Title	Folding of the Immunoglobulin Light Chain : The Mechanism of Unfolding and Refolding, the Role of the Intrachain Disulfide Bond, and the Mechanism of the Disulfide Bond Formation
Author(s)	Goto, Yuji
Citation	大阪大学, 1982, 博士論文
Version Type	VoR
URL	https://hdl.handle.net/11094/24590
rights	
Note	

Folding of the Immunoglobulin Light Chain

—— The Mechanism of Unfolding and Refolding, the Role of the Intrachain Disulfide Bond, and the Mechanism of the Disulfide Bond Formation ——

YUJI GOTO

Department of Biology, Faculty of Science,
Osaka University

1982

Contents

Abbreviations

ANS	1-Anilino-8-naphtalene sulfonate
CD	Circular dichroism
DTNB	5,5'-Dithiobis-(2-nitrobenzoic acid)
DTT	Dithiothreitol
EDTA	Ethylenediaminetetraacetic acid
GSH	Reduced glutathione
GSSG	Oxidized glutathione
GuHCl	Guanidine hydrochloride
SDS	Sodium dodecyl sulfate
CAM-	Reduced and carboxamidomethylated
CM-	Reduced and carboxymethylated
C_{LS}^{S}	The constant fragment of the immunoglobulin light chain (C_L) with intrachain disulfide bond intact
C_{LSH}^{SH}	C_L fragment in which the intrachain disulfide bond is reduced
C_{LSH}^{SSG}	C_L fragment in which the intrachain disulfide bond is reduced and one of the two cysteinyl residues forms a mixed disulfide with glutathione
C_{LSSG}^{SSG}	C_L fragment in which the intrachain disulfide bond is reduced and the two cysteinyl residues form mixed disulfides with glutathione
C_{LSCAM}^{SSG}	C_{LSH}^{SSG} whose SH group is alkylated with iodoacetamide
C_{LSCAM}^{SCAM}	C_{LSH}^{SH} whose SH groups are both alkylated with iodoacetamide

Chapter 1

General Introduction

A protein takes a unique and ordered three-dimensional structure (native conformation) even though a great diversity of possible conformations, and a particular biological function of each protein depends critically upon such a native conformation. Therefore, how and why a protein folds to such a unique conformation from the nacent polypeptide chain synthesized in cells are fundamental problems for understanding the structure and function of proteins. Nowadays, the structure of native proteins and its relation to the function of respective proteins have been elucidated in considerable detail especially by use of X-ray crystallography (Fersht, 1977). On the other hand, the mechanism of protein folding remains many uncertainties in spite of its indispensable importance for protein chemistry.

It is difficult to study the folding in vivo of the nacent proteins in cells. Fortunately, however, the native conformation is determined without any additional information beyond that contained in the amino acid sequence of the protein. This was demonstrated convincingly by Anfinsen and his co-workers (Anfinsen, 1973) by showing the reversible denaturation of ribonuclease A which accompanies the reduction and reoxidation of the four intrachain disulfide bonds. This indicated that we can study the mechanism of protein folding by use of the reversible denaturation in vitro.

Whereas the refolding in vitro starts from a totally unfolded protein by denaturant, heat, acid, or by the reduction of the intra-

chain disulfide bond, the folding in vivo should proceeds at least to some extent as it is synthesized on ribosome. Thus an exact mechanism may be different between the folding in vivo and the refolding in vitro. However, as is apparent from the fact that the native conformation is determined solely by its amino acid sequence, the principles that govern protein folding should be the same. To understand the protein folding is to interprete the principles of the protein folding and it is fairly expected to interprete the principles from the studies in vitro.

The problem of protein folding consists of two aspects. One is the nature and magnitude of interactions necessary to determine the specific native conformaiton. The other is the pathway in which the structureless polypeptide chain converts to the native conformation.

The first aspect of protein folding seems to be elucidated to a greater extent (Tanford, 1968, 1970; Anfinsen & Scheraga, 1975; Hamaguchi, 1976; Schulz & Schirmer, 1979). The first systematic and quantitative studies of protein denaturation were carried out by Tanford and his co-workers (Tanford, 1968, 1970). They studied the denaturation in terms of the structure and stability of proteins and found that generally the denaturation of proteins are highly cooperative process fairly approximated by a two-state transition:

$$D \longleftrightarrow N \,, \qquad \text{(Mechanism 1.1)}$$

where N is native protein and D is denatured (or unfolded) protein nearly equal to a random-coil state. They showed that the stability of protein in physiological condition is only marginal (about 10 kcal/mol) irrespective of protein species (see also Pace, 1975).

A contribution of conformational entropy term is roughly estimated to favor the unfolded state by several hundred kcal per mol of protein (Schulz & Schirmer, 1979). The driving force for folding which compensates such a large conformational entropy is a sum of several terms. The main contribution for folding should be the hydrophobic interactions and the properties of the interactions have been studied extensively (Tanford, 1970; Hamaguchi, 1978; Schulz & Schirmer, 1979). The hydrogen bond, salt bridge, and intrachain disulfide bond are also the important factors for protein folding. The native structure of a protein is a delicately balanced system and its balance is largely influenced by subtle modification of proteins. Fortunately this often aided the elucidation of property and magnitude of above factors in the studies (e.g., using mutant proteins) (Yutani, 1978).

On the other hand, the different approach has elucidated the nature of interaction which determines the specific native structure. By use of the detailed X-ray structure of several proteins, a correlation of amino aicd sequence and the secondary structure became apparent. The fair agreement of the predicted structure from amino acid sequence with the X-ray structure indicated the importance of short-range interaction in determining the native structure (Chou & Fasman, 1974a, b, 1978). However, the prediction is applicable only to the intact protein. Fragments of a protein generally lose their native structure. These and other experiments of fragment-complementation (Anfinsen & Scherage, 1975) indicated that long-range interactions are also important in determination of the native structure.

Our knowledge as to the nature and magnitude of forces that determine the native structure is thus accumulated. However, it seems yet far from constructing a native conformation from a polypeptide chain without any knowledge other than amino acid sequence. The study of the second aspect of protein folding, i.e., the pathway of protein folding, is inevitable for further interpretation of protein folding.

There have been many studies as to the pathway of protein folding (Wetlaufer & Ristow, 1973; Baldwin, 1975; Anfinsen & Scheraga, 1975; Creighton, 1978; Baldwin & Creighton, 1980). However, it is a more difficult problem and our interpretation today may be yet a primitive one. As described above, the remarkable and probably the most important property of protein folding is the high cooperativity of folding transition. The situation today may be that we know little more than the two-state transition as to the pathway of protein folding. Several models have been proposed as to the pathway of protein folding based on the nature and magnitude of interactions which stabilize the native conformation (Burgess & Scheraga, 1975; Ptitsyn & Rashin, 1975; Karplus & Weaver, 1976; Lim, 1978; Nemethy & Scheraga, 1979; Baldwin, 1978, 1980). Nevertheless, a rate-limiting step of folding pathway, which is the most fundamental problem, is still in controversy. The investigation of folding pathway based on the exact experimental evidence is only begining.

The two-state transition means a scarce accumulation of an intermediate. On the other hand, an elucidation of the intermediate is necessary and probably essential for an interpretation of the folding pathway. Through detecting and characterizing the intermediate in

terms of energetics and kinetics of folding transition, we may interprete the pathway of protein folding. Based on this idea, the intermediate of folding (or unfolding) has been examined extensively by several methods (Baldwin, 1975). In early period, the fast kinetic methods was expected to elucidate the intermediate, because deviations from a two-state transition became apparent in several proteins which exhibit a two-state transition by equilibrium measurements (Ikai et al., 1973; Tanford et al., 1973). Contrary to the initial expectation, the apparent complicated kinetic behavior was subsequently shown to be largely due to the proline isomerism (see Chapter 5.1). The problem is not so easy to be solved.

The more successful information has been obtained by an indirect method in which the intrachain disulfide bonds were used as a kinetic trap of the intermediate of folding (Creighton, 1978). Since Anfinsen's findings, the mechanism of disulfide bond formation is one of the most important theme of protein folding. As described above, the intrachain disulfide bond is one of the important factors that stabilize the native conformation. Generally, the cleavage of the intrachain disulfide bonds leads to destruction of the native conformation (Creighton, 1978; Torchinsky, 1981). There have been many studies as to the pathway of disulfide bond formation, and the relation between the disulfide bond formation and the formation of the native conformation has been inferred (Creighton, 1978; Utiyama, 1980; Torchinsky, 1981). The presence of several disulfide bonds in many proteins, however, made difficult a detailed interpretation of the mechanism mainly due to the complexity of the analysis.

Only recently, Creighton (1978) has elucidated the exact pathway of formation of the three disulfide bonds of bovine pancreatic trypsin inhibitor. He found that the pathway of the oxidation and reduction of the disulfide bonds followed an ordered sequence. From kinetic and energetic properties of the pathway and conformational properties of the trapped intermediates, he attempted to correlate the pathway of disulfide bond formation with the pathway of the conformational transition of the protein or with the pathway of folding wihtout disulfide bond formation. As a result, Creighton (1978, 1980a) proposed an idea that the rate-limiting transition in folding is very close to a native state. He (1980a, 1980b) also studied the folding kinetics of several other proteins and suggested a general validity of the idea obtained in trypsin inhibitor.

His strategy seems to be a reasonable and appropriate for studying the pathway of folding in a condition where the direct detection of the folding intermediate is very difficult, and it may be the nearest way for an elucidation of folding pathway. There are, however, two critical problems in such studies. One is that we do not know exactly the role of intrachain disulfide bond in a conformation and stability of proteins. Although a theoretical explanation for the mechanism of the stabilization by disulfide bond had been proposed more than twenty years ago (Flory, 1956; Poland &Scheraga, 1965), the presence of several disulfide bonds in many proteins obstructed an exact experimental study of the role of the respective disulfide bonds. While there are many qualitative data (Creighton, 1978; Torchinsky, 1981), quantitative data as to the role of the respective disulfide

bonds in proteins are only a few. The other is that the relation between one disulfide bond formation and the conformational transition of the protein molecule is known only a little. The only one clear case was obtained for the third disulfide bond of the bovine pancreatic trypsin inhibitor (Creighton, 1978). The third disulfide bond of the trypsin inhibitor is located at the surface of the molecule and its proximity greatly accelerates the disulfide bond formation through thiol-disulfide interchange reaction. Thus, the interpretation of Creighton (1978, 1980a) is based on a critical assumption obtained from the third disulfide bond of the trypsin inhibitor, i.e., the varying tendencies of the possible pairs of cysteine residues of the polypeptide chain to form disulfide bonds reflect their tendencies to come into suitable proximity, due to the conformational properties of the protein at each stage of folding. In other words, he assumed that the proximity of two SH groups always results in the disulfide bond formation. As will be described in Chapter 7, my results denied the general validity of his assumption.

Creighton (1979) further studied the pathway of disulfide bond formation in ribonuclease A, which has four disulfide bonds, but the analysis is largely inferior to that of trypsin inhibitor. Only one increase in the number of disulfide bond made increasingly difficult the study. This is mainly due to the above uncertainties of the property of disulfide bond. These problems of the disulfide bond suggest that we must further study a fundamental property of disulfide bond in a more simple system in which we can directly interprete the role of disulfide bond in the structure of protein, and in which a

correlation of disulfide bond formation with the conformational transition of the protein molecule is possible. The distinct information concerning a single disulfide bond may progress the experimental approach for an elucidation of the pathway of protein folding. In these viewpoints, the domain of immunoglobulin is very suitable.

Immunoglobulins are serum glycoproteins synthesized by vertebrates as antibodies against antigens. There are perhaps countless different immunoglobulin molecules in normal serum. On the other hand, myeloma proteins which are homogeneous immunoglobulin are produced by single clones of malignant plasma cells. From the extensive studies of amino acid sequences, physicochemical properties, and X-ray diffraction of myeloma proteins and its fragments, the detailed three-dimentional structure and its relation to the several functions of immunoglobulins were elucidated (Edelman & Gall, 1969; Davies et al., 1975; Beale & Feinstein, 1976; Kabat, 1978; Amzel & Poljak, 1979). Recent studies using gene technology is just going to elucidate the mechanism of an expression of immunoglobulin gene which accompanies gene rearrangement responsible for diversity and class-switch of immunoglobulin molecules.

Immunoglobulins generally consist of four polypeptide chain: two heavy (H) chain and two light (L) chain (mw of 50,000 and 25,000, respectively) (Figure 1.1). They are divided into five major classes (IgM, IgG, IgA, IgD, and IgE) characterized by their H chain types and each class carries a different role in immune system. Light chains are also classified into two types (κ and λ) independent of

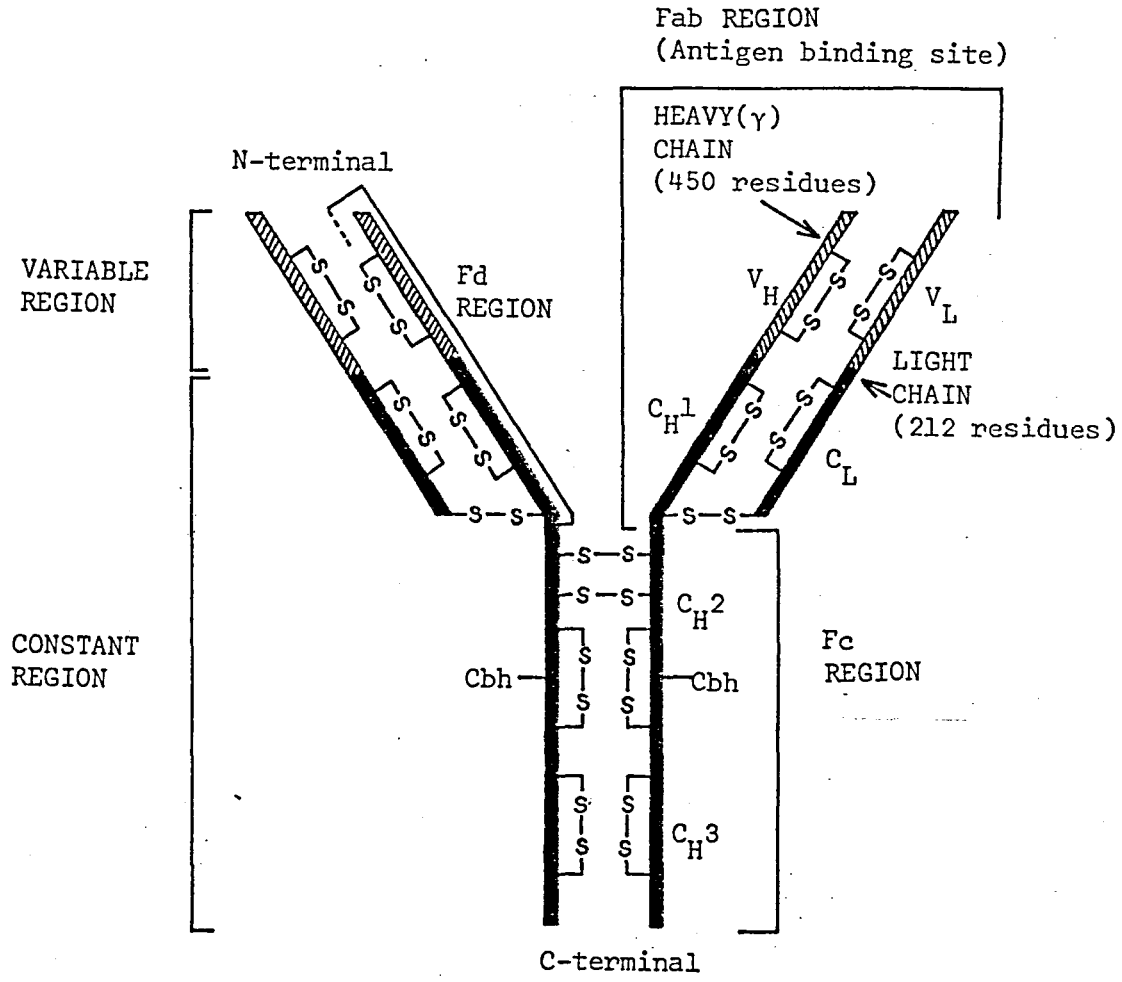

Fig. 1.1. Diagrammatic representation of the four-chain structure of immunoglobulin (IgG1) molecule showing both inter- and intrachain disulfide bonds and homology regions.

heavy chain classes. The distinguished structural property of immunoglobulin molecules is the domain structure. H and L chain consist of four (V_H, C_H1, C_H2, and C_H3) and two (V_L and C_L) homologous regions called domain, respectively (Figure 1.1). Each domain consists of 110 amino acids and contains one intrachain disulfide bond (Figure 1.2). The native conformations of domains are retained even in the isolated domains and it indicates an independent folding of the domains. X-ray crystallography revealed that all of these domains share a common pattern of three-dimentional chain folding called immunoglobulin-fold (Figure 1.2). It consists of two antiparallel β-pleated sheets which are formed by three and four antiparallel β-strands. The internal volume of two β-sheets is tightly packed with hydrophobic side chains and one intrachain disulfide bond, which connects the two β-sheets, is buried in the center of the molecule.

Several functions of immunoglobulins are attributed to respective domains. The binding site against antigens is formed by the interaction of amino-terminal V_L and V_H domains. The C_H2 domain in IgG binds C_{1q} to initiate the classical complement sequence, while an adherance to the monocyte surface is mediated through carboxy-terminal C_H3 domain.

Based on these structural and functional properties of immunoglobulin molecule, we can regard the respective isolated domains as relatively small globular proteins. And the intrachain disulfide bond present in each domain is a very typical intrachain disulfide bond in that it is buried in the interior hydrophobic region of the molecule and in that the loop formed by the disulfide bond is very

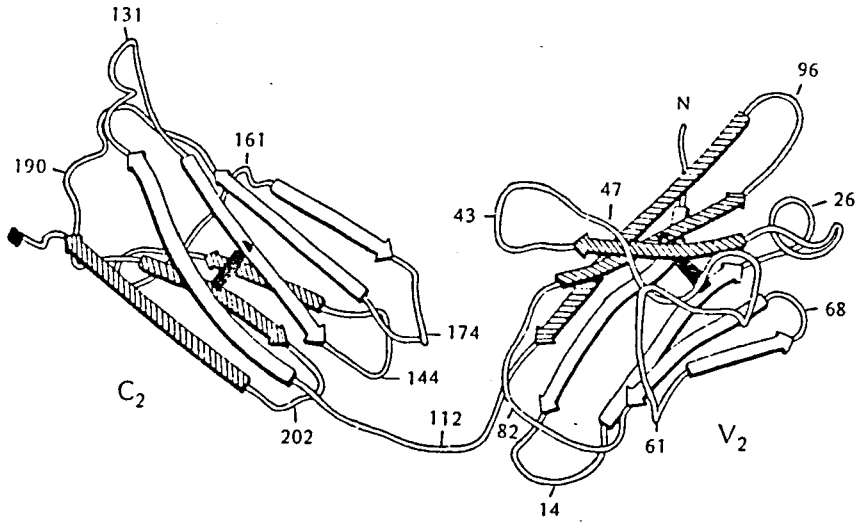

Fig. 1.2. A schematic drawing of the tertiary structure of type λ light chain. V_2 and C_2 refer to the variable and constant domains, respectively. The arrows indicate the β-pleated sheets and direction of polypeptide chain. The solid bars are the disulfide bonds, and the numbers are amino acid residues. (Reproduced from Schiffer et al., 1973)

large (about 60 amino acid residues). Therefore studying the folding of the immunoglobulin domains with an emphasis on the intrachain disulfide bond was expected to provide a useful and distinct information as to the role of the disulfide bond in the folding of the domains. As described above, the result in such a simple system will be the most fundamental one and will be useful in consideration of the role of intrachain disulfide bonds in general proteins with several disulfide bonds. Furthermore, we can study the folding of complicated system by preparing the fragments consisting of two or more domains (e.g., whole light chain, which consists of V_L and C_L domains (Figure 1.2)). The result may be considered in relation to the folding of its constituent domains. Such stepwise study may not only shed light on the problem of how complex structure of immunoglobulin molecule is formed but also become a fundamental model for folding of proteins consisting of several domains and oligomeric enzyme. Based on these ideas, I prepared an isolated C_L domain (C_L fragment) by a proteolytic digestion of Bence Jones protein Nag, which is a homogeneous light chain secreted in the urine of myeloma patient, and carried out several experiments concerning the folding of the C_L fragment and the whole light chain, with a main interest on the intrachain disulfide bond.

Firstly, in Chapter 3, I studied the conformation and stability of the C_L fragment whose disulfide bond had been reduced and compared with those of intact C_L fragment. The results obtained showed that the reduced C_L fragment has a native-like conformation in the absence of denaturant although the stability is much decreased. As far as

I know, the C_L fragment is the first protein to show that the native conformation is retained even if the intrachain disulfide bond which is buried in the interior of the protein molecule is reduced. The decrease in stability after reduction of the disulfide bond was explained in terms of the increase in entropy in the denatured state after the reduction of the bond.

In Chapters 4 and 5, I studied the unfolding and refolding kinetics of the intact and reduced C_L fragments, respectively, to interprete the role of the intrachain disulfide bond in detail. Unfolding and refolding kinetics of both proteins were complex. I analysed the kinetic data quantitatively and found that the kinetics of both proteins follow fundamentally the three-species mechanism:

$$U_1 \longleftrightarrow U_2 \longleftrightarrow N \,, \qquad \text{(Mechanism 1.2)}$$

where U_1 and U_2 are the slow-folding and fast-folding species, respectively, of unfolded protein and N is native protein. In equilibrium measurement, this mechanism cannot be distinguished from the two-state mechanism (mechanism 1.1). I compared the respective rate constants of the intact C_L fragment with those of the reduced C_L fragment and found that the kinetic role of intrachain disulfide bond is to increase only the refolding rate. The kinetic results not only confirmed the entropic role of disulfide bond inferred from the equilibrium measurements, but also suggested the location of the rate-limiting step of folding transition of the C_L fragment. The presnece of two forms of the unfolded species (U_1 and U_2) were also considered in detail.

In Chapter 6, I studied the folding mechanism of light chain which consists of two domains (V_L and C_L) based on the folding kinetics of isolated V_L and C_L fragments. The results indicated that the folding kinetics of the light chain was essentially explained by a sum of the independent folding of two domains, although some deviations from the entire independent folding were also apparent.

The two SH groups of the reduced C_L fragment are buried in the interior of the protein molecule. Such buried SH groups may appear during the reoxidation of other reduced proteins with several disulfide bonds. Thus, the mechanism of disulfide formation in such buried SH groups is important in the study of protein folding. In Chapter 7, I studied the mechanism of disulfide bond formation in the reduced C_L fragment. I found that the burial of the SH groups in the interior of the protein molecule greatly retards the disulfide bond formation, even though the two SH groups locate in close proximity.

The results obtained were simple but reasonable. I believe that all of them are essential to the consideration of the problem of protein folding.

Chapter 2

Experimental

2.A. Materials

2.A.1. Reagents

GuHCl (specially prepared grade) was obtained from Nakarai Chemicals Co. and was used without further purification. A stock solution of GuHCl was filtered through a 0.22 μm Millipore filter, type GSWP, before use.

The ammonium salt of ANS was purchased from Nakarai Chemicals Co. ANS was purified by preparing the magnesium salt and repeatedly recrystallizing it. ANS concentration was determined spectrophotometrically using a molar extinction coefficient of 4.95×10^3 at 350 nm (Weber & Young, 1964).

Urea (specially prepared grade), DTT, DTNB, iodoacetamide, iodoacetate, and EDTA were obtained from Nakarai Chemicals Co. GSH and GSSG were obtained from Sigma Chemical Co. All other reagents were of reagent grade and were used without further purification.

2.A.2. Bence Jones proteins

Type λ Bence Jones protein Nag was purified from the urine of patient Nagai with multiple myeloma. The urine was precipitated with 80% ammonium sulfate and was dialyzed against 0.02 M phospate buffer at pH 8.0. The crude solution of Bence Jones protein was subjected to ion exchange chromatography on a DEAE-Sephadex A-50 column equilibrated with 0.02 M phospate buffer at pH 8.0. The major component

eluted with a linear gradient from 0 to 0.4 M KCl in the same buffer were pooled and dialyzed against 0.01 M acetate buffer at pH 5.5. Then the protein solution was subjected to ion exchange chromatography on a CM-cellulose column equilibrated with 0.01 M acetate buffer at pH 5.5. The component which did not adsorb the column was a homogeneous Bence Jones protein from the analysis by polyacrylamide gel electrophoresis both in the presence and absence of sodium dodecyl sulfate. This component was dialyzed against distilled water and then lyophilized.

The other Bence Jones proteins used in this work: five type λ Bence Jones proteins (Tod, Ni, Sh, Kob, and Fu) and two type κ Bence Jones proteins (Ta and Ham), were kindly provided by Dr. S. Migita of Kanazawa University.

The results of SDS-polyacrylamide gel electrophoresis showed that Kob protein is a dimer with an interchain disulfide bond and that Sh, Ni, and Nag proteins contain both dimers with an interchain disulfide and monomer. The interchain disulfide bonds of Tod, Nag, Ni and Fu proteins were reduced with 10 mM DTT in 0.1 M Tris-HCl buffer containing 0.15 M KCl, 1 mM EDTA at pH 8 for 30 min at room temperature and then alkylated by the addition of two-fold molar excess of iodoacetamide over the SH groups. The reaction was continued for 30 min in dark and then the reaction mixture was dialyzed against the desired buffer solution or distilled water. Sh and Kob proteins were used without reducing and alkylating the interchain disulfide bond.

2.A.3. C_L fragments

The C_L fragment of type λ Bence Jones protein Nag was obtained by tryptic digestion or papain digeston.

Tryptic digestion was carried out as follows. A 2-3 % solution of Bence Jones protein Nag in which the interchain disulfide bond had been reduced and alkylated was digested at 37°C for 50 min with trypsin, with a substrate-to-enzyme ratio of 50 : 1 (W/W) in 0.01 M Tris-HCl buffer, pH 8.0, containing 0.15 M KCl. The digestion was stopped by the addition of soybean trypsin inhibitor with an inhibitor-to-enzyme ratio 1.5 : 1 (W/W). The digested solution was applied to a Sephadex G-75 column equilibrated with 0.01 M Tris-HCl buffer at pH 8.6. Five peaks were separated (Figure 2.1). The first and second peaks corresponded to aggregates and the undigested protein, respectively. The third peak contained a fragment with a molecular weight of about 12,000 as estimated by SDS-polyacrylamide gel electrophoresis. The fourth and fifth peaks contained several smaller fragments. The fractions of the third peak were pooled and subjected to ion exchange chromatography on a DEAE-cellulose column equilibrated with 0.01M Tris-HCl buffer at pH 8.6. Two peaks were eluted with a linear gradient from 0 to 0.1 M KCl in the same buffer (Figure 2.2). The first and major peak contained the C_L fragment, which was identified on the basis of an immunodiffusion test using rabbit antiserum against a type λ Bence Jones protein. The pooled fractions from the main peak were dialyzed against water and then lyophilized.

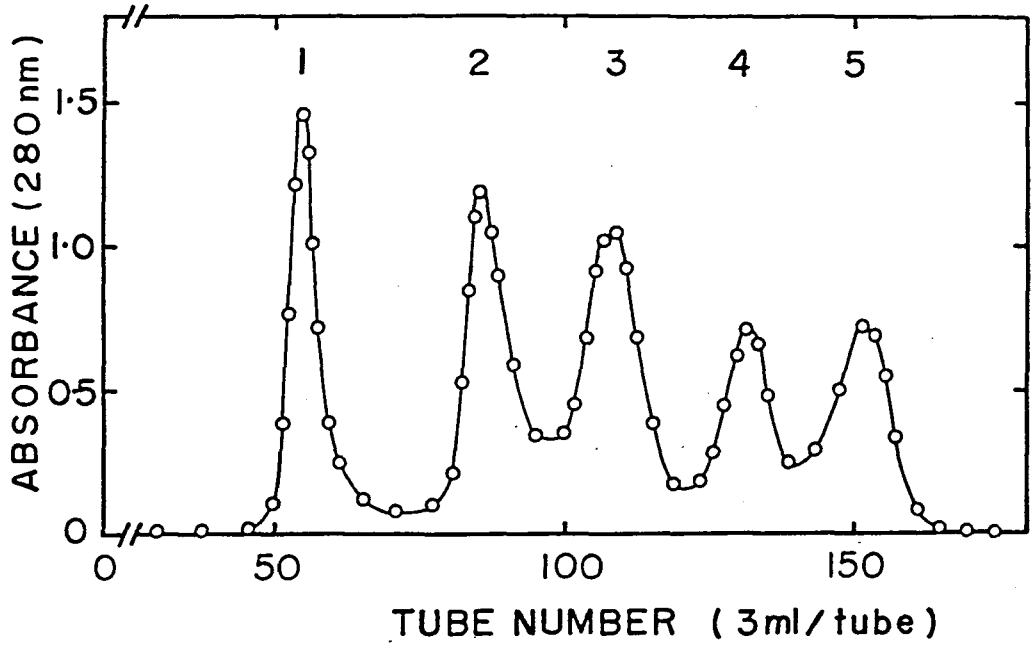

Fig. 2.1. Gel filtration on Sephadex G-75 of a tryptic digest of reduced and alkylated Bence Jones protein Nag. Five ml of digest was applied to a 3 x 100 cm column equilibrated with 0.01 M Tris-HCl buffer at pH 8.6 and fractions of 3 ml were collected. See the text for experimental details.

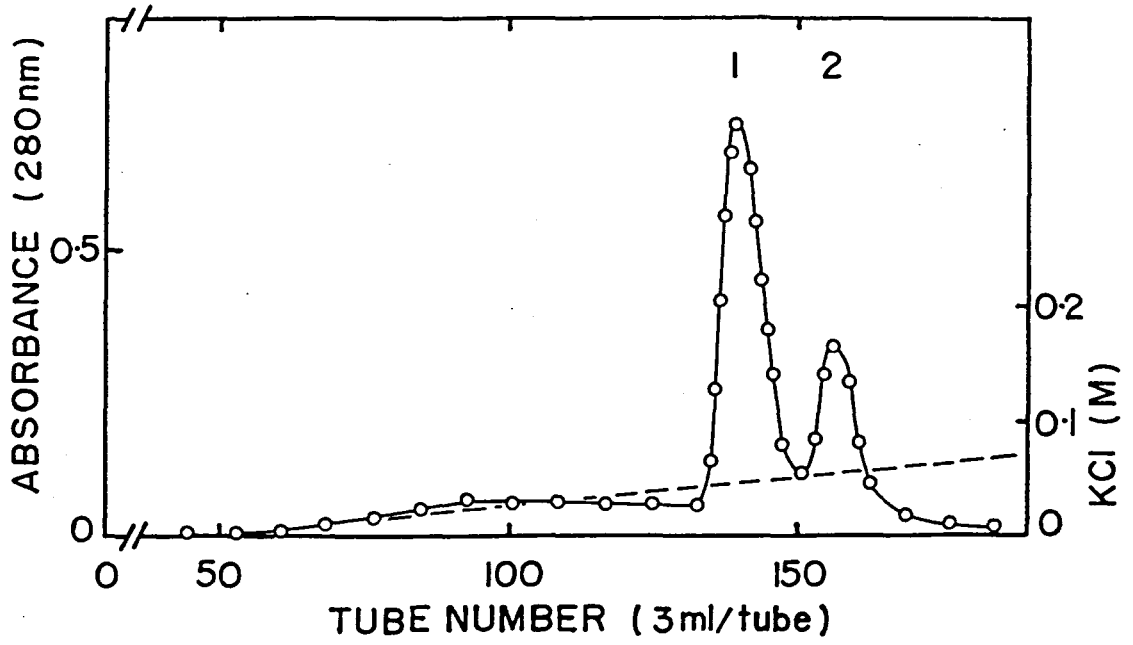

Fig. 2.2. Ion exchange chromatography on DEAE-cellulose (DE 52) of the third peak obtained by the gel filtration of the tryptic digest of Bence Jones protein Nag. Fifty ml of the protein solution was applied to a 2 x 20 cm column equilibrated with 0.01 M Tris-HCl buffer at pH 8.6. Elution was performed with 500 ml of the same buffer in a gradient from 0 to 0.1 M KCl and fractions of 3 ml were collected.

Papain digestion was carried out as follows. A 1-2 % solution of Bence Jones protein Nag in which the interchain disulfide bond had been reduced and alkylated with iodoacetamide was digested at 37°C for 40 min with papain with a substrate-to-enzyme ratio of 250 : 1 (W/W) in a 0.1 M phosphate buffer at pH 7.0 containing 4 mM cysteine and 1 mM EDTA. The digestion was stopped by adding 5 mM iodoacetamide and cooling the reaction mixture to 4°C. Identification and purification of the C_L fragment were made following the same procedure as used for typtic digestion. Figure 2.3 shows the gel filtration (Sephadex G-75) pattern of the digested solution at pH 8. Three peaks were separated. The first, second, and third peaks corresponded to the undigested protein, the C_L fragment, and several smaller fragments, respectively. The fractions of the second peak were then subjected to ion exchange chromatography on DEAE-cellulose column at pH 8.0 (Figure 2.4). The main peak eluted with a linear gradient from 0 to 0.1 M KCl contained the C_L fragment. The pooled fractions from the peak were dialyzed against water and then lyophilized.

The C_L fragment whose intrachain disulfide bond is reduced (reduced C_L fragment or $C_{L}^{SH}{}_{SH}$) was prepared as follows. About 0.5 % (W/V) C_L fragment in 0.1 M Tris-HCl buffer containing 4 M GuHCl (or 8 M urea) and 1 mM EDTA at pH 8.0 was allowed to react with 20 mM DTT for 30 min at room temperature. After the reaction the reduced fragment was separated from the residual reagents on a column of Sephadex G-25 equilibrated with 5 mM potassium acetate buffer at pH 5.0 containing 1 mM EDTA and 0.15 M KCl. Unless otherwise specified, all the buffers used for preparing solutions of reduced C_L fragment were degassed

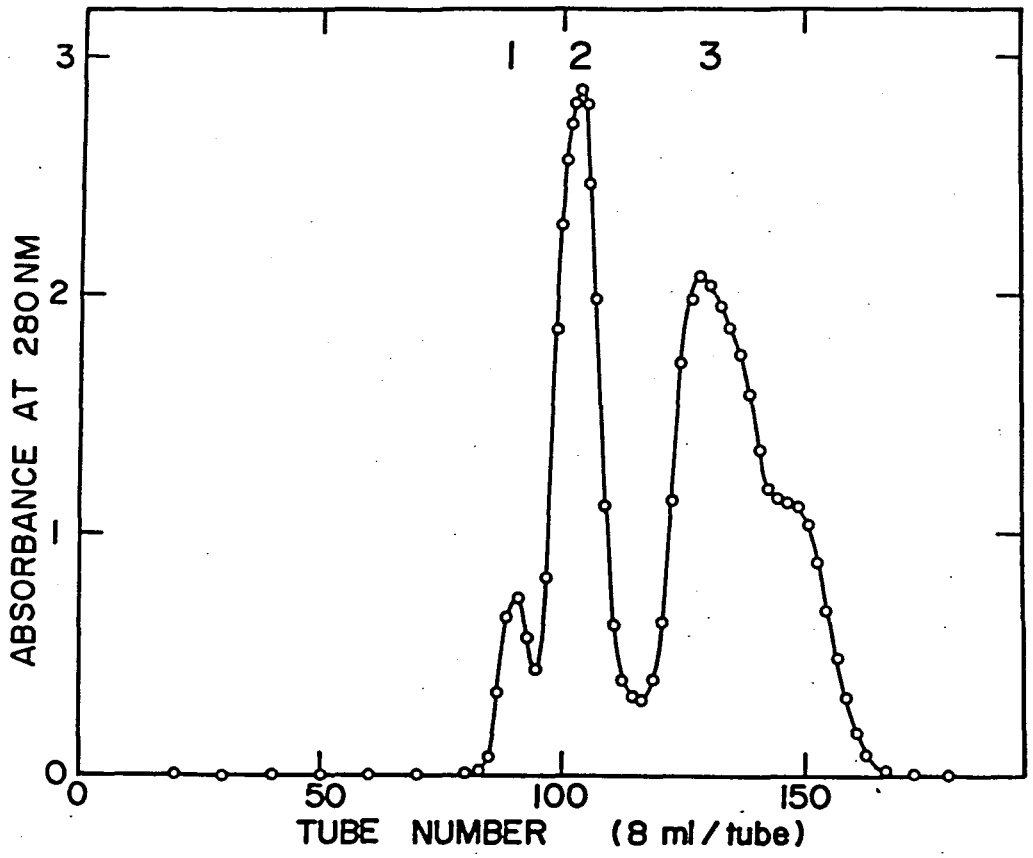

Fig. 2.3. Gel filtration on Sephadex G-75 of a papain digest of reduced and alkylated Bence Jones protein Nag. Thirty ml of digest was applied to a 3.6 x 105 cm column equilibrated with 0.01 M Tris-HCl buffer at pH 8.6 and fractions of 8 ml were collected. See the text for experimental details.

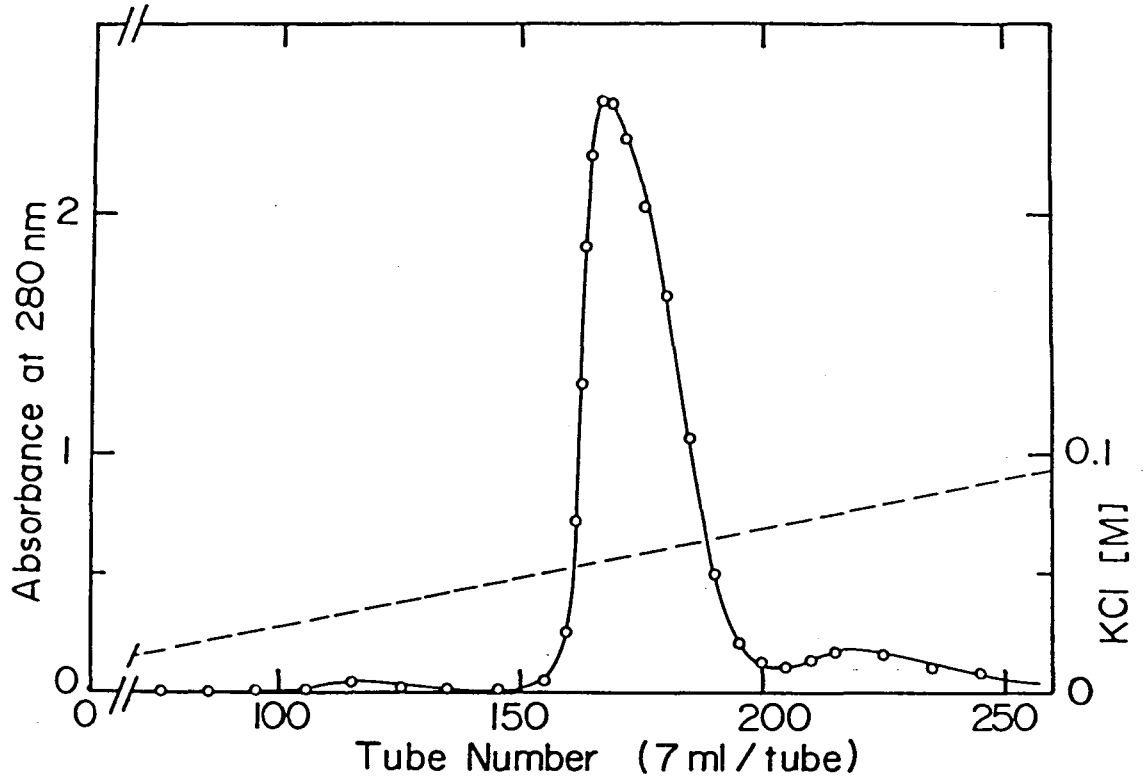

Fig. 2.4. Ion exchange chromatography on DEAE-cellulose (DE 52) of the second peak obtained by the gel filtration of the papain digest of Bence Jones protein Nag. 300 ml of the protein solution was applied to a 3.8 x 50 cm column equilibrated with 0.01 M Tris-HCl buffer at pH 8.6. Elution was performed with 2000 ml of the same buffer in a gradient from 0 to 0.1 M KCl and fractions of 7 ml were collected.

and subsequently saturated with oxygen-free nitrogen.

The C_L fragment whose intrachain disulfide bond is reduced and alkylated by iodoacetamide (CAM-C_L fragment or C_{LSCAM}^{SCAM}) or iodoacetate (CM-C_L fragment or C_{LSCM}^{SCM}) was prepared as follows. The SH groups of about 0.1 % (W/V) reduced C_L fragment in 0.1 M Tris-HCl buffer at pH 8.0 containing 4 M GuHCl were alkylated by the addition of two-fold molar excess of iodoacetamide or iodoacetic acid over the SH groups. The reaction was continued for 30 min and then the reaction mixture was dialyzed against 0.05 M Tris-HCl buffer at pH 7.5.

The C_L fragment in which the intrachain disulfide bond is reduced and the two cysteinyl thiols form mixed disulfides with glutathione (C_{LSSG}^{SSG}) was prepared as follows. About 0.1 % (W/V) reduced C_L fragment was allowed to react with 50 mM GSSG in 0.2 M Tris-base at pH 8.5 containing 4 M urea and 1 mM EDTA. After 30 min at room temperature, C_{LSSG}^{SSG} was isolated by gel filtration through a column of Sephadex G-25 equilibrated with 1 mM EDTA and was then lyophilized.

2.A.4. V_L fragments

The urine of patients, Tod, Fu, and Ta contained V_L fragments in addition to the parent Bence Jones proteins. The V_L fragments of Tod (type λ), Fu (type λ), and Ta (type κ), which were purified by ion exchange chromatography and gel filtration (Azuma et al., 1978), were kindly provided by Dr. K. Hamaguchi.

2.B. Methods

2.B.1. CD measurement

Unless otherwise specified, all the experiments were carried out in 0.05 M Tris-HCl buffer at pH 7.4 - 7.6 containing 0.15 M KCl. CD measurement was carried out with a Jasco J-20 spectropolarimeter equipped with a CD attachment, previously calibrated with d-10-camphorsulfonic acid (Urry & Pettegrew, 1967; Cassim & Yang, 1969). The results are expressed as mean residue ellipticity [θ], which is defined as

$$[\theta] = \frac{100 \times \theta_{obs}}{l \times c} \qquad (2.1)$$

where θ_{obs} is the observed ellipticity in degrees, c is the concentration in residue mol per liter, and l is the length of the light path in centimeters. For calculation of c, a value of 108 was used as the mean residue molecular weight for all proteins. CD spectra were measured at a protein concentration of about 0.2 mg/ml with a 2.0-or 4.0-cm cell from 320 to 250 nm, with a 1.0-or 0.5-cm cell from 260 to 230 nm, and with a 0.1-cm cell from 250 to 200 nm. Kinetic measurement was made at a fixed wavelength at a protein concentration of 0.1 mg/ml with a 0.5-cm cell or 0.2 mg/ml with a 0.1-cm cell. The temperature was controlled with a thermostatically controlled cell holder. The dead time of the kinetic measurement was about 1 min.

2.B.2. Fluorescence measurement

Fluorescence measurement was carried out with a Hitachi fluorescence spectrophotometer, model MPF-4, equipped with a spectral

corrector. Square cells of 1-cm path length were used. Temperature was kept at 25°C or 5°C using a thermostatically controlled cell holder. Tryptophyl fluorescence was measured by using 280 nm or 295 nm light for the excitation. Absorbance of the protein in a 1-cm cell was less than 0.05 at the excitation wavelength. The fluorescence of ANS was measured with excitation at 365 or 440 nm, and the absorbance was less than 0.1 at 365 and 440 nm. The dead time of the kinetic measurement was about 20 sec.

2.B.3. Ultraviolet absorption measurement

Difference absorption spectra of Bence Jones proteins and C_L fragment were recorded with a Cary model 118 spectrophotometer. The protein concentration was 0.07 %. The change in the molar extinction coefficient ($\Delta\varepsilon$) was calculated by assuming the molecular weight of Bence Jones protein monomer and C_L fragment to be 23,000 and 11,500, respectively. The refolding processes of Bence Jones proteins and C_L and V_L fragments were followed by measuring the change with time in the absorption at around 293 nm using a Hitachi 323 spectrophotometer. In the reference cell, 50 µl of denatured protein in 4 M GuHCl was added to 3 ml of Tris-HCl buffer at pH 7.5 and the mixture was allowed to stand for a sufficient time to renature the protein. Fifty µl of the same denatured protein solution was then added to 3 ml of the same buffer in the sample cell, and the absorption change was followed. All the absorption measurements were carried out at 25°C using a thermostatically controlled cell holder. The dead time of the kinetic measurement was about 20 sec.

2.B.4. Stopped-flow measurement

For measurements of fast kinetics a Union Giken stopped-flow spectrophotometer, model RA-401, which is equipped with a data processer, RA-450, was used. The fluorescence accessory in conjunction with the Xenon lamp accessory was used. The excitation wavelength was set at 280 nm and a Toshiba UV-33 glass filter was used to cut off the fluorescence at wavelengths shorter than 330 nm. The original mixing apparatus was used to measure fast reactions which are complete within 10 sec and a modified mixing apparatus, in which the distance between the mixer and the observation cell is longer than that of the original apparatus (about 50 mm), was used to measure reactions slower than the above. In the case where the mixing of unequal volume of protein and diluent is needed, I introduced a constriction in the flow channel from the resorvoir of protein solution to the mixer as was described by Kato et al. (1981). The mixing ratio was checked by a known solution of tryptophan. The resorvoir and the observation cell were thermostated by rapidly circulating water at 25°C. The dead time was determined as 5 msec for the original apparatus and 30 msec for the modified apparatus from the measured rate of reducing reaction of 2,6-dichlorophenol-indophenol sodium with L-ascorbic acid (Tonomura et al., 1978). The fluorescence change was monitored on a memory oscilloscope and was recorded with an X-Y recorder through a data processer. The protein conentration was 0.02 mg/ml.

2.B.5. Titration of SH groups with DTNB

The SH content of reduced C_L fragment was checked by titration with DTNB just after the spectroscopic measurements. To a 2.5 ml solution of reduced C_L fragment was added 0.5 ml of freshly prepared 5 mM DTNB solution in 1 M Tris-HCl buffer at pH 8.2 containing 4 M GuHCl, and its absorbance was measured against a freshly prepared reagent blank with a Hitachi Model 323 spectrophotometer. The final pH of the reaction mixture was about 8. The molar extinction coefficient of reduced DTNB at pH 8 was assumed to be 13,600 M^{-1} cm^{-1} at 412 nm (Gething & Davidson, 1972). The SH content of reduced C_L fragment was always between 1.9 and 2.1.

The reactivities of the two SH groups of the reduced C_L fragment toward DTNB at various concentrations of GuHCl were used to follow protein unfolding reaction. To a 2.5 ml solution of the reduced C_L fragment in 0.05 M Tris-HCl buffer containing 0.15 M KCl, 1 mM EDTA, and a given concentration of GuHCl at pH 7.5 was added 0.5 ml of freshly prepared 3 mM DTNB solution in the same buffer containing the same concentration of GuHCl, and its absorbance at 412 nm was measured against a freshly prepared reagent blank.

2.B.6. Data analysis of kinetic measurements

All the kinetic data can be described by an equation of the form

$$F(t) - F(\infty) = \sum_{i=1}^{n} F_i \cdot \exp(-\lambda_i t) \qquad (2.2)$$

where F(t) is the value of a particular physical property at time t, $F(\infty)$ is the value after equilibration, λ_i is the apparent rate constant of phase i, and F_i is the amplitude of the phase. From the first-order plot of reaction, the apparent rate constant and the amplitude of the slowest phase were first determined. This component was then subtracted from the original time course and the logarithm of the residue was again plotted against time to determine the rate and amplitude of the second phase. When two exponential terms were insufficient to describe the total change, the procedure was repeated again. All the kinetic data obtained in this work were described by at most three exponential terms.

2.B.7. Thiol-disulfide interchange reaction

The thiol-disulfide interchange reaction of reduced C_L fragment with GSSG in the absence of urea was performed as follows. Freshly prepared reduced C_L fragment was diluted to a final concentration of about 5×10^{-5} M into 0.1 M Tris-HCl, 0.15 M KCl, 1 mM EDTA with a final pH of 8.1. The reaction was started by adding to this solution an equivalent volume of a solution of GSSG at an appropriate concentration in 0.1 M Tris-HCl (pH 8.1), 0.15 M KCl, 1 mM EDTA. The reaction of reduced C_L fragment with GSSG was carried out in the same buffer containing 8 M urea. The reaction of intact C_L fragment and C_L fragment which formed mixed disulfide with glutathione (C_{LSSG}^{SSG}), with GSH in the absence and presence of urea was carried out in a similar manner.

The thiol-disulfide interchange reaction in the absence of urea was quenched by adding 0.1 ml of 0.2 M iodoacetamide in 0.1 M potassium acetate (pH 5.0) containing 8 M urea to 0.1 ml of protein solution. The reaction in the presence of 8 M urea was quenched by addition of an equivalent volume of 0.2 M iodoacetamide in the same buffer without urea. The quenched solution was kept for a few minutes at room temperature and then the products were analyzed by polyacrylamide gel electrophoresis. The pH of the quenched solution was about 7.

All the buffers used were degassed, and for the reactions that were continued for more than 1 hour, the buffers were degassed and then saturated with oxygen-free nitrogen.

2.B.8. Electrophoresis

Electrophoresis for the analysis of the thiol-disulfide interchange reaction was carried out at pH 9.5 in 15 % (W/V) polyacrylamide gel according to the method of Davis (1964). Samples (0.05 ml) containing 4 M urea at about pH 7 were layered on the stacking gels and electrophoresis was carried out for 5 to 8 hours at 1.5 mA/tube. Gels were stained with 0.5 % (W/V) Coomassie brilliant blue in 45 % (V/V) methanol, 7.5 % (V/V) acetic acid, and destained in 5 % (V/V) methanol, 7.5 % acetic acid. Densitometric scanning of the gels was done at 565 nm using a Toyo DMU 33c digital densitometer.

Electrophoresis for the analysis of purity of proteins was carried out at pH 9.5 in 7.5 % (W/V) polyacrylamide gel according to the method of Davis (1964), and in 15 % (W/V) polyacrylamide gel in the presence of SDS according to the method of Weber and Osborn (1969).

2.B.9. Protein concentration

Concentrations of intact C_L fragment was determined spectrophotometrically using a value of $E^{1\%}_{1cm}$ = 14.6 at 280 nm (Karlsson et al., 1972). Concentrations of reduced C_L fragment, CM-C_L fragment, and CAM-C_L fragment were estimated assuming values of $E^{1\%}_{1cm}$ = 14.5, 13.6, and 13.6 at 280 nm, respectively. These values were obtained by measuring the difference spectra of intact C_L fragment, reduced C_L fragment, CM-C_L fragment, and CAM-C_L fragment in 4 M GuHCl against a reference of each protein in Tris-HCl buffer at pH 7.5 and assuming that the absorption coefficient at 280 nm of these proteins in 4 M GuHCl are all the same.

2.B.10. pH measurement

pH was measured with a Radiometer PHM 26c meter at 25°C.

2.B.11. Amino terminal sequence determination

The amino terminal sequences of the C_L fragments obtained by tryptic and papain digestion were determined by manual Edman degradation (Blombäck et al., 1966) and phenylthiohydantoin derivatives of amino acids were identified by thin layer chromatography.

2.B.12. Amino acid analysis

The amino acid composition of V_L (Tod) fragment was determined with a Beckman amino acid analyzer, model 120B, according to the method of Spackman et al. (1958). The sample was hydrolyzed in an evacuated, sealed tube for 24 or 72 hours. Tryptophan was analyzed after hydrolysis with 6 N HCl containing 4 % thioglycolic acid (Matsubara & Sasaki, 1969).

Chapter 3

Role of intrachain disulfide bond in conformation and stability of C_L fragment

3.A. Introduction

The domains of immunoglobulin molecules share a common pattern of three-dimensional chain folding called immunoglobulin-fold (Figure 1.2) consisting of two antiparallel β-pleated sheets. The internal volume of the β-sheets is tightly packed with hydrophobic side chains and one intrachain disulfide bond, which connects the two-β sheets, is buried in the center of the molecule. At first sight, the disulfide bond is indispensable for the maintainance of the immunoglobulin-fold.

In the present Chapter, I describe the conformation and stability of the intact C_L fragment and the C_L fragment whose disulfide bond has been reduced. The result obtained showed that the intrachain disulfide bond is not essential for the immunoglobulin-fold of the C_L fragment.

There have been many studies as to the role of the disulfide bonds in the conformation of the proteins (Creighton, 1978; Torchinsky, 1981). A complete reduction of the intrachain disulfide bonds of Taka-amylase A (Takagi & Isemura, 1966), ribonuclease A (Takahashi et al., 1977), lysozyme (Bradshaw et al., 1967; White, 1976; Acharya & Taniuchi, 1976) induced the unfolding of the proteins. A few cases in which the reduction of the disulfide bond does not alter the native structure have been reported. The third disulfide bond of the bovine

pancreatic trypsin inhibitor (Vincent et al., 1971; Creighton, 1978) and the single disulfide bond of protease inhibitor I from potato tubes (Plunkett & Ryan, 1980) are such cases. The other examples have been summarized by Torchinsky (1981). These disulfide bonds are located on the surface of the molecule and reduction was carried out in the absence of denaturant. Although Straub (1967) reported several cases of the reduction of disulfide bonds without loss of activity, their reliability is obscure. Therefore, while the reduction of the disulfide bonds which locate at the surface of the molecule was often possible without destruction of the native structure, those disulfide bonds which locate in the interior of the molecule have been regarded to be essential for acquisition of their native structure. The disulfide bond of the C_L fragment is thus the first case of buried disulfide bond whose reduction does not alter the native structure. This finding is very important for the study of protein folding.

3.B. Results

3.B.1. Structure of intact C_L fragment

The amino terminal sequence of the C_L fragment obtained by tryptic digestion was determined to be

$$\overset{105}{\text{Leu}} - \text{Thr} - \text{Val} - \text{Leu} - \text{Ser} - \text{Gln} - \overset{111}{\text{Pro}} -^{\dagger},$$

which corresponds to the sequence of the switch region of type λ light chain. The amino terminal sequence of the C_L fragment obtained by papain digestion was determined to be

$$\overset{109}{\text{Ser}} - \text{Gln} - \overset{111}{\text{Pro}} -.$$

Thus the former fragment was four residues longer than the latter. While the amino acid sequence for the constant domain is very homologous for chains belong to the same types(κ or λ), alternatives called isotypes have been found at several positions. From the proton nuclear magnetic resonance study and the peptide analysis of the tryptic digests of the C_L fragment obtained by papain digestion, Shimizu et al. (1980) determined the isotypes of Bence Jones protein Nag to be Mcg (-), Kern (-), and Oz (+) (see also Arata & Shimizu, 1979). Thus the amino acid sequences of the C_L fragments obtained by tryptic and papain digestion were determined as Figure 3.1.

Table 3.I shows the amino acid composition of the C_L fragment obtained by papain digestion. Molecular weight determined from amino acid composition are 11,700 for C_L fragment obtained by tryptic digestion and 11,500 for C_L fragment by papain digestion. Mobilities

---

† Numbering of residues is in terms of the sequence of Bence Jones protein (New) (Chen & Poljak, 1974)

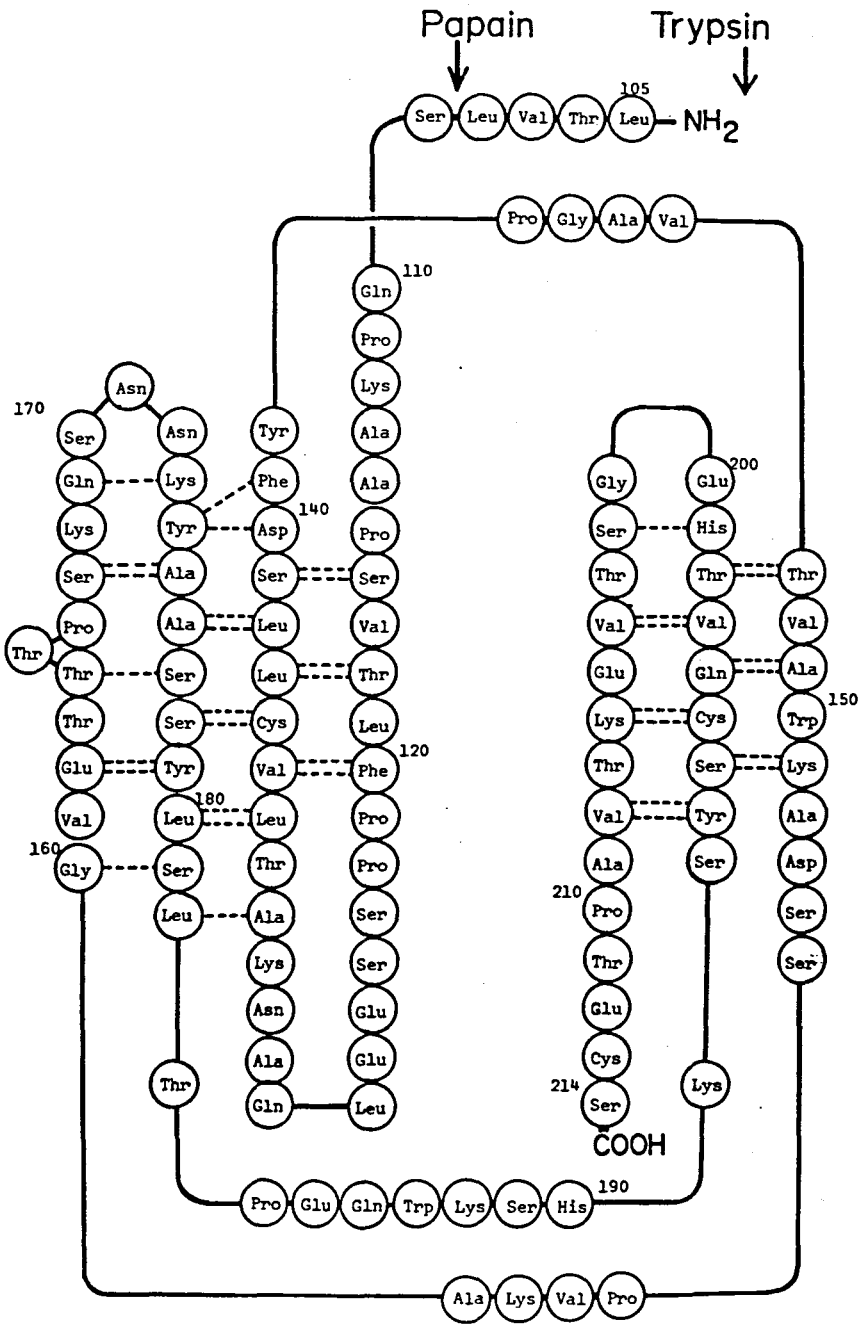

Fig. 3.1. Diagram of amino acid sequence and hydrogen bonding (broken line) between the main chain atoms of C_L fragment. The hydrogen bonded clusters correspond to the two β-sheet structures of the domain. Produced from the original diagram by Amzel and Poljak (1979).

TABLE 3.I. Amino acid composition of type λ C_L fragment obtained by papain digestion of Bence Jones protein Nag.

Amino acid	Residue per molecule
Lysine	8
Histidine	2
Arginine	1
Aspartic acid	2
Asparagine	3
Threonine	11
Serine	17
Glutamic acid	7
Glutamine	5
Proline	9
Glycine	3
Alanine	11
Cystein	3
Valine	9
Isoleucine	1
Leucine	8
Tyrosine	4
Phenylalanine	2
Tryptophan	2
Total	106

in 15 % polyacrylamide gel electrophoresis in the presence of SDS and the elution positions on Sephadex G-75 gel filtration (see below) for the C_L fragments were consistent with these values of molecular weight. Isoelectric point for the C_L fragment was suggested to be about 8 from the mobilities in 7.5 % polyacrylamide gel electrophoresis at pH 9.5 and at pH 4.0 and from the amino acid composition, although I did not determine the exact value.

Although the C_L fragment obtained by papain digestion was four residues shorter than the C_L fragment obtained by tryptic digestion, there was no conformational difference between the two fragments as far as I examined (i.e., CD and Fluorescence spectra of intact and reduced fragments, and unfolding transitions of intact fragments by GuHCl). Because a yield of the C_L fragment by papain digestion was several times higher than that by tryptic digestion, the following studies were carried out mainly by use of the C_L fragment obtained by papain digestion. The C_L fragment described below represents the fragment obtained by papain digestion.

The CD spectrum of C_L fragment is shown in Figure 3.2. It is very similar to that of C_L fragment reported by other authors (Ghose, 1972, Karlsson et al., 1972b). In the region of 250 to 200 nm, the CD spectrum had a negative maximum at 218 nm, which is characteristic of β- sheet conformation. The mean residue ellipticity at the maximum is about - 7,000 degrees cm^2 decimole. When denatured with 4 M GuHCl, the negative meximum at 218 nm disappeared and the CD spectrum in the region of 320 to 200 nm showed the absence of any ordered structure.

The fluorescence spectra of C_L fragment in the absence and

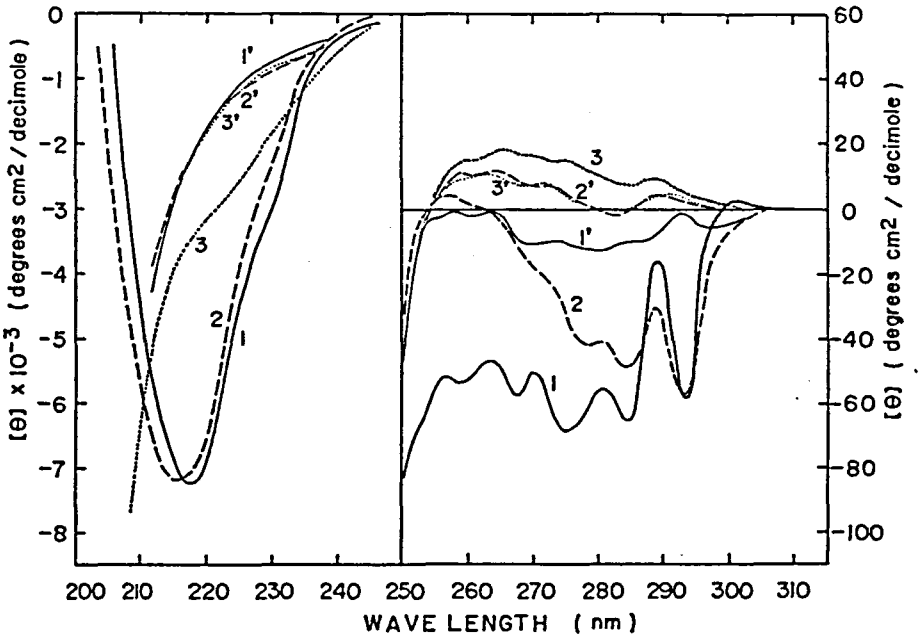

Fig. 3.2. CD spectra of intact C_L (solid lines), reduced C_L (broken lines), and CAM-C_L (dotted lines) fragments at 25°C. 1, 2, and 3 indicate the spectra in 0.05 M Tris-HCl buffer at pH 7.5 containing 0.15 M KCl and 1', 2', and 3' indicate the spectra in the buffer at pH 7.5 containing 4 M GuHCl.

presence of GuHCl are shown in Figure 3.3. It is known that the fluorescence spectrum of a tryptophyl residue in full contact with water shows a maximum at around 350 nm (Teale, 1960). The sepctrum in the presence of 4 M GuHCl had a maximum at 350 nm and showed that two tryptophyl residues of C_L fragment are completely exposed to the solvent. For the native C_L fragment, however, the maximum wavelength was 325 nm and the fluorescence intensity was 35 % relative to the intensity of the denatured C_L fragment with 4 M GuHCl. It is well known that with an increase of the hydrophobicity of the environment of the tryptophyl residue, the maximum of the fluorescence spectrum shifts to shorter wavelength with accompanying increase in fluorescence intensity. Thus this showed that the tryptophyl residues of C_L fragment are buried in the interior hydrophobic region of the molecule and the fluorescence is greatly quenched.

The difference spectrum of the C_L fragment in 4 M GuHCl referred to the protein in the absence of GuHCl is shown in Figure 3.4. The spectrum had minima at 286 and 292 nm. The value of $\Delta\varepsilon$ at 292 nm for the C_L fragment was - 1,700 M^{-1} cm^{-1}, which corresponds to the change in the molar extinction coefficient accompanying exposure of one tryptophyl residue from the interior of the protein molecule to the aqueous environment.

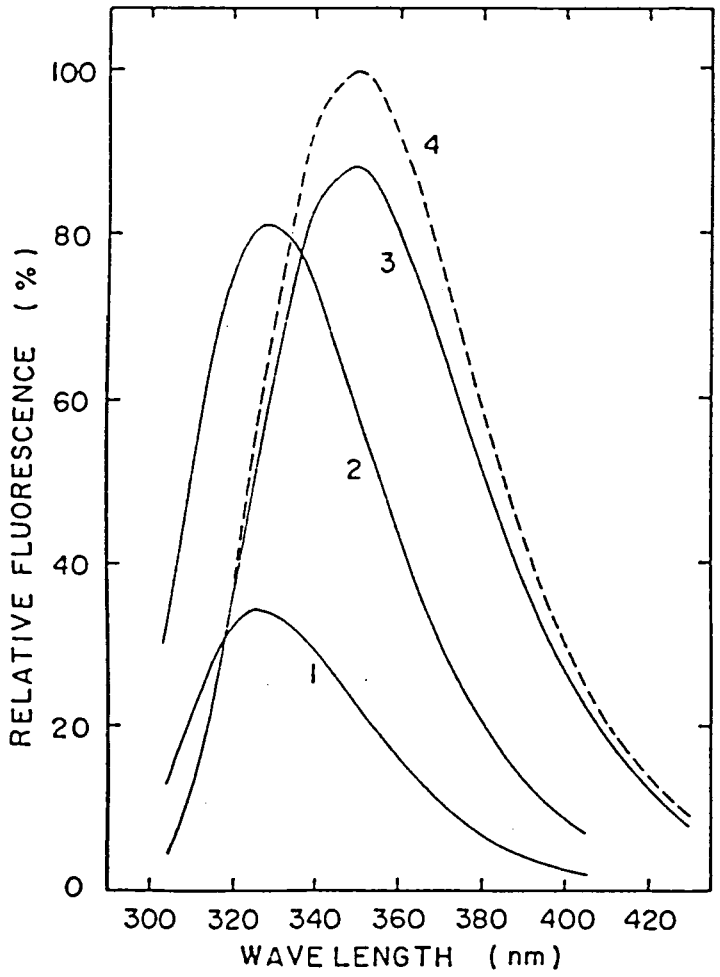

Fig. 3.3. Fluorescence spectra of intact C_L fragment (1), reduced C_L fragment (2), and CM-C_L fragment (3) in Tris-HCl buffer at pH 7.5 and at 25°C, and the denatured proteins (4) in 4 M GuHCl at pH 7.5 and at 25°C. The ordinate represents the fluorescence relative to that in the presence of 4 M GuHCl. Excitation was at 295 nm.

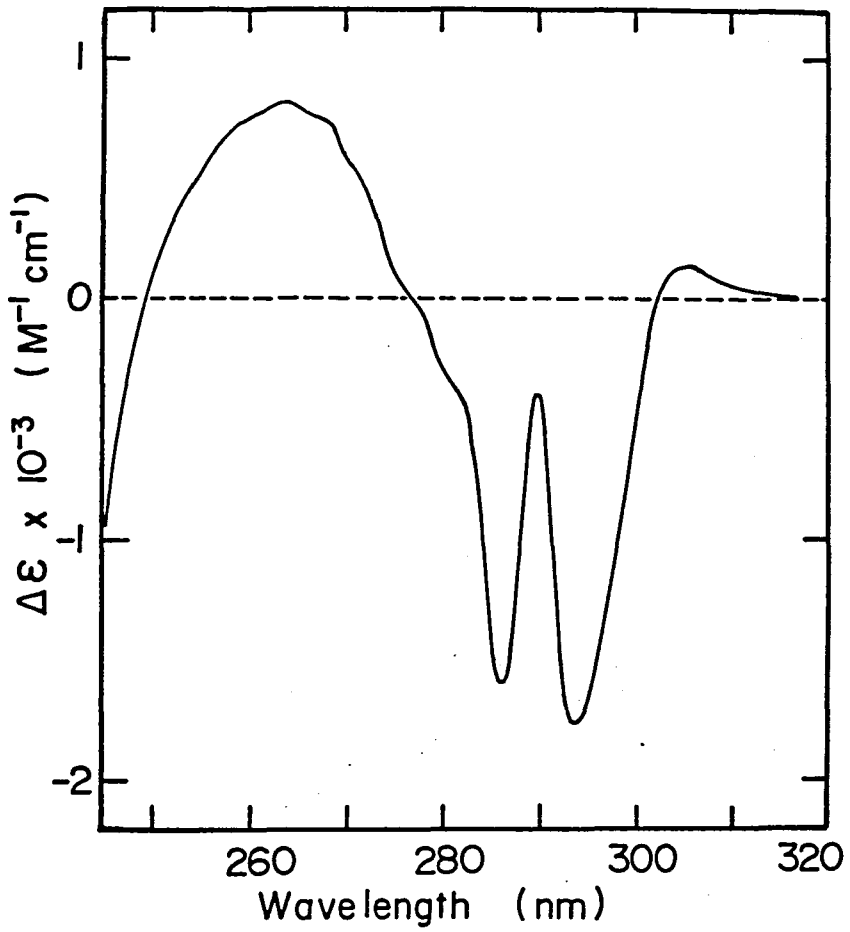

Fig. 3.4. Difference absorption spectrum of C_L fragment in 4 M GuHCl referred to the protein in Tris-HCl buffer at pH 7.5. 25°C.

3.B.2. Structure of reduced C_L fragment

Figure 3.2 shows the CD spectra of reduced C_L fragment and CAM-C_L fragment in the absence and presence of GuHCl. In the region of 250 to 200 nm, the CD spectrum of reduced C_L fragment in Tris-HCl at pH 7.5 had a negative maximum at 216 nm, which is very similar to the spectrum of intact C_L fragment. This indicates that the β-sheet conformation of reduced C_L fragment is similar to that of intact C_L fragment. However, reduction and alkylation of the intrachain disulfide bond caused a drastic change in the CD spectrum. The negative maximum at 218 nm completely disappeared and a shoulder was seen at 230 nm in the CD spectrum of CAM-C_L fragment. This spectrum was also different from the spectrum of denatured protein in 4 M GuHCl. The CD spectra in the region of 250 to 200 nm of the proteins in 4 M GuHCl were all the same. In the region of 300 to 250 nm, the CD spectra of intact C_L fragment, reduced C_L fragment, and CAM-C_L fragment in the absence of GuHCl were different from one another. In the presence of 4 M GuHCl, the spectrum of reduced C_L fragment was the same as that of CAM-C_L fragment but differed from that of intact C_L fragment. These results will be discussed later (3.C.1). The spectrum of CM-C_L fragment was the same as that of CAM-C_L fragment in the absence and presence of 4 M GuHCl, over the wavelengths studied.

The fluorescence spectra of reduced C_L fragment and CM-C_L fragment in Tris-HCl buffer at pH 7.5 are shown in Figure 3.3 with that of the protein in 4 M GuHCl. The spectra of these proteins in 4 M GuHCl were all the same and had a maximum at 350 nm. The fluorescence

spectrum of reduced C_L fragment had a maximum at 328 nm, which is close to the maximum emission wavelength for intact C_L fragment, but the intensity was much greater than that for intact C_L fragment (80 % relative to the intensity of the denatured protein). The fluorescence spectrum of CM-C_L fragment had a maximum at 350 nm, which is the same as the maximum wavelength for the denatured protein, and the intensity was about 90 % relative to the intensity for the denatured protein. The fluorescence spectrum of CAM-C_L fragment was very similar to that of CM-C_L fragment.

The states of tryptophyl residues in reduced C_L fragment and reduced and alkylated C_L fragment were studied by means of difference absorption spectroscopy. Since it is difficult to prepare solutions of intact C_L fragment, reduced C_L fragment, and reduced and alkylated C_L fragment at exactly the same concentration, I did not measure directly the difference spectrum of reduced C_L or reduced and alkylated C_L fragment vs. intact C_L fragment. Instead, I determined these difference spectra on the basis of the difference spectrum of each of these proteins in 4 M GuHCl against the protein in Tris-HCl buffer at pH 7.5. Assuming that the absorption spectra of these proteins in 4 M GuHCl are all the same, I obtained the difference spectrum of reduced C_L (or reduced and alkylated C_L) fragment against intact C_L fragment in the buffer by subtracting the difference spectrum of reduced C_L (or reduced and alkylated C_L) fragment in 4 M GuHCl against the protein in the buffer from the difference spectrum of intact C_L fragment in 4 M GuHCl against the protein in the buffer. The results are given in Figure 3.5.

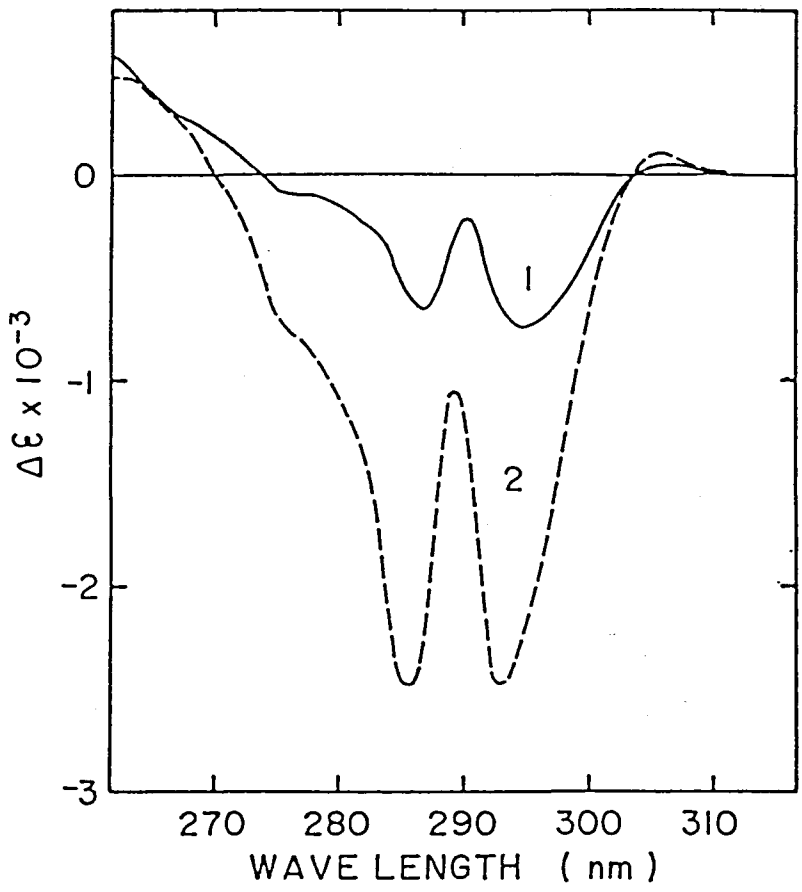

Fig. 3.5. Difference absorption spectra of reduced C_L fragment vs. intact C_L fragment (1) and CM-C_L fragment vs. intact C_L fragment (2). pH 7.5, 25°C (see the text for details).

The difference spectrum of CM-C_L fragment vs. intact C_L fragment had negative peaks at 285 and 293 nm and a small positive peak at 305 nm. The value of $\Delta\varepsilon$ at 293 nm was about -2,500 M^{-1} cm^{-1}. The differnece spectrum of reduced C_L fragment vs. intact C_L fragment also had negative peaks at 287 and 295 nm and a small positive peak at 305 nm, but the value of $\Delta\varepsilon$ at 295 nm, - 750 M^{-1} cm^{-1}, was considerably smaller than the value at 293 nm in the difference spectrum of CM-C_L fragment vs. intact C_L fragment.

I studied the reactivities of the SH groups of reduced C_L fragment toward DTNB in the absence and presence of GuHCl. The time course of SH titration with DTNB was followed at 412 nm at pH 7.5 and 25°C (Figure 3.6). In the presence of 4 M GuHCl, the SH groups of reduced C_L fragment reacted with DTNB within the dead time (20 sec) of the measurement and about two SH groups per mol of reduced C_L fragment were titrated. In the absence of GuHCl, on the other hand, the SH groups of reduced C_L fragment first reacted rapidly and then slowly with DTNB. The slow phase followed first-order kinetics with a rate constnat of 1.0×10^{-3} s^{-1} (Figure 3.6, inset). The absorbance change in the slow phase corresponded to about 95 % of the total change.

Effect of reduction of the intrachain disulfide bond on a hydrodynamic volume of the C_L fragment was studied by a gel filtration on Sephadex G-75 column. Figure 3.7 shows the chromatography pattern of the intact C_L, reduced C_L, and CAM-C_L fragments. The apparent molecular weight was estimated from the molecular weight of the intact C_L fragment (11,500) and marker proteins (Figure 3.7(b)).

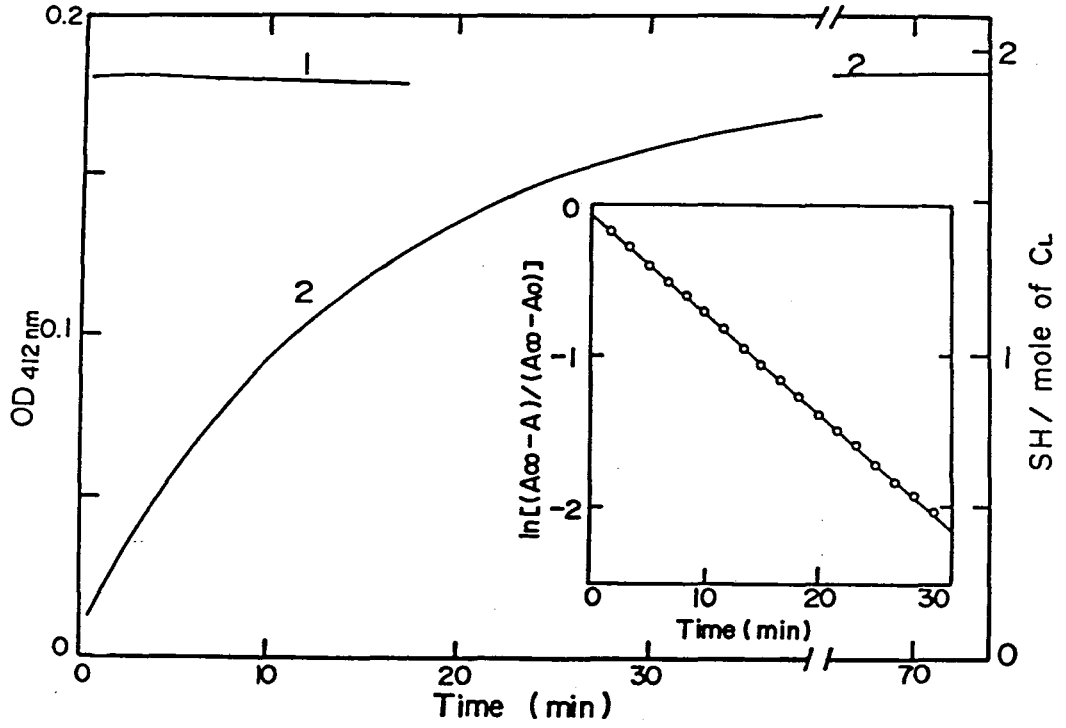

Fig. 3.6. Titration of the SH groups of reduced C_L fragment with DTNB in the presence (1) and absence of 4 M GuHCl (2). Absorbance change at 412 nm were measured at pH 7.5 and at 25°C. The inset shows the first-order plot of the absorbance change at 412 nm in the absence of GuHCl.

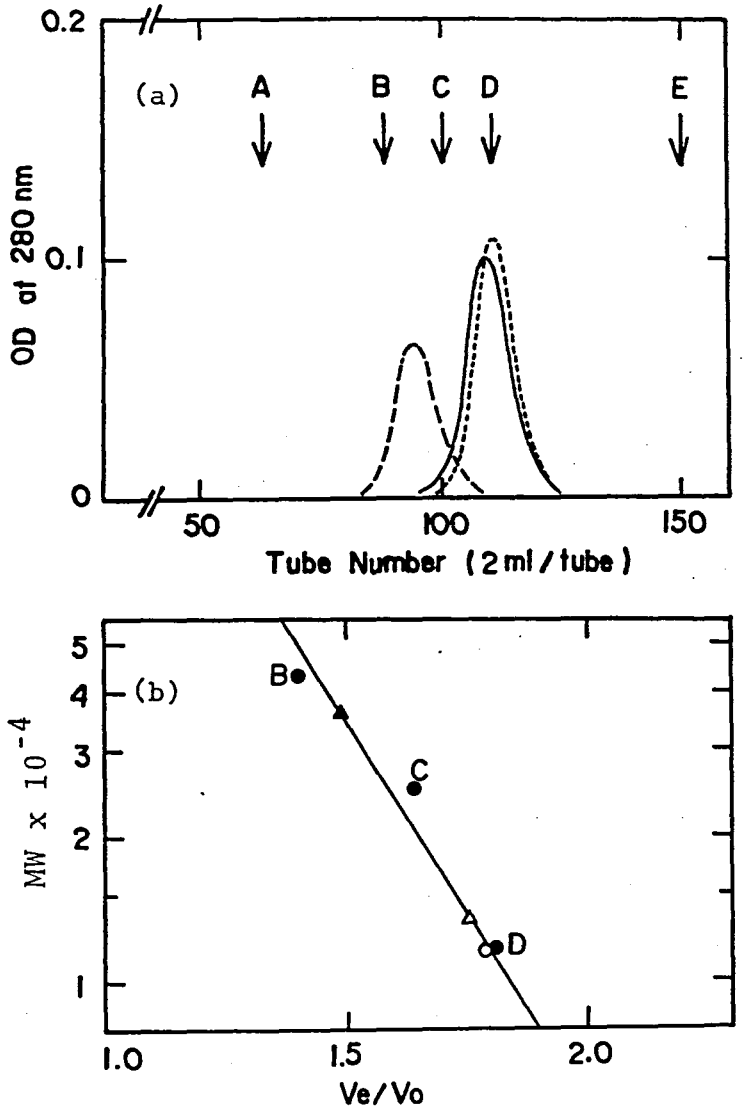

Fig. 3.7. Gel filtration patterns (a) of intact C_L fragment (dotted line), reduced C_L fragment (solid line), and CAM-C_L fragment on a Sephadex G-75 column (1.6 x 164 cm) equilibrated with 5 mM acetate buffer at pH 6.1 containing 1 mM EDTA and 0.15 M KCl, and estimation of apparent molecular weight (b) of intact C_L fragment (○), reduced C_L fragment (△), and CAM-C_L fragment (▲). One to two mg of the protein samples were applied to the column. Blue dextran (A), ovalbumin (B), α-chymotrypsinogen (C), cytochrome c (D), and dithiothreitol (E) were run on the same column as standards. Their absorbance peak positions are indicated by arrows. Abscissa in (b) indicates the ratio of elution volume (Ve) to void volume (Vo).

The estimated values were 13,500 for reduced C_L fragment and 35,000 for CAM-C_L fragment.

3.B.3. Stability of intact and reduced C_L fragments

The results described above suggest that reduced C_L fragment has a conformation very similar to intact C_L fragment. In order to clarify the difference in stability between intact C_L fragment and reduced C_L fragment, I studied the unfolding equilibrium of these proteins.

Figure 3.8 shows the unfolding transitions by GuHCl of intact and reduced C_L fragments measured by CD at 218 nm. A cooperative transition with an apparent midpoint of 1.2 M GuHCl was observed for intact C_L fragment. The stability of reduced C_L fragment was much lower than that of intact C_L fragment, but reduced C_L fragment was also denatured by GuHCl cooperatively with a midpoint of 0.4 M GuHCl. The change in the ellipticity at 218 nm above 2 M GuHCl was the same for both proteins.

Figures 3.9 and 3.10 show the fluorescence spectra of intact and reduced C_L fragments at various concentrations of GuHCl, respectively. Figures 3.11, 3.12, and 3.13 show the unfolding transitions measured at 350 nm for intact C_L fragment, at 350 nm for reduced C_L fragment, and at 400 nm for reduced C_L fragment, respectively. There exists an isoemissive point at 315 nm in the spectra of intact C_L fragment (Figure 3.9) and at 338 nm in the spectra of reduced C_L

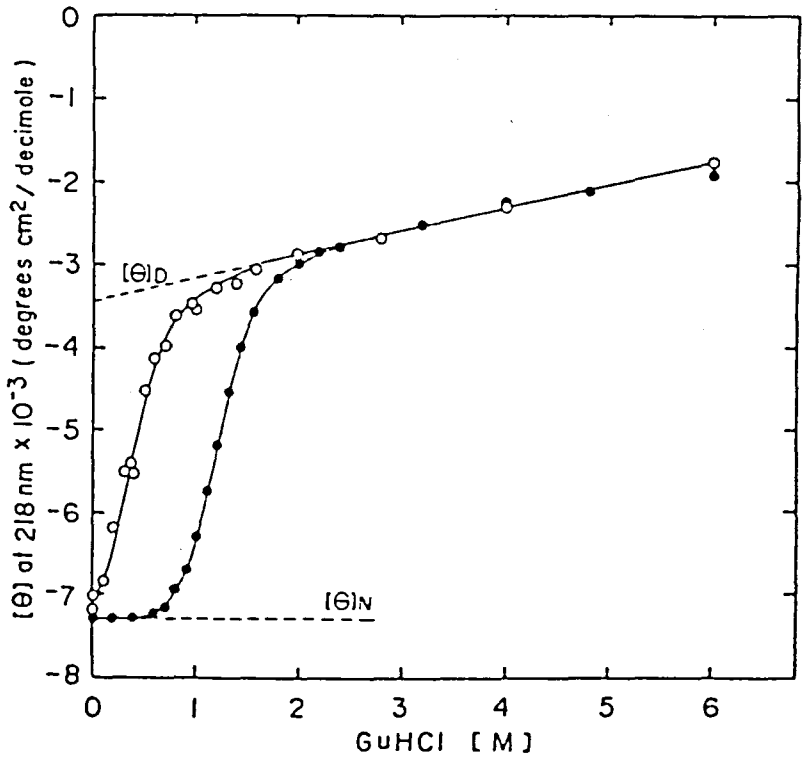

Fig. 3.8. Ellipticity at 218 nm of intact C_L fragment (●) and reduced C_L fragment (○) as a function of GuHCl concentration. pH 7.5, 25°C. Solid lines indicate theoretical curves constructed using Eqs. (3.1) and (3.2) and the values of Δn and $\Delta G_D^{H_2O}$ obtained on the basis of k = 0.6 (Table 3.II).

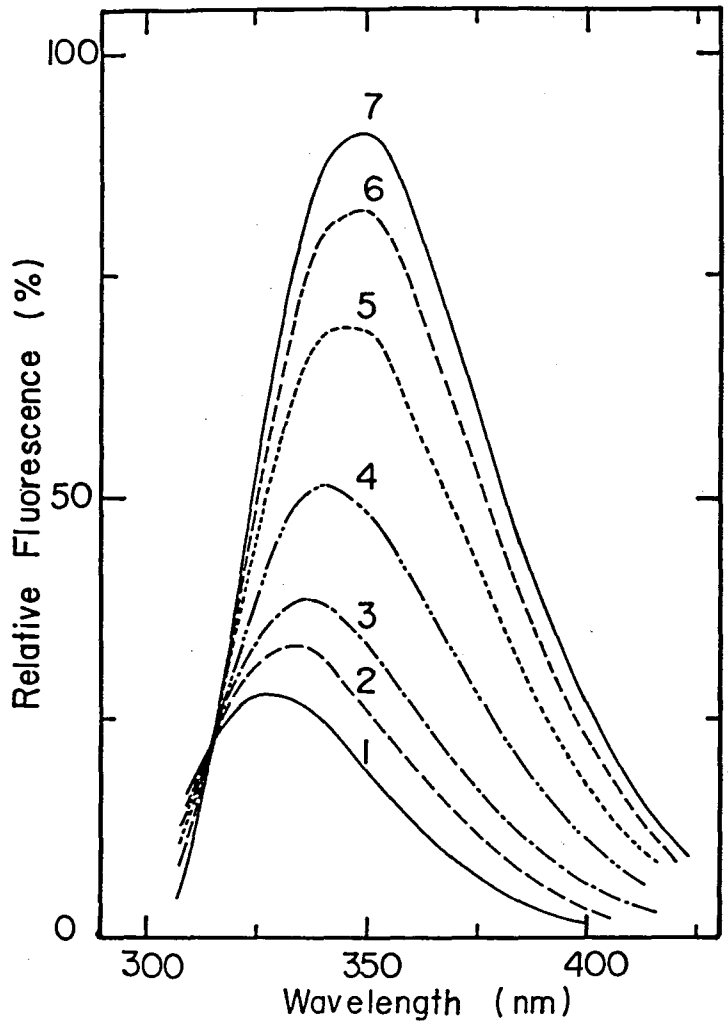

Fig. 3.9. Fluorescence spectra of intact C_L fragment at various GuHCl concentrations. pH 7.5, 25°C. Excitation wavelength, 295 nm; protein concentration, 0.04 mg/ml. 1, 0 M; 2, 0.7 M; 3, 0.9 M; 4, 1.1 M; 5, 1.32 M; 6, 1.56 M; 7, 2.0 M GuHCl.

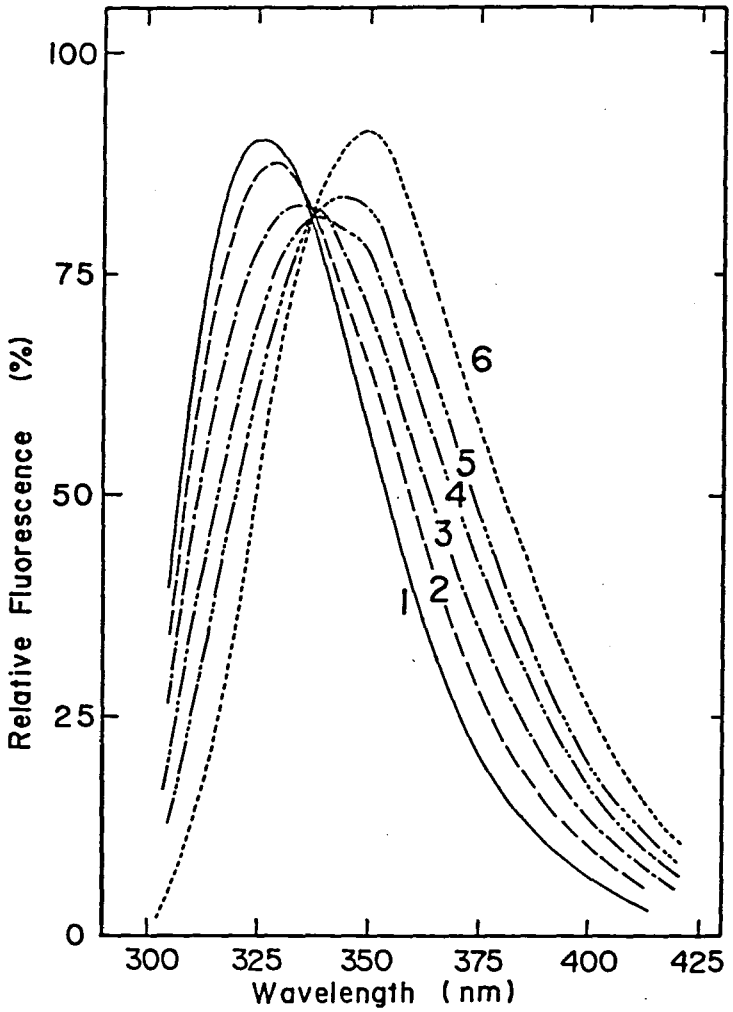

Fig. 3. 10. Fluorescence spectra of reduced C_L fragment at various GuHCl concentrations. pH 7.5, 25°C. Excitation wavelength, 295 nm; protein concentration, 0.04 mg/ml. 1, 0 M; 2, 0.2 M; 3, 0.3 M; 4, 0.4 M; 5, 0.5 M; 6, 1.2 M GuHCl.

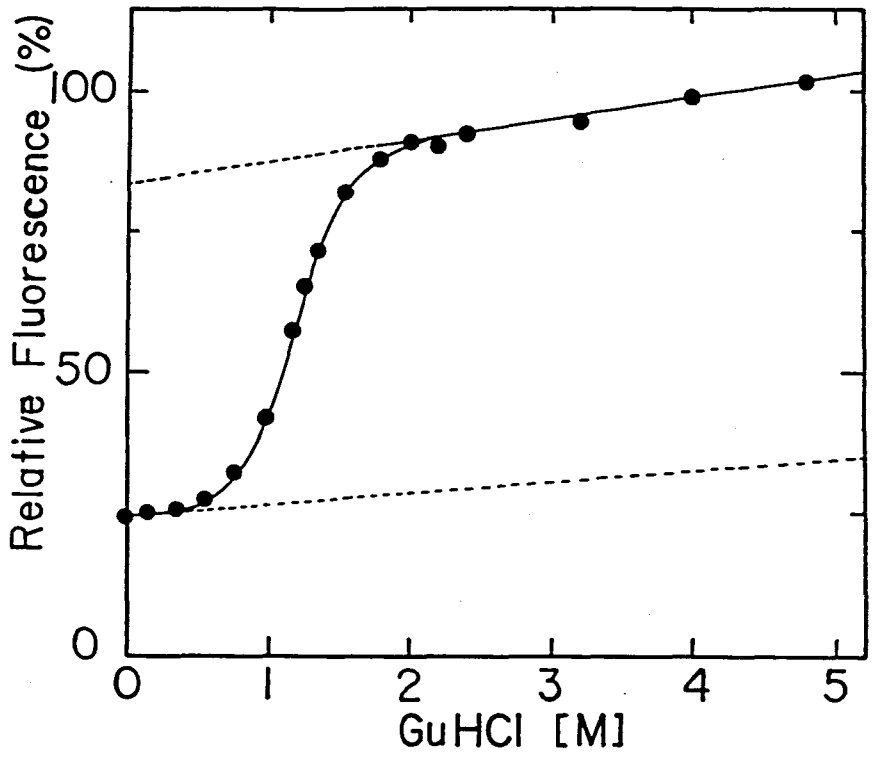

Fig. 3.11. Fluorescence at 350 nm of intact C_L fragment as a function of GuHCl concentration. pH 7.5, 25°C. Excitation wavelength, 295 nm; protein concentration, 0.04 mg/ml. Solid line indicates theoretical curve constructed using Eqs. (3.1) and (3.2) and the values of Δn and $\Delta G_D^{H_2O}$ obtained on the basis of k = 0.6 (Table 3.II).

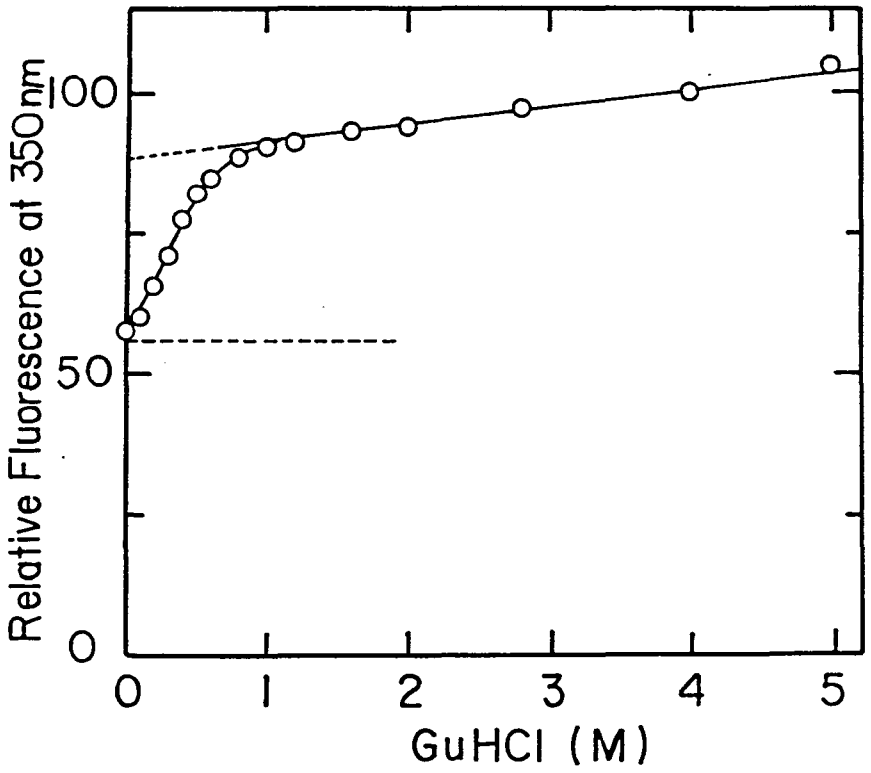

Fig. 3.12. Fluorescence at 350 nm of reduced C_L fragment as a function of GuHCl concentration. pH 7.5, 25°C. Excitation wavelength, 295 nm; protein concentration, 0.04 mg/ml. Solid line indicates theoretical curve constructed using Eqs. (3.1) and (3.2) and the values of Δn and $\Delta G_D^{H_2O}$ obtained on the basis of k = 0.6 (Table 3.II).

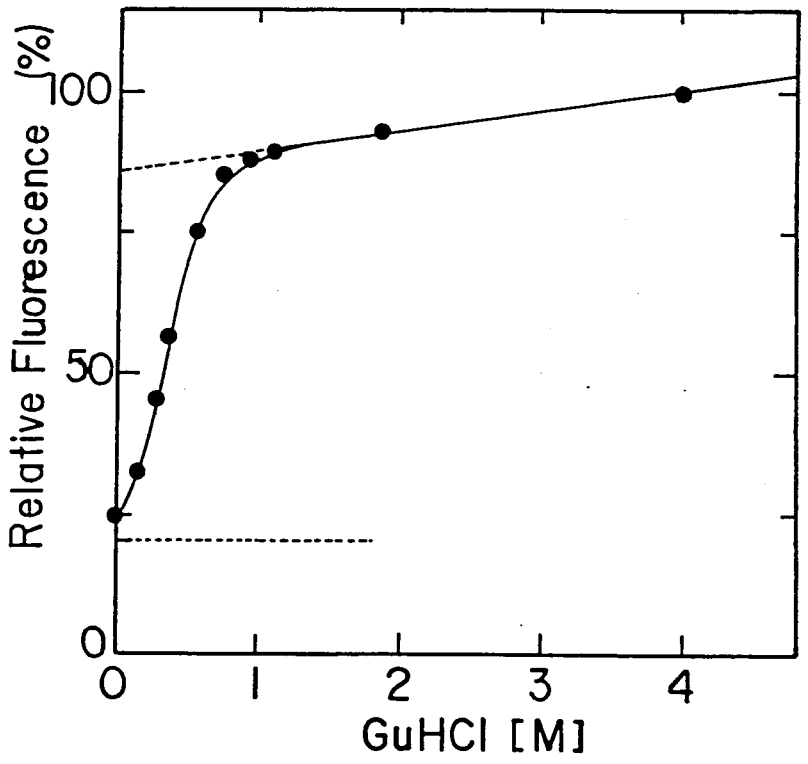

Fig. 3.13. Fluorescence at 400 nm of reduced C_L fragment as a function of GuHCl concentration. pH 7.5, 25°C. Excitation wavelength, 295 nm; protein concentration, 0.04 mg/ml. Solid line indicates theoretical curve constructed using Eqs. (3.1) and (3.2) and the values of Δn and $\Delta G_D^{H_2O}$ obtained on the basis of $k = 0.6$ (Table 3.II).

fragment (Figure 3.10). The transition curves for unfolding of intact and reduced C_L fragments were very similar to the respective curves observed by CD at 218 nm and had apparent midpoints of 1.2 M and 0.4 M GuHCl, respectively.

Figure 3.14 shows the unfolding transitions by urea of intact and reduced C_L fragments measured by CD at 218 nm. Although about two-fold high concentrations of denaturant was necessary to denature the proteins compared with the denaturation by GuHCl, the unfolding transitions were qualitatively similar to those by GuHCl. Both proteins showed a cooperative transition for unfolding and a midpoint of reduced C_L fragment (1 M urea) was much lower than that of the intact C_L fragment (3 M urea).

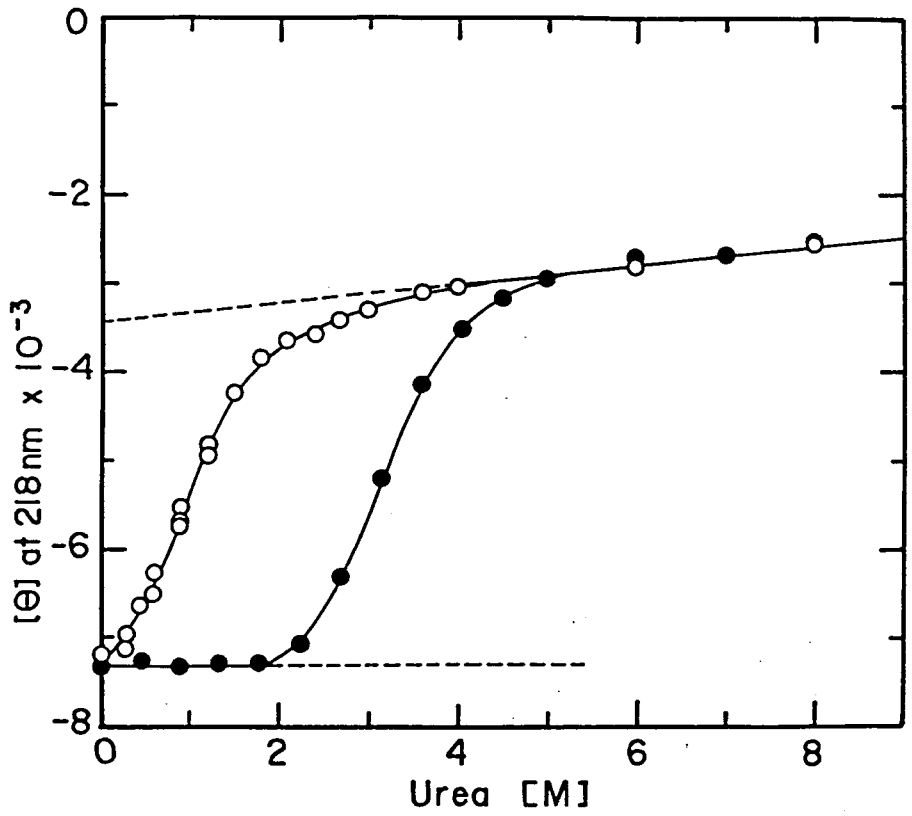

Fig. 3.14. Ellipticity at 218 nm of intact C_L fragment (●) and reduced C_L fragment (○) as a function of urea concentration. pH 7.5, 25°C. Protein concentration, 0.2 mg/ml.

3.C. Discussion

3.C.1. Conformation

I obtained the two C_L fragment by proteolytic digestion of Bence Jones protein Nag. Although the C_L fragment obtained by papain digestion was four residues shorter than the C_L fragment obtained by tryptic digestion, there was no difference in their conformational properties. The amino-terminal about five residues of the C_L fragment obtained by tryptic digestion are belong to a switch region of light chain (Davies et al., 1975; Beale & Feinstein, 1976; Amzel & Poljak, 1979). Thus the conformational and folding properties of the isolated C_L domain may be independent of the presence or absence of the amino-terminal extra residues.

As shown in Figure 3.2, the CD spectrum of reduced C_L fragment was very similar to that of intact C_L fragment in the region of 200 to 250 nm, indicating that the C_L fragment retains β-sheet conformation even though the intrachain disulfide bond is reduced. However, introduction of bulky groups such as carboxymethy or carboxamidomethyl group into the sulfhydryl groups destroys the β-sheet conformation of reduced C_L fragment, though it does not result in completely denatured conformation. This suggests that the tightly packed hydrophobic region between the two β-sheets plays an important role in the acquisition of the β-sheet conformation.

The C_L fragment contains two tryptophyl residues, and X-ray crystallographic studies show (Davies et al., 1975), that one of them is located close to the intrachain disulfide bond and the other is near or on the surface of the protein molecule. The tryptophyl

fluorescence maximum of reduced C_L fragment shifted only slightly to a longer wavelength, though the fluorescence intensity was much higher, compared with the fluorescence of the intact C_L fragment (Figure 3.3). It is known that the tryptophyl fluorescence of Bence Jones proteins are quenched to a great extent (Pollet et al., 1972; Longworth et al., 1976, see also Chapter 6). Since disulfides are known to quench tryptophyl fluorescence (Cowgill, 1967), enhancement of the fluorescence intensity with an accompanying slight shift of the maximum wavelength indicates that only the quenching effect is removed with no accompanying great conformational change, on reduction of the intrachain disulfide bond. On the other hand, the fluorescence spectra of CM-C_L fragment and CAM-C_L fragment had a maximum at 350 nm, which is the same as the maximum wavelength for the denatured proteins. This indicates that the conformation of intact C_L fragment is greatly changed on reduction and alkylation, and the tryptophyl resiudes in CM-C_L and CAM-C_L fragments are completely exposed to the aqueous environment. The finding that the fluorescence intensity of CM-C_L or CAM-C_L fragment is about 10 % less than the fluorescence of the proteins in 4 M GuHCl may be explained in terms of the solvent perturbation effect of GuHCl on the fluorescence.

The difference absorption spectrum of reduced C_L vs. intact C_L fragment (Figure 3.5) suggests that tryptophyl residues are perturbed on reduction of the intrachain disulfide bond of the C_L fragment. However, the value of $\Delta\varepsilon$ at 295 nm, - 750 M^{-1} cm^{-1}, is considerably smaller than the value of $\Delta\varepsilon$ at 293 nm, - 2,500 M^{-1} cm^{-1}, in the difference spectrum of CM-C_L against intact C_L fragment. The latter

figure is close to the value expected for transfer of one tryptophyl resiude from the interior of the protein molecule to aqueous environment (Hamaguchi & Kurono, 1963). These findings show that the tryptophyl residues in CM-C_L fragment are completely exposed to solvent but those in reduced C_L fragment are only slightly perturbed.

The gel filtrations on Sephadex G-75 of the reduced C_L fragment and the reduced and alkylated C_L fragment showed that the hydrodynamic volume of reduced C_L fragment is similar to that of intact C_L fragment and that the volume of reduced and alkylated C_L fragment is about three-fold of that of intact C_L fragment. These results confirmed the above indication obtained by spectrophotometric measurements, i.e., while the reduction of the intrachain disulfide bond does not alter the conformation of intact C_L fragment in water, the reduction and alkylation of the disulfide bond largely unfold the native conformation.

The SH groups of reduced C_L fragment are far less reactive in the absence of GuHCl than in its presence. This is expected from the native-like conformation of reduced C_L fragment, where the two SH groups are buried in the interior of the molecule. The very slow rate of titration in the presence of high concentration of DTNB suggests that the intramolecular process of the reduced C_L fragment (unfolding process) is rate-limiting and not the reaction of the exposed SH groups with DTNB. The SH titration will be described in detail in Chapter 5.

If no great conformational change occurs on reduction of the intrachain disulfide bond of the C_L fragment, the CD spectrum of the disulfide bond may be obtained by comparing the CD spectrum of intact C_L fragment with that of reduced C_L fragment. Figure 3.15 shows the difference spectra obtained by subtracting the spectrum of reduced C_L fragment from that of intact C_L fragment in the absence and presence of 4 M GuHCl.

The difference spectrum in the presence of GuHCl has a negative maximum at around 270 nm. It is known from studies on model compounds (Takagi & Ito, 1972; Takagi et al., 1973) and proteins (Takagi & Izutsu, 1974; Yoshida et al., 1976) that the CD spectra of disulfide bonds usually have a negative maximum at around 260 nm. Thus, the CD band at 270 nm is due to the optical activity of the intrachain disulfide bond in the denatured C_L fragment. The value of residue molar ellipticity, - 18 degrees cm^2 $dmol^{-1}$, at 270 nm represents the molar ellipticity of a disulfide of - 1,910 degrees cm^2 $dmol^{-1}$. This figure can be compared with the molar ellipticity at 260 nm of a disulfide in denatured ribonuclease A in 6 M GuHCl (- 1,700 degrees cm^2 $dmol^{-1}$ at 20°C) (Takagi & Izutsu, 1974) and with the molar ellipticity at 265 nm of N,N'-diacetyl-L-cystine bismethylamide (about - 1,300 degrees cm^2 $dmol^{-1}$ at 20°C) (Takagi & Izutsu, 1974). In the absence of GuHCl, the difference CD spectrum has positive maxima at 290 and 297 nm in addition to a negative maximum at 254 nm. The CD maxima at 290 and 297 nm may be due to a change in the state of tryptophyl residue, located near the intrachain disulfide bond (Davies et al., 1975), caused by reduction of the disulfide bond. The negative

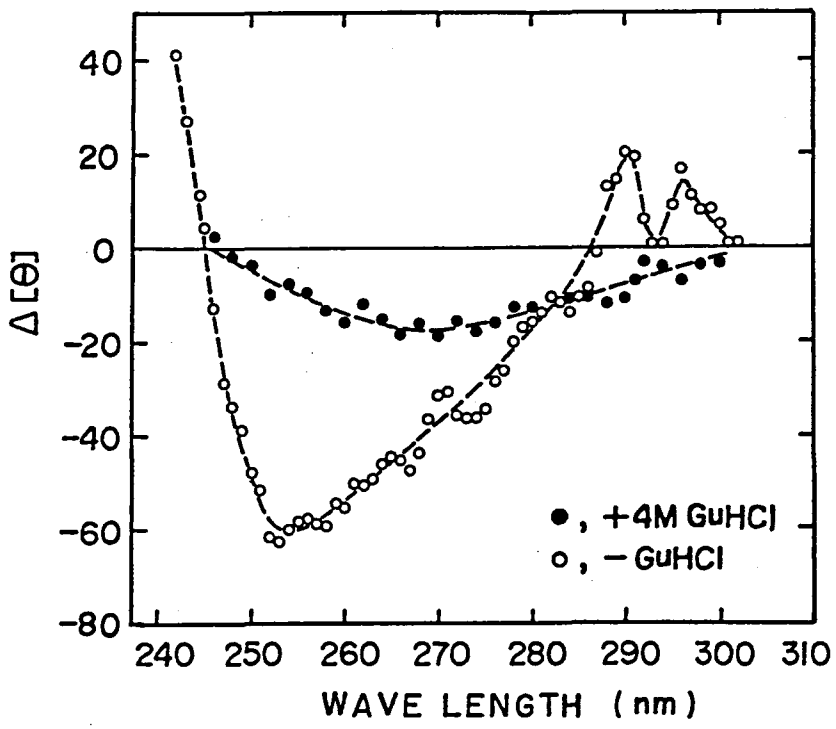

Fig. 3.15. Difference CD spectra obtained by subtracting the spectrum of reduced C_L fragment from the spectrum of intact C_L fragment (see Fig. 3.2). ○, in the absence of GuHCl; ●, in the presence of 4 M GuHCl.

maxima at 254 nm may be due largely to the optical activity of the intrachain disulfide bond of intact C_L fragment, although there may be some contribution from aromatic amino acid residues to this CD band. The residue molar ellipticity at 254 nm, - 60 degrees cm^2 $dmol^{-1}$, means the molar ellipticity of a disulfide of - 6,360 degrees cm^2 $dmol^{-1}$, which is considerably larger than the corresponding value for intact C_L fragment in 4 M GuHCl. There are two conformers of a cystine residue that have different optical activities (Takagi & Ito, 1972; Takagi et al., 1973). The intrachain disulfide bond of the C_L fragment is fixed at one of the two conformers. X-ray crystallographic analysis of the Fab fragment of human immunoglobulin New (Poljak et al., 1973) showed the torsion angles of the C—C↘S↘S↘C—C linkage of the intrachain disulfide of the C_L domain to be - 173°, - 95°, and - 169°, respectively. In the presence of 4 M GuHCl, however, the disulfide exists as a mixture of two conformers. This may explain the larger ellipticity in the absence of GuHCl than in its presence.

All the findings described above show that the conformation of the C_L fragment does not change greatly on reduction of the intrachain disulfide bond but greatly changes on reduction and alkylation.

3.C.2. Stability

Although reduced C_L fragment is less resistant than intact C_L fragment to GuHCl or urea, a sharp cooperative transition is also observed for reduced C_L fragment (Figures 3.8, 3.12, 3.13, and 3.14). Previously, Isenman et al. (1975) used β_2-microglobulin as a model of an isolated immunoglobulin domain and compared the conformation of the intact protein with that of reduced protein in the presence of 1 M GuHCl. They concluded that the intrachain disulfide bond of β_2-microglobulin is essential in the acquisition of the native conformation and this may be applicable to the other domains of immunoglobulin molecule. As can be seen from Figures, however, in the presence of 1 M GuHCl, reduced C_L fragment is denatured almost completely, while intact C_L fragment is not. Thus only after a structure of reduced protein far below the transition zone for intact protein is examined, the definite conclusion may be made.

I analysed the transition curves measured by CD at 218 nm (Figure 3.8) using a two-state approximation for the denaturation of intact C_L and reduced C_L fragments, and determined the free energy change, ΔG_D, for the reaction N(native) $\longleftrightarrow$ D(denatured) at a given GuHCl concentration in the transition region using the equation,

$$\Delta G_D = - RT \cdot \ln \frac{\Theta_N - \Theta}{\Theta - \Theta_D} \qquad (3.1)$$

where Θ is the observed ellipticity at 218 nm, and Θ_N and Θ_D are the ellipticities of the native and denatured states. The Θ_N value for reduced C_L fragment was assumed to be the same as that for intact C_L fragment.

I then estimated the free energy change, $\Delta G_D^{H_2O}$, for the reaction $N \leftrightarrow D$ in the absence of GuHCl using the following equation proposed by Tanford (1970),

$$\Delta G_D = \Delta G_D^{H_2O} - \Delta nRT \cdot \ln(1 + ka_{\pm}) , \qquad (3.2)$$

where Δn is the difference in the number of binding sites between the denatured and native states, k is the average binding constants of these sites, and $a_{\pm}$ is the mean ion activity of GuHCl. The value of $a_{\pm}$ were calculated using the equation described by Pace and Vanderburg (1979):

$$a_{\pm} = 0.6761[M] - 0.1468[M]^2 + 0.02475[M]^3 + 0.001318[M]^4, \qquad (3.3)$$

where [M] is the molar concentration of GuHCl.

A value of k = 1.2 was widely used in tha analysis of the denaturation of proteins by GuHCl (Pace, 1975), but Pace and Vanderburg (1979) have recently shown that 0.6 should be used as the value of k. I analyzed the denaturation curves of intact C_L and reduced C_L fragments using both values of k. Use of either of the values gave a good straight line for the plot of ΔG_D against $\ln(1 + ka_{\pm})$, and the vlaues of $\Delta G_D^{H_2O}$ and Δn obtained are given in Table 3.II.

The $\Delta G_D^{H_2O}$ value for intact C_L fragment, about 6 kcal mol^{-1}, is in agreement with the value, 5.5 kcal mol^{-1}, estimated by Rowe and Tanford (1973) for the each domain of a Bence Jones protein. The smaller $\Delta G_D^{H_2O}$ value for reduced C_L fragment, about 1.8 kcal mol^{-1} compared with the value for intact C_L fragment indicates that reduced C_L fragment in water is considerably less stable than itact C_L fragment.

TABLE 3.II. Values of $\Delta G_D^{H_2O}$ and Δn of intact C_L fragment and reduced C_L fragment. pH 7.5, 25°C.

Protein	k = 0.6		k = 1.2	
	$\Delta G_D^{H_2O}$ (kcal·mol^{-1})	Δn	$\Delta G_D^{H_2O}$ (kcal·mol^{-1})	Δn
Intact C_L fragment	5.5	29.5	6.3	18.6
Reduced C_L fragment	1.7	20.3	1.9	13.1

The transition curves for unfolding in Figures 3.8, 3.11, 3.12, and 3.13 were constructed using equations (3.1) and (3.2), the values of Δn and $\Delta G_D^{H_2O}$ obtained on the basis of k = 0.6 (Table 3.II), and the appropriate values of N and D states. Agreement of the observed transition curves measured by fluorescence with the theoretical curves (Figures 3.8, 3.11, 3.12, and 3.13) confirmed the establishment of the two-state approximation.

Johnson et al. (1978) studied the thermal transition of intact lysozyme and cross-linked oxindolalanine lysozyme and showed that the difference in the stability between these proteins can be explained in terms of the decreased entropy of denatured protein following introduction of the cross-link. Their procedure can also be applied to our case. For the following cycle in water,

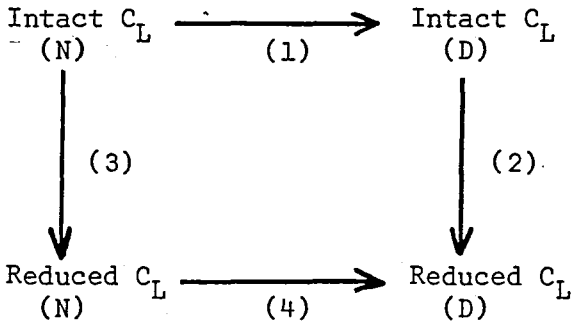

(Mechanism 3.1)

the following relation holds,

$$\Delta G_1 + \Delta G_2 = \Delta G_3 + \Delta G_4 , \qquad (3.3)$$

where

$$\Delta G_1 = \Delta H_1 - T\Delta S_1$$

$$\Delta G_2 = \Delta H_2 - T\Delta S_2$$

$$\Delta G_3 = \Delta H_3 - T\Delta S_3$$

and

$$\Delta G_4 = \Delta H_4 - T\Delta S_4$$

ΔG_1 and ΔG_4 were determined as 5.7 and 1.7 kcal mol^{-1}, respectively, on the basis of k = 0.6 (Table 3.II)

Provided that no conformational change occurs on reduction of the intrachain disulfide bond and that there is no strain in the disulfide bond (Johnson et al., 1978; Lapanje & Rupley, 1979), ΔS_3 equals zero and ΔH_3 and ΔH_2 are the same. Therefore, the difference in the value of $\Delta G_D^{H_2O}$ between processes (1) and (4) may be written as

$$\Delta G_1 - \Delta G_4 = \Delta G_3 - \Delta G_2$$
$$= \Delta H_3 - \Delta H_2 - T\Delta S_3 + T\Delta S_2 = T\Delta S_2 \ , \qquad (3.4)$$

and the decreased stability of reduced C_L fragment compared with intact C_L fragment may be explained in terms of the increased entropy of the C_L fragment following reduction of the intrachain disulfide bond in the denatured state. On the basis of the theory of Flory (Flory, 1956; Poland & Scheraga, 1965), the entropy change associated with formation of a cross-linked loop is calculated as

$$\Delta S = 1.5 \times R[\ \ln(N/2) + 3\ ] \qquad (3.5)$$

where N is the number of residues in the loop. The cross-linked loop of the C_L fragment consists of 60 residues and the entropy change is estimated to be - 19 e.u., which contributes to the free energy by - 5.7 kcal mol^{-1}. This value is comparable with, though slightly larger than, the value of $(\Delta G_1 - \Delta G_4)$ (4 kcal mol^{-1}). I may therefore conclude that although there may be small change in entropy in process (3), the lesser stability of reduced C_L fragment is due mostly to the entropy of reduced C_L fragment being larger than that of intact C_L fragment in the denatured state. The role of the disulfide bond from a kinetic viewpoint will be described in detail in Chapter 5.C.2.

Chapter 4

Folding mechanism of intact C_L fragment

4.A. Introduction

As described in Chapter 1, unfolding and refolding transitions of proteins are highly cooperative and a two-state approximation is generally valid for equilibrium measurements. On the other hand, the kinetic measurements for several proteins (Baldwin, 1975) revealed distinct deviations from a two-state transition and suggested transient accumulation of a folding intermediate (I) as,

$$U \rightleftarrows I \rightleftarrows N.$$

These observations provided hope to protein chemists that characterization of the intermediate is possible in the near future.

Refolding of ribonuclease A also showed a complex kinetics, in which fast (20% of total) and slow (80% of total) phases were observed (Tsong et al., 1972; Garel & Baldwin, 1973). From the detailed studies of unfolding and refolding of ribonuclease A, however, Baldwin and his co-workers (Garel & Baldwin, 1975; Garel et al., 1976; Hagerman & Baldwin, 1976) proposed the three-species mechanism:

$$U_1 \rightleftarrows U_2 \rightleftarrows N,$$

where U_1 and U_2 are two forms of the unfolded species and N is the native protein. They showed that interconversion between U_1 and U_2 is slow compared with the direct folding transition of U_2 to N, so that, while U_2 refolds fast, U_1 refolds slowly after the slow conversion of U_1 to U_2. In this mechanism, the two-state transition is valid because there is no structural intermediate, and the deviation

in kinetic measurement from the two-state behavior is merely due to the presence of two forms of the unfolded molecule.

At the same time, Brandts et al (1975) proposed the same mechanism from the study of the same protein. They further explained the existence of the two forms of unfolded molecule by a cis-trans isomerization of X-Pro peptide bond:

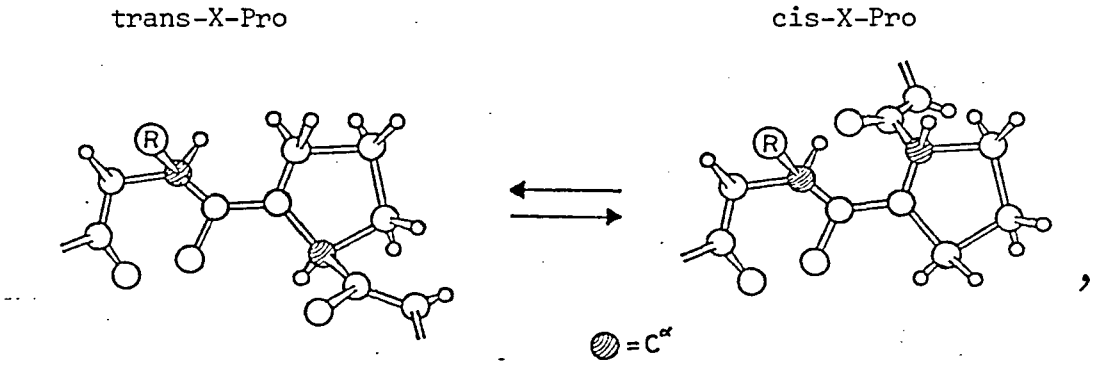

where X being any preceding amino acid residue. Whereas the peptide bonds formed by residues other than proline greatly favor the trans form, that of proline takes cis form easily and its interconversion is very slow due to the high energy of nonplanar form. The proportion of trans form of prolyl peptide bond is 0.7 to 0.9. Brandts et al. (1975) suggested that, while the peptide bonds are locked in either cis or trans in native molecule, they isomerize to different form in unfolded molecule and those molecules that have different cis-trans form of prolyl peptide bonds produce the slow-refolding species (U_1). They also suggested that all of the experimental data which had been reported for other proteins are also explained simply by the three-species mechanism and proline isomerism. Provided that

this is the case, the attempt to elucidate the pathway of protein folding from the usual kinetic study is very difficult. Therefore, whether the three-species mechanism due to the proline isomerism is general for unfolding and refolding of proteins containing prolyl resiudes or not is a critical problem for the study of protein folding.

I studied the kinetics of the reversible denaturation of the intact C_L fragment by GuHCl in detail. Then, I found that the three-species mechanism due to the proline isomerism is valid fundamentally for the C_L fragment. However, it was also found that the incorrect proline residues are not a critical factor for folding of the C_L fragment in the condition where the native protein is stable.

4.B. Results

4.B.1. Unfolding kinetics of intact C_L fragment

The kinetics of unfolding of the C_L fragment by GuHCl were measured fluorimetrically using manual mixing for reactions which last more than one minute and using stopped-flow mixing for reaction which are complete within a few minutes. Figure 4.1(a) shows the unfolding kinetics at 1.7 M GuHCl obtained by stopped-flow measurement and Figure 4.2(a) shows the semilog plot of the kinetics. The unfolding kinetics inside the transition zone were described by two exponential decay terms,

$$F(t) - F(\infty) = F_1 \exp(-\lambda_1 t) + F_2 \exp(-\lambda_2 t) , \qquad (4.1)$$

where λ_1 and λ_2 are the apparent rate constants of the slow and fast phases, respectively, and F_1 and F_2 are the amplitudes of the respective phases. The amplitudes of the slow and fast phases relative to the total fluorescence change are described by α_1 and α_2, respectively, where $\alpha_1 + \alpha_2 = 1$. The relative amplitudes varied greatly with GuHCl concentration and the total change in the fluorescence above 2.5 M GuHCl was expressed by first-order process (Figures 4.1(b) and 4.2(b)).

Figure 4.3 shows the dependence on the final concentration of GuHCl of the two apparent rate constants (λ_1 and λ_2) and the relative amplitude (α_2) of the fast phase. Figure 4.4 shows the transition curve for unfolding observed by the stopped-flow apparatus and the initial points of the fast and slow phases which were obtained by extrapolation to time zero of the respective phases. It can be seen that the initial points of the fast phase fell on a strainght line extending the fluorescence values before the transiton.

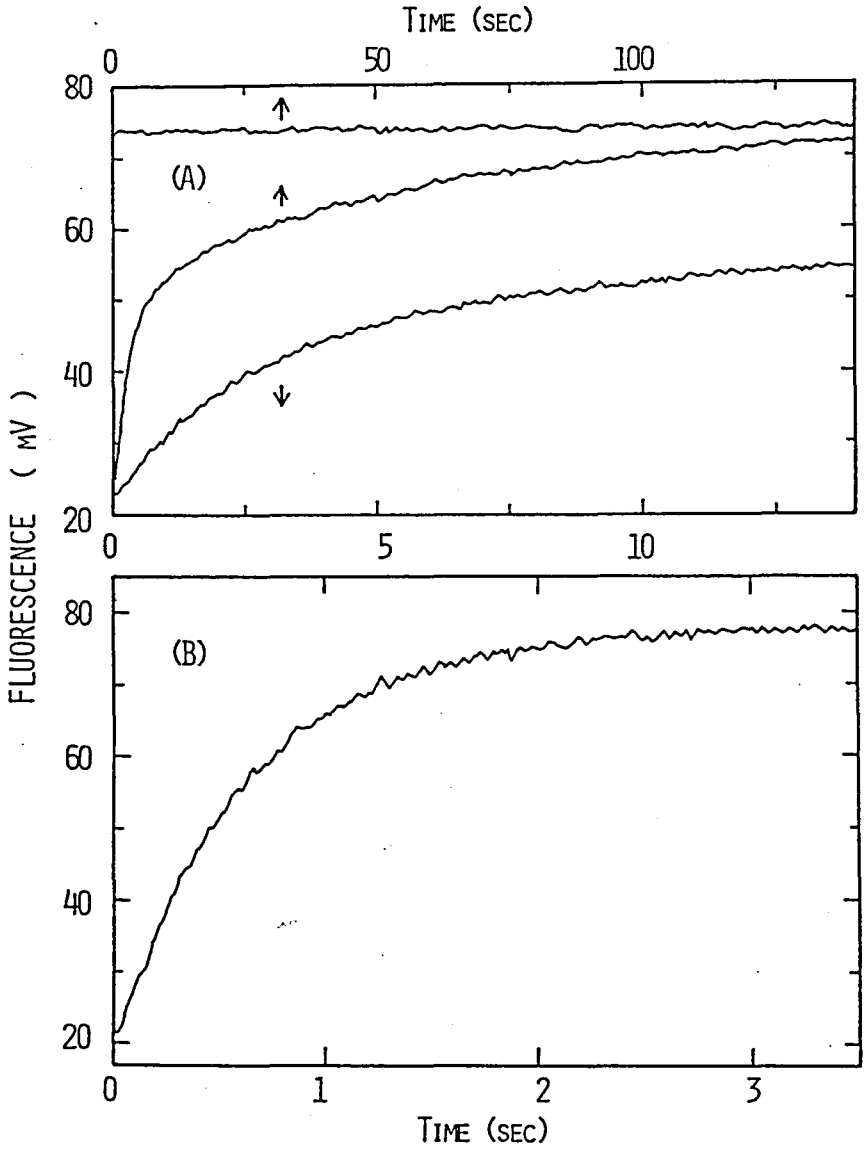

Fig. 4.1. Unfolding kinetics of the C_L fragment obtained by stopped-flow fluorescence measurements at 1.7 M GuHCl (A) and 2.75 M GuHCl (B). pH 7.5, 25°C, protein concentration: 0.02 mg/ml. The initial concentrations of GuHCl and the C_L fragment were 0 M and 0.04 mg/ml, respectively. The upper horizontal line in (A) indicates the change over the time range 200 to 350 sec.

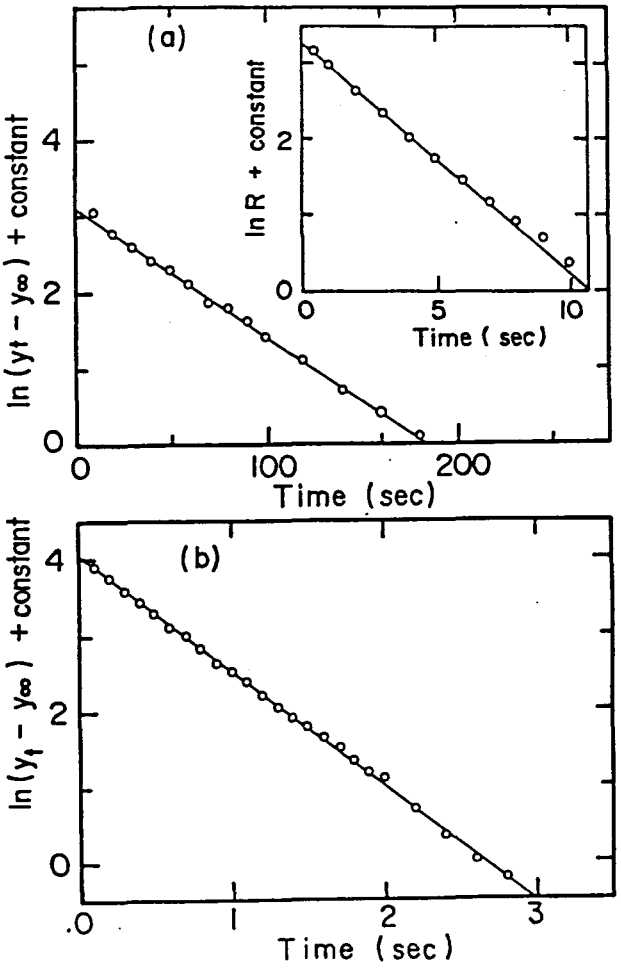

Fig. 4.2. First-order plots of the unfolding kinetics of the C_L fragment at 1.7 M GuHCl (a) and 2.75 M GuHCl (b). The conditions are described in the legend to Fig. 4.1. The inset in (a) shows the first-order plot for the fast phase (see the text).

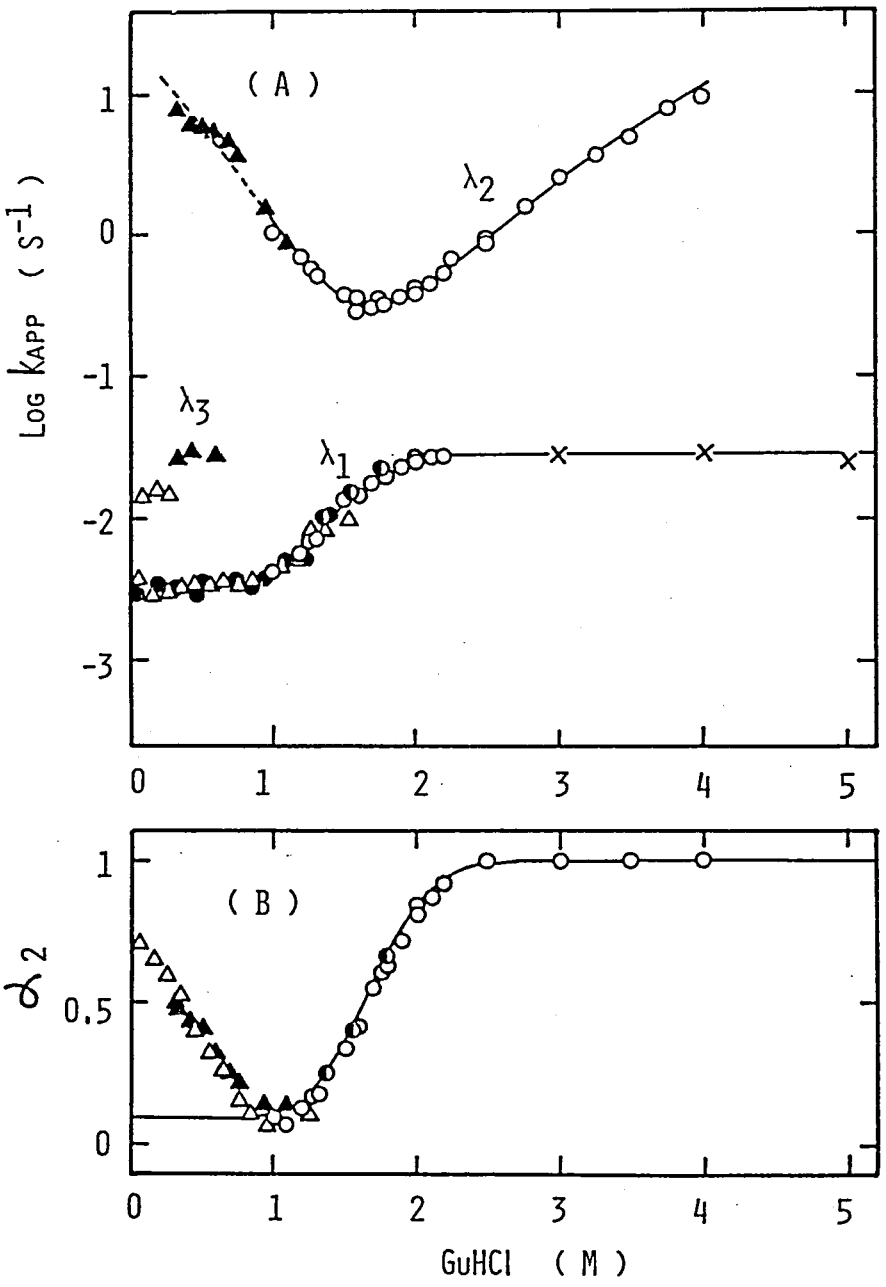

Fig. 4.3. See the next page.

Fig. 4.3. The dependence on GuHCl concentration of the apparent rate constants (λ_1, λ_2, and λ_3) (A) and the relative amplitude (α_2) of the fast phase (B) for unfolding and refolding kinetics of the C_L fragment at pH 7.5 and 25°C. (○), from unfolding kinetics obtained by stopped-flow fluorescence measurements. The conditions are as described in the legend to Fig. 4.4; (◐), from unfolding kinetics measured by fluorescence at 350 nm using manual mixing. The initial and final concentrations of the C_L fragment were 1 and 0.02 mg/ml, respectively; (▲), from refolding kinetics obtained by stopped-flow fluorescence measurements. The conditions are as described in the legend to Fig. 4.4; (△), from refolding kinetics measured by fluorescence at 350 nm using manual mixing. Initial conditions: protein concentration, 1 mg/ml; 4 M GuHCl; final conditions: protein concentration, 0.02 mg/ml; the indicated concentration of GuHCl; (●), from refolding kinetics measured by CD at 218 nm. The conditions are as described in the legend to Fig. 4.8; (×), the apparent rate constant of the isomerization process of U_2 to U_1 in mechanism 4.1 after unfolding measured by double-jump experiments. The conditions are as described in the legend to Fig. 4.5. The solid line in (B) indicates the values of α_2 calculated using K_{21} = 10 and the values of f_N obtained from equilibrium measurement (see equation (4.9)). The values of α_2 for the unfolding (◐) and refolding (△) kinetics measured by fluorescence at 350 nm using manual mixing were obtained assuming that the kinetics consists of the same phases as those observed by stopped-flow measurements and that the starting points for unfolding or refolding lie on a linear line extending the linear portion corresponding to the unfolded or native state in the transition curve determined by fluorescence measurements at 350nm (Fig. 3.11).

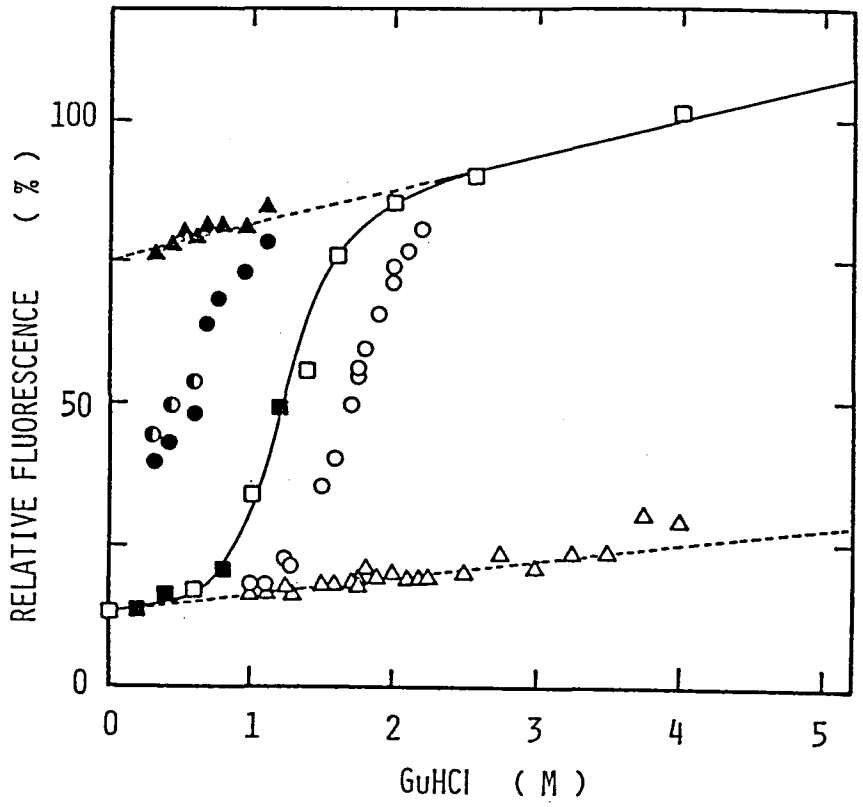

Fig. 4.4. Equilibrium and kinetic data for the denaturation of the C_L fragment by GuHCl, at 25°C and pH 7.5. Measurements were carried out by fluorescence using a stopped-flow apparatus. Unfolding (□) and refolding (■) equilibria were measured at a protein concentration of 0.02 mg/ml. The initial points of the slow and fast phases of unfolding kinetics are shown by ○, and △, respectively, and the initial points of the slow, fast, and intermediate phases of refolding kinetics are shown by ●, ▲, and ◐, respectively. They were obtained by extrapolating the respective phases to time zero. The initial concentrations of GuHCl for the unfolding and refolding kinetic experiments were 0 and 2.5 M, respectively. The initial protein concentration for unfolding and refolding kinetic experiments were 0.04 and 0.15 mg/ml, respectively. All measurements were made at a protein concentration of 0.02 mg/ml. The solid line indicates the theoretical curve constructed using Eqs. (3.1) and (3.2) and the values of Δn and $\Delta G_D^{H_2O}$ obtained on the basis of k = 0.6 (Table 3.II) (see Chapter 3)

This indicates that any phase that escaped the observation is not present and the two exponential terms are sufficient to describe the total change in the fluorescence upon unfolding. As shown in Figure 4.3, the apparent rate constant (λ_2) of the fast phase showed a minimum at about 1.7 M GuHCl, which is the concentration near the upper end of the unfolding transition zone. The apparent rate constant (λ_1) of the slow phase increased sharply from 1 M GuHCl, which is the lowest concentration of GuHCl used in the unfolding experiments, and tended to level off above 2 M GuHCl. This change is similar to the unfolding equilibrium curve shown in Figure 4.4. The value of α_2 increased from about 0.1 at 1.0 M GuHCl to 1.0 above 2.5 M GuHCl. The apparent mid-point of this change was at 1.7 M GuHCl. While the change in α_2 shifts to a higher concentration of GuHCl compared with the conformational transition, they are similar in shape. The values of λ_1 and α_2 obtained by the measurement of fluorescence at 350 nm using manual mixing agreed with the respective values obtained using stopped-flow mixing (Figure 4.3).

The following three-species mechanism has been proposed for the unfolding and refolding kinetics of ribonuclease A (Garel & Baldwin, 1975; Brandts et al., 1975).

$$U_1 \underset{k_{21}}{\overset{k_{12}}{\rightleftharpoons}} U_2 \underset{k_{32}}{\overset{k_{23}}{\rightleftharpoons}} N \qquad \text{(Mechanism 4.1)}$$

where N is native protein, and U_1 and U_2 are the slow-folding and rapid-folding species, respectively, of denatured protein, and k_{12}, k_{21}, k_{23}, and k_{32} are the rate constants for the respective processes.

U_1 and U_2 are indistinguishable from spectroscopic properties. The general solution of mechanism 4.1 is well known (Frost & Pearson, 1961). The same kinetics as equation (4.1) is obtained for mechanism 4.1 and the two apparent rate constants (λ_1 and λ_2) are given by

$$\lambda_{1(2)} = \left\{ \Sigma k \text{ -(+) } \left[(\Sigma k)^2 - 4\Pi k \right]^{1/2} \right\} / 2 \qquad (4.2)$$

where

$$\Sigma k = k_{12} + k_{21} + k_{23} + k_{32} = \lambda_1 + \lambda_2 \qquad (4.3)$$

and

$$\Pi k = k_{12}k_{23} + (k_{12} + k_{21})k_{32} = \lambda_1\lambda_2 \qquad (4.4)$$

The theoretical considerations for the mechanism for ribonuclease A have been given by Hagerman and Baldwin (1976). Under the conditions where the value of

$$K_{21} = k_{21}/k_{12} \qquad (4.5)$$

is independent of GuHCl concentration, the relative amplitudes of the slow and fast phases (α_1 and α_2) are independent of the initial conditions and have the same values in unfolding and refolding in the same final conditions. Then α_2 is given by

$$\alpha_2 = \left\{ 1 + \frac{|\lambda_1 - k_{12} - k_{21}|}{|\lambda_1 - k_{12} - k_{21}|} \right\}^{-1} \qquad (4.6)$$

Under the limiting conditions where $\lambda_2/\lambda_1 \gg 1$ and where k_{23}, $k_{32} \gg k_{12}$, k_{21}, the parameters, λ_1, λ_2, and α_2, are given by the following limiting forms,

$$\lambda_1 = k_{12} + \frac{k_{21}}{1 + (k_{23}/k_{32})} \qquad (4.7)$$

$$\lambda_2 = k_{23} + k_{32} \qquad (4.8)$$

and

$$\alpha_2 = (1 + f_N K_{21})^{-1} \qquad (4.9)$$

where f_N is the fraction of native protein in the final conditions and is given by $k_{12}k_{23}/\lambda_1\lambda_2$.

Under the above limiting conditions, the kinetic behavior is predicted as follows (Hagerman & Baldwin, 1976); (1) The minimum of λ_2 is located near the midpoint of the equilibrium transition, (2) the value of λ_1 increases sharply along by the transition zone and has a constant value of k_{12} and a constant value of $(k_{12} + k_{21})$ below and above the transition zone, respectively, and (3) the value of α_2 increases from a low limiting value of $1/(1 + K_{21})$ to 1 with a somewhat delayed increase compared with the equilibrium transition. When the above limiting conditions do not hold and λ_1 and λ_2 are not well separated, the value of α_2 is predicted to be smaller than the limiting value (Hagerman, 1977).

The dependence on GuHCl concentration of the kinetic parameters (λ_1, λ_2, and α_2) obtained from the unfolding experiments of the C_L fragment accords well with the predictions under the above limiting conditions. This strongly suggests that there are two forms of the unfolded C_L molecule and that the unfolding kinetics of the C_L fragment follows mechanism 4.1, where K_{21} is independent of GuHCl concentration.

I made double-jump experiments (Brandts et al., 1975; Nall et al., 1978) to confirm further the mechanism that explains the observed unfolding kinetics of the C_L fragment. Figure 4.5 shows the dependence on the time of exposing the C_L fragment to 3 M GuHCl of the amplitude of the slow phase observed in the refolding condition of 0.8 M GuHCl. Unfolding of the C_L fragment in 3 M GuHCl was complete within 2 sec. The refolding condition of 0.8 M GuHCl was chosen because at this concentration almost all the protein molecules refold to the native molecule (Figure 4.4, see Chapter 3) and the value of α_1 is sufficiently large to obtain reliable results (see section 4.B.2). The amplitude of the slow phase increased form zero at time zero with increasing the time of exposure to 3 M GuHCl (Figure 4.5). The apparent rate constant of the slow phase of refolding observed in the double-jump experiments was independent of the time of exposure (3×10^{-3} s^{-1}). These findings indicate that there exist two forms of the unfolded C_L molecule; one refolds rapidly and the other refolds slowly, and that the former converts slowly to the latter. The apparent rate constant of this interconversion was determined to be 3.2×10^{-2} s^{-1}. The results obtained by similar double-jump experiments at 4 and 5 M GuHCl with the same refolding condition of 0.8 M GuHCl showed that the rate for the interconversion between the two unfolded forms is independent of GuHCl concentration to which the C_L fragment is exposed. The apparent rate constants obtained by these experiments are plotted against GuHCl concentration in Figure 4.3. It can be seen that they fall on a horizontal line obtained by extending the plot of the apparent rate constants (λ_1) of the slow phases determined from the unfolding

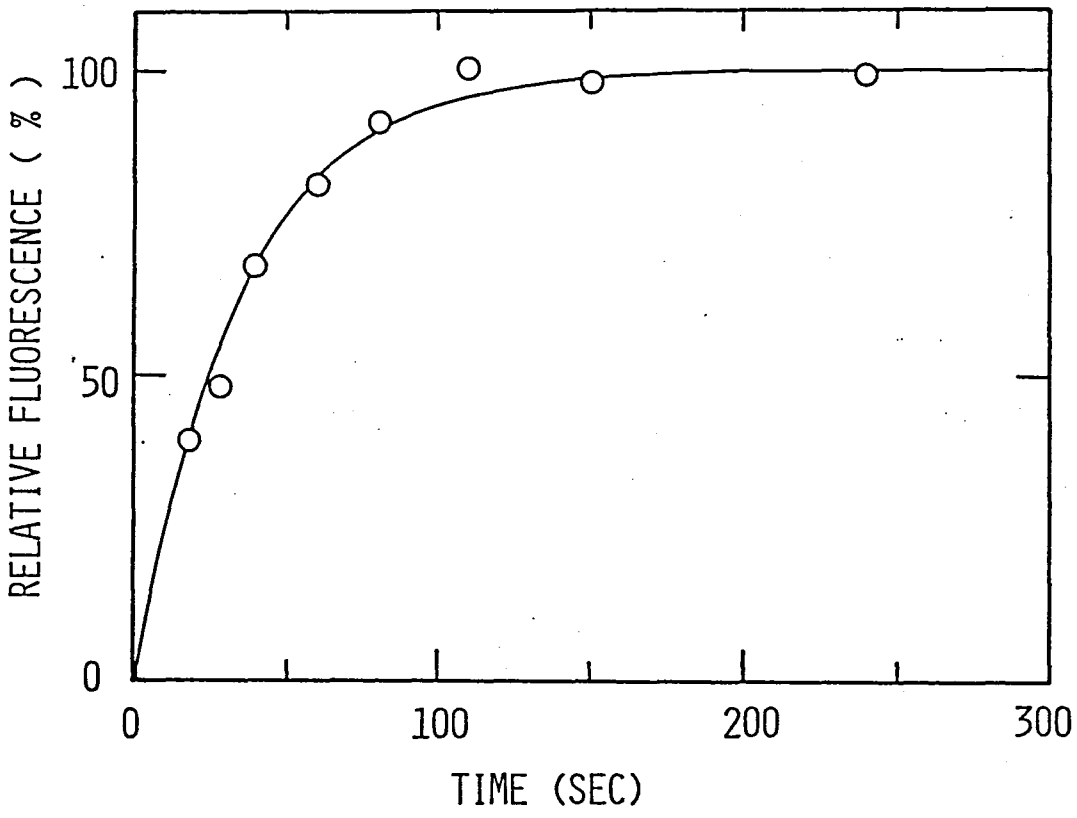

Fig. 4.5. A double-jump experiment measuring the process of U_2 to U_1 in mechanism 4.1 after unfolding. pH 7.5, 25°C. Formation of U_1 species was monitored by taking samples at the indicated times of unfolding and measuring the refolding kinetics by fluorescence at 350 nm. All the mixing procedures were made manually. The ordinate shows the fluorescence change for the slow phase observed in refolding process relative to the maximum fluorescence change obtained at infinite time in the unfolding conditions. Unfolding conditions: 3 M GuHCl; protein concentration, 0.6 mg/ml. Refolding conditions: 0.8 M GuHCl; protein concentration, 0.02 mg/ml. The solid line indicates the theoretical curve with a rate constant of 3.2×10^{-2} s^{-1}.

reactions. This result is explained on the basis of mechanism 4.1 in which the rates for the interconversion between U_1 and U_2 are independent of GuHCl concentration, and the apparent rate constant for the interconversion obtained by the double-jump experiments should be given by $(k_{12} + k_{21})$, which is the maximum value of λ_1 expected for unfolding kinetics above the transition zone as described above.

4.B.2. Refolding kinetics of intact C_L fragment

The kinetics of refolding of the C_L fragment upon dilution of GuHCl were measured fluorimetrically using manual mixing and stopped-flow mixing. Figure 4.6 shows the kinetics of refolding of the C_L fragment in 0.7 M GuHCl from 2.5 M GuHCl obtained by stopped-flow mixing. It is seen that the reaction consists of fast and slow phases and the slow phase is well separated from the fast phase. The slow phase was measured separately by manual mixing using a fluorescence change at 350 nm. Then the fast phase was obtained by subtraction of the slow phase, which was estimated form the apparent rate constant of the slow phase determined by manual mixing and the equilibrium value of fluorescence obtained by stopped-flow apparatus (see Figure 4.4), from the total fluorescence change.

The kinetics of refolding of the C_L fragment in 0.7 - 1.1 M GuHCl were expressed by two exponential terms and the values of λ_1 and λ_2 agreed well with those determined by the unfolding experiments described above (see Figure 4.3(a)). However, for the refolding kinetics below 0.6 M GuHCl, in addition to these two terms a third

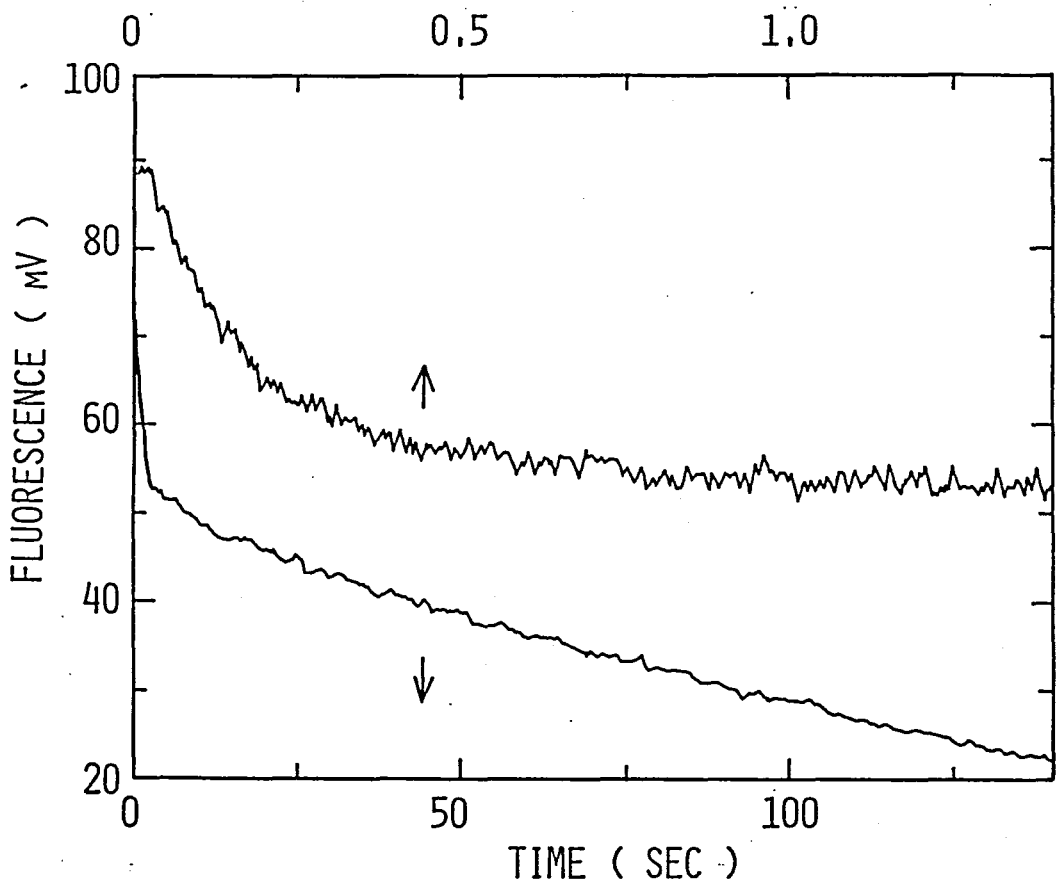

Fig. 4.6. Stopped-flow refolding kinetics of the C_L fragment measured by fluorescence. pH 7.5, 25°C. Initial conditions: 2.5 M GuHCl; protein concentration, 0.15 mg/ml. Final conditions: 0.7 M GuHCl; protein concentration, 0.02 mg/ml.

exponential term was necessary to describe the total fluorescence change. This additional term had a relatively small amplitude (α_3) and an apparent rate constant (λ_3) which is intermediate between the rate constants for the fast and slow phases (Figure 4.3). The change with GuHCl conentration in the amplitude (α_2) of the fastest phase determined by the refolding experiments is shown in Figure 4.3(b). Figure 4.4 includes the initial points obtained by extrapolation of each phase to time zero. It can be seen that the initial points for the fast phase fell on a line extending the curve above 2 M GuHCl to lower concentration region. This indicates that the total change in the fluorescence is seen in the refolding experiments.

The apparent rate constant (λ_1) of the slow phase of refolding was constant (3×10^{-3} s^{-1}) below the transition zone and increased inside the transition zone, where the values of λ_1 obtained by unfolding and refolding experiments were the same (Figure 4.3(a)). The apparent rate constant (λ_2) of the fast phase of refolding agreed well with those obtained by unfolding experiments inside the transition zone, and increased sharply with decreasing GuHCl concentration. The relative amplitudes of the fast phases obtained by the unfolding and refolding experiments were the same and the relative amplitude of the slow phase was about 0.9 at 1 M GuHCl (Figure 4.3(b)). The value of α_2 increased markedly below 1 M GuHCl. The apparent rate constant (λ_3) of the intermediate phase was near the rate constant for the slow phase and its amplitude was less than 0.1 (see Figure 4.4).

The agreement of the kinetic parameters (λ_1, λ_2, and α_2) obtained by unfolding experiments with those by refolding experiments inside

the transition zone establishes mechanism 4.1 in which K_{21} is independent of GuHCl concentration. Below the transition zone, however, the value of α_2 increased markedly with decreasing GuHCl concentration. This is not expected from mechanism 4.1, for which the value of α_2 should be constant in the region (the solid line in Figure 4.3(b)), where the limiting conditions are held (see equation (4.9)). Furthermore, a third phase appeared below 0.6 M GuHCl. This cannot be explained on the basis of mechanism 4.1 either.

Refolding kinetics of the C_L fragment were also studied by CD. In my CD measurements, I could follow only at a later stage of the reaction owing to the dead time of mixing being long (1 min). Figure 4.7 shows the kinetics of refolding of the C_L fragment in 0.1 M GuHCl from 4 M GuHCl obtained by the CD change at 218 nm. The reaction consisted of very fast phase which completes within the dead time of mixing and a slow phase. The observable process followed first-order kinetics (Figure 4.7, inset). In Figure 4.3 are included the apparent rate constants for the slow phases measured by CD at 218 nm at various concentrations of GuHCl. It is seen that these values are in good agreement with those for the slow phases of refolding measured by fluorescence. Figure 4.8 shows the initial points at various concentrations of GuHCl obtained by extrapolation to time zero of the slow phase of refolding kinetics measured by CD at 218 nm. These initial points change markedly with GuHCl concentration. This is very similar to the change in the amplitude of the slow phase measured by fluorescence (Figure 4.4).

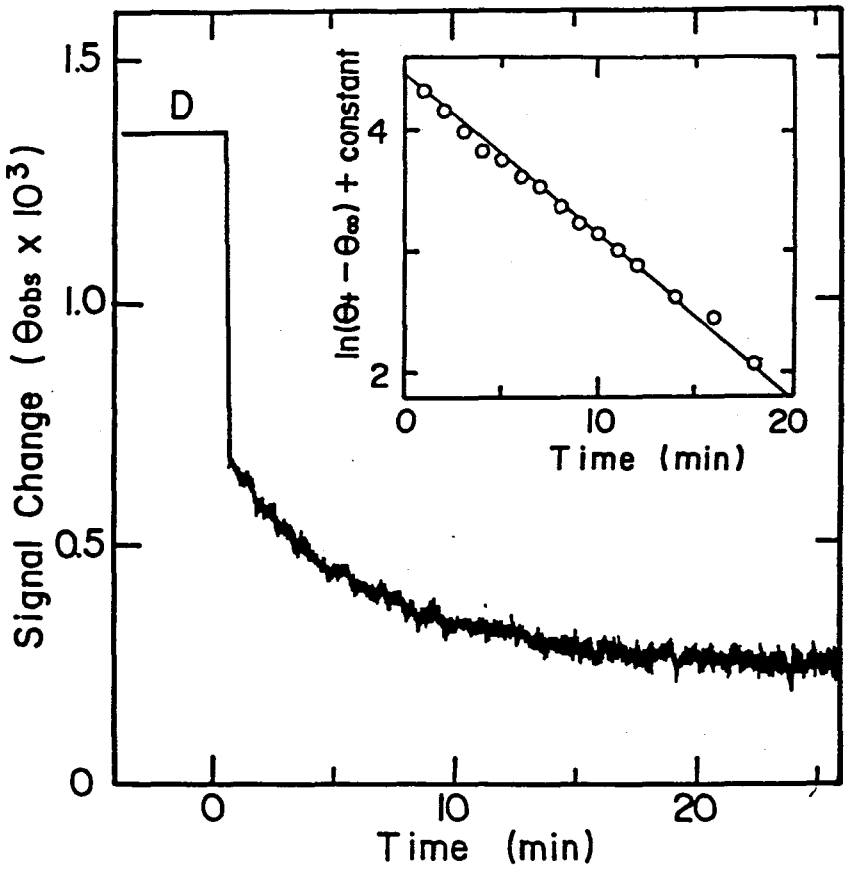

Fig. 4.7. Refolding kinetics of the C_L fragment measured by CD at 218 nm. pH 7.5, 25°C. Initial conditions: protein concentration, 7 mg/ml; 4 M GuHCl. Final conditions: protein concentration, 0.2 mg/ml; 0.1 M GuHCl. D represents the CD value in the presence of 4 M GuHCl. The inset shows the first-order plot of the kinetics.

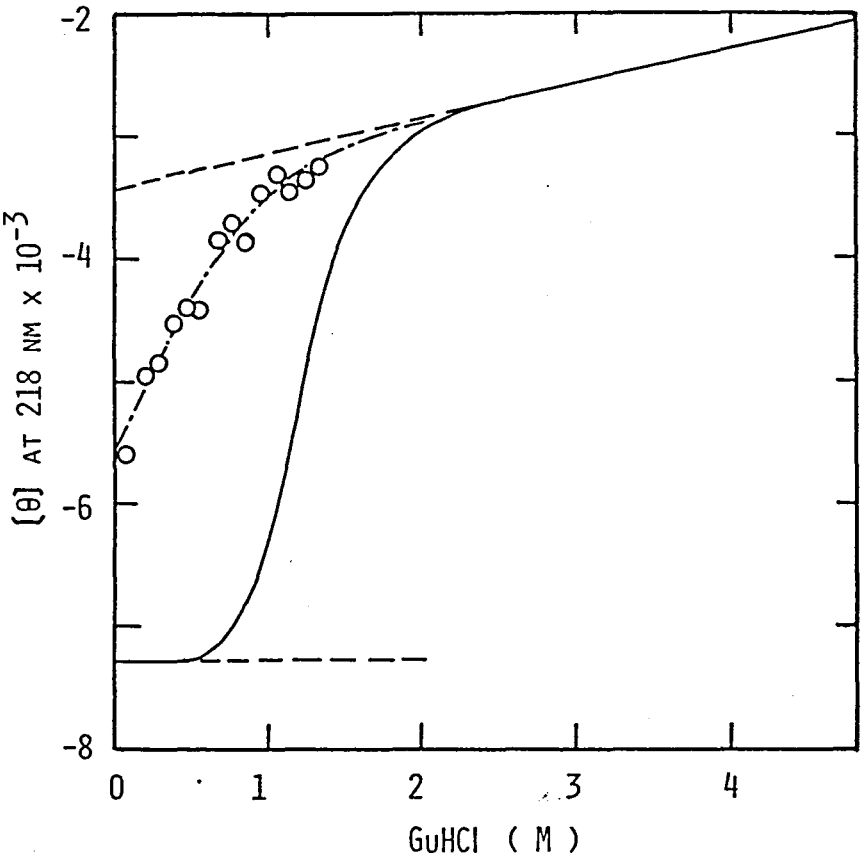

Fig. 4.8. The dependence on GuHCl concentration of the initial points for the slow phases of the refolding kinetics measured by CD at 218 nm. pH 7.5, 25°C. Initial conditions: protein concentration, 7 mg/ml; 4 M GuHCl. Final conditions: protein concentration, 0.2 mg/ml, the indicated concentration of GuHCl. The solid line indicates the transition curve determined by equilibrium measurement shown in Fig. 3.8.

Refolding kinetics of the C_L fragment were also measured in terms of ultraviolet absorption. The refolding kinetics obtained by the absorption change at 293 nm were very similar to those by fluorescence and CD and consisted of fast and slow phases. The slow phase had an apparent rate constant of 3×10^{-3} s^{-1} and the relative amplitude of 0.2 in 0.1 M GuHCl and 0.5 in 0.4 M GuHCl.

When the refolding kinetics of the C_L fragment are measured by CD at various wavelengths, slow phases with the same rate constant but with different relative amplitudes were observed. Figure 4.9 shows the initial points of the slow phases of the refolding kinetics measured at various wavelengths in 0.1 M GuHCl from 4 M GuHCl. The CD spectrum thus obtained was similar to that of intact C_L fragment in shape and had a minimum at about 215 nm. This suggests that β-structure similar to the structure present in the intact molecule is formed during the early stage of refolding.

In the same way, the fluorescence spectra were obtained by exptrapolating to time zero the slow phase of the refolding kinetics of the C_L fragment in 0.1 M and 0.4 M GuHCl from 4 M GuHCl measured at various wavelengths (Figure 4.10). It was found that the extrapolated spectrum in 0.1 M GuHCl has a maximum at around 330 nm and the fluorescence is greatly quenched compared with the fluorescence of the unfolded molecule. In 0.4 M GuHCl, the extrapolated spectrum changed, and the maximum shifted to 340 nm and the intensity increased greatly. For further study of the change of the extrapolated spectrum depending on GuHCl concentration, I measured fluorescence spectra immediately after dilution of a solution of the C_L fragment in 4 M

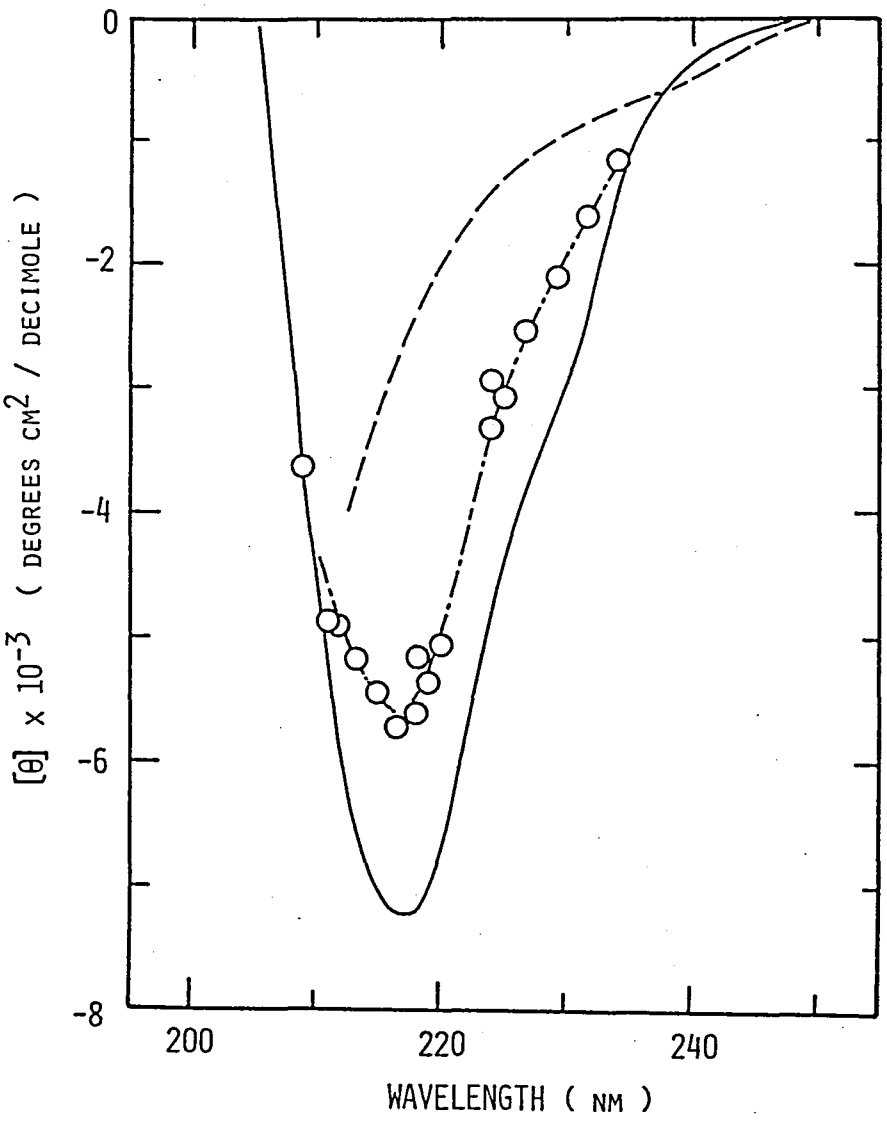

Fig. 4.9. The initial points for the slow phases of refolding kinetics of the C_L fragment measured by CD at various wavelengths. pH 7.5, 25°C. Initial conditions: 4 M GuHCl; protein concentration, 7 mg/ml. Final conditions: 0.1 M GuHCl; protein concentration, 0.2 mg/ml. The solid and broken lines indicate the spectra of native protein and unfolded protein in 4 M GuHCl, respectively.

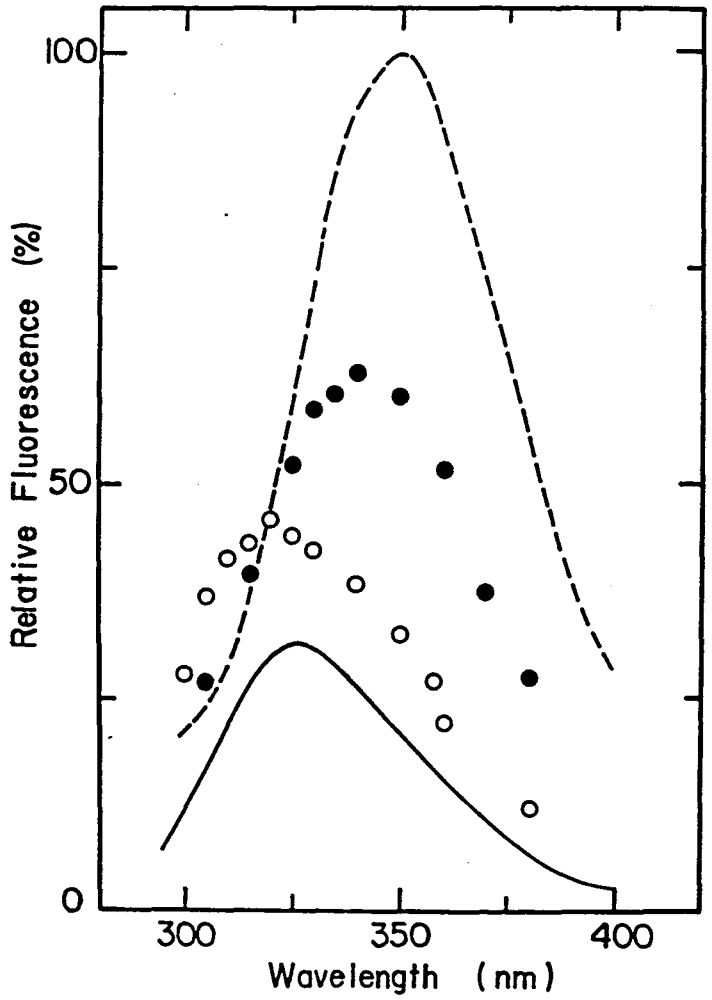

Fig. 4.10. The initial points for the slow phases of refolding kinetics of the C_L fragment in 0.07 M GuHCl (○) and 0.4 M GuHCl (●) measured by fluorescence at various wavelengths. pH 7.5, 25°C. Initial conditions: protein concentration, 1 mg/ml; 4 M GuHCl. Final protein concentration, 0.02 mg/ml. The solid and broken lines indicate the spectra of native protein and unfolded protein in 4 M GuHCl, respectively.

GuHCl to various concentrations of GuHCl at a lower temperature. At 5°C, the apparent rate constant of the slow phase dropped more than ten-fold (2×10^{-4} s^{-1}). However, the fast phase was complete within the dead time of manual mixing (30 sec) even at 5°C. Although the equilibrium and kinetics of unfolding of the C_L fragment at 5°C have not been examined in detail, the amplitude of the slow phase of refolding measured by CD at 225 nm was independent of the temperature from 5°C to 40°C (see below). Since it takes only 1 min to record the whole fluorescence spectrum in the region of 300 to 400 nm, essentially no change occurs with time during the measurement after dilution. Therefore, the spectrum thus obtained represents the spectrum obtained by extrapolation to time zero of the slow phase. The spectrum at the lowest concentration of GuHCl (0.07 M) used had a maximum at 335 nm which is close to the maximum wavelength for the intact C_L fragment and the fluorescence was much quenched compared with the fluorescence of denatured protein (Figure 4.11). This spectrum and the spectrum in 0.4 M GuHCl are similar to the extrapolated spectra at 25°C (Figure 4.10). There exists an isoemissive point at 315 nm in the spectra at various final concentrations of GuHCl and the spectrum of reduced and alkylated C_L fragment with no significant ordered structure (Chapter 3), but not in these spectra and the spectrum of native C_L fragment. This finding is not explained by the presence of native and unfolded molecules of the C_L fragment only, but indicates that an intermediate which has a conformation different from native protein appears during the refolding process. The amount of the intermediate formed was larger at lower final concentration

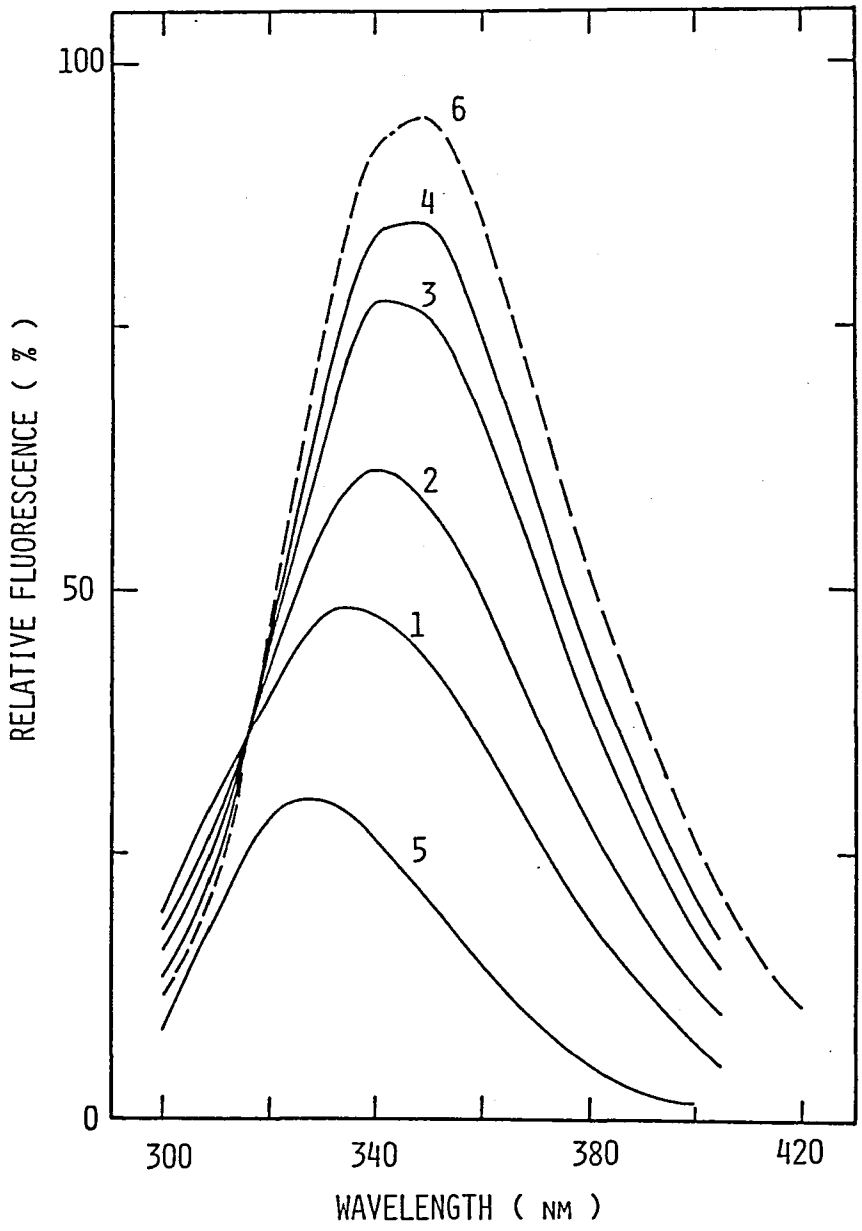

Fig. 4.11. Dependence on the final concentration of GuHCl of the fluorescence spectrum of the C_L fragment measured immediately after initiation of refolding. pH 7.5, 25°C. Initial conditions: protein concentration, 1 mg/ml; 4 M GuHCl. Final conditions: protein concentration, 0.02 mg/ml; (1), 0.07 M; (2), 0.26 M; (3), 0.46 M; (4), 0.66 M GuHCl. Curves 5 and 6 show the fluorescence spectra of native C_L fragment and reduced and alkylated C_L fragment, respectively.

of GuHCl. The fluorescence spectrum of the intermediate should have a maximum below 335 nm and its fluorescence is quenched but not so greatly as the fluorescence of native C_L fragment.

The kinetics of refolding in 0.1 M GuHCl from 4 M GuHCl were measured by CD at 225 nm over the temperature range of 5°C to 40°C. Over the wide temperature range, the relative amplitude of the slow phase was constant and was about 0.6. The dependence of the apparent rate constant (λ_1) of slow phase on temperature was plotted as log λ_1 versus (1/T) (Arrhenius plot) in Figure 4.12. The Arrhenius plots fit a straight line and the slope gives an activation energy of 20 kcal mol^{-1}.

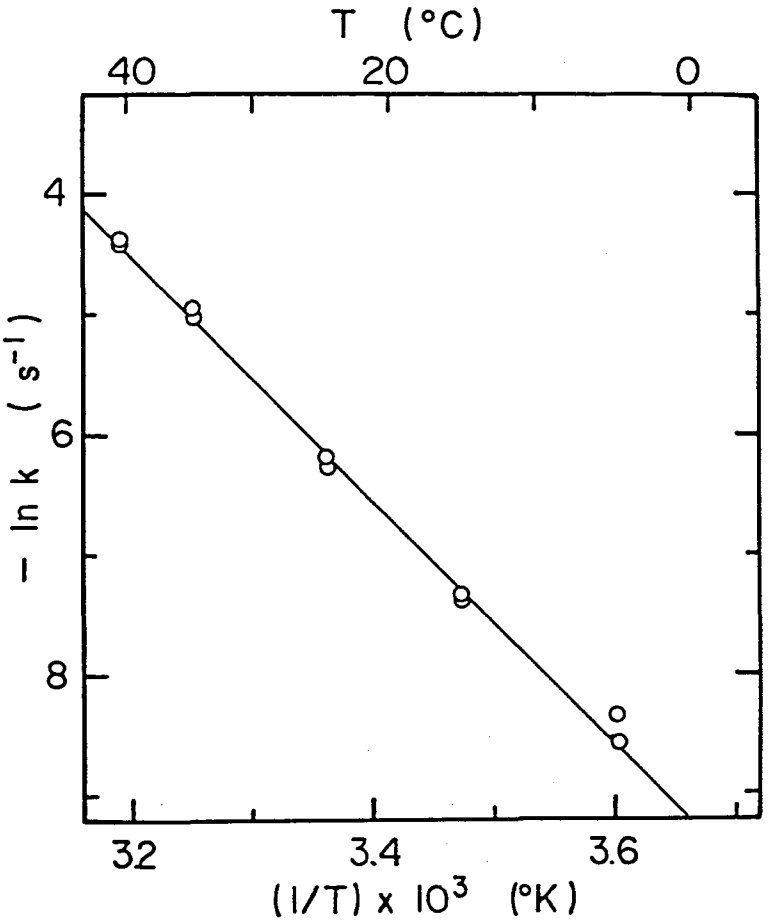

Fig. 4. 12. Arrhenius plot of the apparent rate constant (λ_1) of the slow phase of refolding of C_L fragment measured by CD at 225 nm. pH 7.5. Initial conditions: 4 M GuHCl; protein concentration, 7 mg/ml; 25°C. Final conditions: 0.1 M GuHCl; protein concentration, 0.2 mg/ml.

4.C. Discussion

4.C.1. Folding mechanism of intact C_L fragment

As described in Results, all the kinetic data of unfolding of the C_L fragment can be explained on the basis of mechanism 4.1. The kinetic parameters in this mechanism can be determined as follows. From the double-jump experiments at 3, 4, and 5 M GuHCl (Figures 4.3 and 4.5), the value of $(k_{12} + k_{21})$ was determined to be 3.2×10^{-2} s^{-1}. I first assumed that the value of λ_1 below the transition zone equals to k_{12} under the limiting conditions (see equation (4.7)). Then the value of k_{12} was estimated to be 3×10^{-3} s^{-1}. Thus the values of k_{21} can be estimated and hence $K_{21} = k_{21}/k_{12}$. It can be seen form equations (4.3) to (4.6) that the value of K_{21} thus assumed ($K_{21} = 10$) and the values of λ_1, λ_2, and α_2 determined experimentally are sufficient to give the values of k_{12}, k_{21}, k_{23}, and k_{32} without employing the limiting conditions. Then the values of f_N at various concentrations of GuHCl were determined using the relation $f_N = k_{12}k_{23}/\lambda_1\lambda_2$. In the region far above the transition zone the value of λ_2 equals to k_{32} because k_{23} should be small (equation (4.8)). Figure 4.13(a) shows the microscopic rate constants thus obtained and Figure 4.13(b) shows the values of f_D ($= 1 - f_N$) calculated using these values at various concentrations of GuHCl. The values of k_{12} and k_{21} are essentially constant at all the GuHCl concentrations studied and the values of k_{12} thus estimated are in good agreement with the values of λ_1 below the transition zone. This shows that the above assumption is correct. The transition curve calculated using only the kinetic data agrees quite well with that obtained

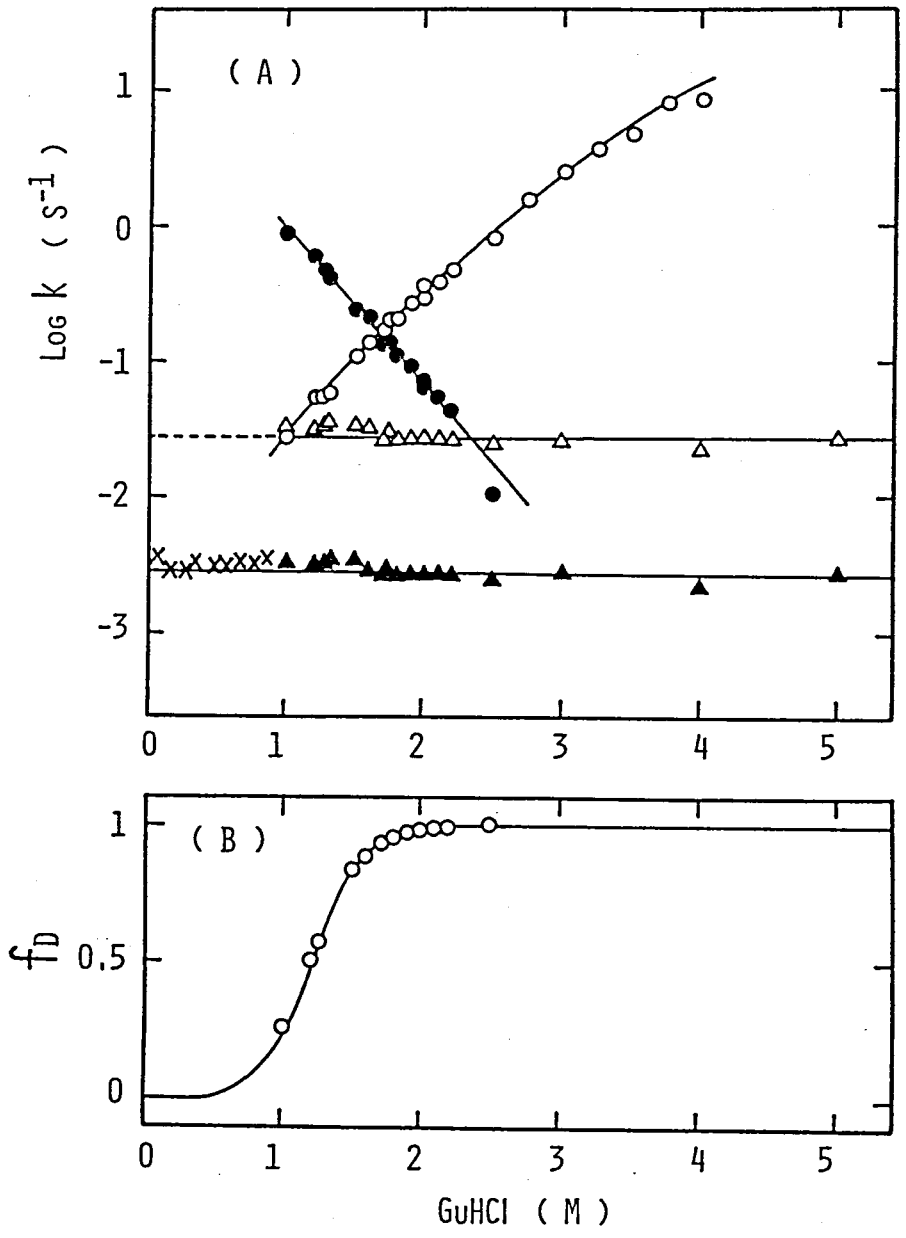

Fig. 4.13. Dependence on GuHCl concentration of the microscopic rate constants estimated based on mechanism 4.1 for folding of the C_L fragment (A) and the transition curve for unfolding calculated using the microscopic rate constants (B). pH 7.5, 25°C. (○), k_{32}; (●), k_{23}; (△) , k_{21}; (▲), k_{12}. The crosses represent the values of λ_1 taken from Fig. 4.3. The solid line in (B) indicates the transition curve for unfolding obtained from equilibrium measurement.

from the equilibrium measurement. These results show that the kinetics of unfolding of the C_L fragment can be explained thoroughly on the basis of mechanism 4.1.

With increasing GuHCl concentration, k_{23} decreases and k_{32} increases sharply. This is expected for the rates of conformational transition of proteins. It should be noted that the values of k_{23} and k_{32} are the same at 1.7 M GuHCl (Figure 4.13) and the value of λ_2 is minimum at this concentration (Figure 4.3). Although the apparent midpoint of the equilibrium transition is at 1.2 M GuHCl (Figure 4.4, see also Chapter 3), the GuHCl concentration of 1.7 M should be the true midpoint for the conformational transition of the C_L fragment. The apparent equilibrium constant (K_{app}) of native protein to the total unfolded protein is expressed by

$$K_{app} = \frac{(U_1) + (U_2)}{(N)} = K_{32}(1 + K_{21}), \qquad (4.10)$$

where

$$K_{32} = (U_2)/(N) = k_{32}/k_{23}.$$

Therefore, when two forms (U_1 and U_2) are present in the unfolded state and the equilibrium constant between them (K_{21}) is large, the true equilibrium constant (K_{32}) becomes smaller than the apparent equilibrium constant (K_{app}) and hence the true midpoint lies at a higher concentration of GuHCl than the apparent midpoint depending on the value of K_{21}.

Whereas the kinetics of refolding of the C_L fragment inside the transition zone are consistent with mechanism 4.1 and the kinetic parameters in this zone are in agreement with those obtained by the

the unfolding experiments (Figure 4.3), the refolding kinetics below the transition zone are not explained only on the basis of mechanism 4.1. The constancy of λ_1 and the increase of λ_2 with decreasing GuHCl concentration are expected but a marked increase of α_2 with decreasing GuHCl concentration is unexpected from mechanism 4.1. The value of 10 for K_{21} means that the proportion of the slow-refolding species (U_1) is about 90 % of the total unfolded protein. Therefore the refolding process is governed to a great extent by the refolding of U_1. The results of Figures 4.10 and 4.11 show that an intermediate, of which fluorescence spectrum is similar to that of native protein, appears during the fast refolding process and it is in eqiulibrium with the unfolded protein depending on GuHCl concentration. The CD spectrum obtained by extrapolating the slow phases of the refolding kinetics in 0.1 M GuHCl to time zero (Figure 4.9) has a minimum at around 215 nm. If an intermediate accumulates during the fast refolding process as is indicated by the fluorescence result, this shows that the intermediate has β-structure similar to that present in the natvie C_L fragment. I had another complex observation that an intermediate phase appears in the refolding kinetics below 0.6 M GuHCl. In order to interpret the refolding kinetics, however, I first did not take this phase into account because of its small amplitude.

I found that the refolding kinetics below the transition zone are well explained if I assume the following mechanism in which an alternative pathway of refolding of U_1 is involved.

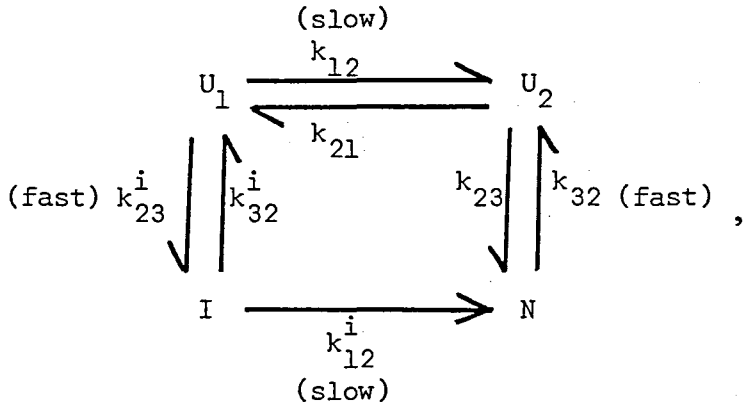

(Mechanism 4.2)

where I represents the intermediate, k^i_{23}, k^i_{32}, and k^i_{12} are the rate constants of the respective processes involving I, and the others are the same as those in mechanism 4.1. The proportion of U_1 is about 90 % of the total unfolded protein (U_1 + U_2). In the alternative pathway, the conformation of I is similar to that of native protein but the stability of I is less than that of native protein, U_1 and I are in a rapid equilibrium, and the rate of refolding of I to N is as slow as that of U_1 to U_2.

Using mechanism 4.2 the results are explained as follows. (i) I is unstable to exist inside and above the transition zone, so that mechanism 4.2 reduces to mechanism 4.1 for the unfolding and refolding kinetics inside and above the transition zone. (ii) Kinetic intermediate I with spectroscopic properties similar to those of native protein appears below the transition zone. With decreasing GuHCl concentration I is stabilized and the rapid equilibrium between U_1 and I shifts to I. The spectral change shown in Figures 4.10 and 4.11, and the change in α_2 with GuHCl concentration shown in Figure 4.3(b), which has a midpoint at about 0.4 M GuHCl, are explained by the shift of this equilibrium depending on GuHCl concentration.

The change in α_2 represents approximately the unfolding curve of I and the sharp change in α_2 is explained in terms of a native-like conformation of I. (iii) The apparent rate constant of the fast phase (λ_2) inside the transition zone represents the rate of refolding of U_2 to N ($k_{23} + k_{32}$). At a low GuHCl concentration, it mainly represents the rate of refolding of U_2 to I ($k^i_{23} + k^i_{32}$). (iv) The constancy of the apparent rate constant of the slow phase (λ_1) is due to the rate of conversion of U_1 to U_2 (k_{12}) being equal to that of I to N (k^i_{12}). These rates are independent of GuHCl.

The constancy of the activation energy of the slow phase for refolding in 0.1 M GuHCl from 4 M GuHCl in the temperature range of 5°C to 40°C (Figure 4.12) establishes mechanism 4.2 over the wide temperature range.

Although most of the kinetic properties of the refolding are explained on the basis of mechanism 4.2, the appearance of the intermediate phase in not clear at present. If the slow phase of refolding is due to the proline isomerization as will be described below (section 4.C.2), the intermediate phase may appear as a result of the presence of different types of prolyl residues.

4.C.2. Role of Pro-143 in folding of C_L fragment

The slow equilibrium between the two forms of unfolded species, one of which refolds fast and the other slowly, was first established for ribonuclease A by Garel and Baldwin (1975). The interconversion between these two forms has been interpreted in terms of the cis-trans isomerization of the prolyl residues (Brandts et al., 1975). It has been shown more recently that wrong proline isomers do not always prevent refolding of ribonuclease A and kinetic intermediates containing wrong proline isomers are formed during refolding process in the conditions where the protein is strongly stable (Cook et al., 1979; Schmid, 1981; Schmid & Blaschek, 1981). Similar results have been obtained for other proteins (Ridge et al., 1981; Jullien & Baldwin, 1981; Kato et al., 1981; Crisanti & Matthews, 1981). Creighton (1980b) has demonstrated directly using urea-gradient electrophoresis that a compact intermediate with probably wrong proline isomers appears during refolding of several proteins below transition zone. On the basis of these observations, the presence of the two forms of unfolded species and appearance of kinetic intermediates have been accepted as a general property of folding in vitro of proteins containing proline residues (Pain, 1981). Levitt (1981) attempted to explain these complex kinetics of refolding on the basis of different types of proline residues which are classified according to the energy difference between the native structure and the folded structure containing wrong proline isomer.

The C_L fragment contains nine proline residues at positions 111, 115, 121, 122, 143, 156, 166, 184, and 210. This proline content is

relatively high compared with other proteins with similar size (Stellwagen, 1979). These proline residues are located in the loops and at the ends of β-strands (Beale & Feinstein, 1976; Amzel & Poljak, 1979) (Figure 4.14). Among these proline residues only Pro 143 is in cis configuration (Marquart et al., 1980) and is located in a sharp turn. It was established by the present experiments that there exist two forms of unfolded species of the C_L fragment and that the rates of interconversion between them are slow and are independent of GuHCl concentration. The activation energy for the slow phase of refolding is 20 kcal mol^{-1} (Figure 4.12). Since these are characteristic of the proline isomerization (Brandts et al., 1975; Cheng & Bovey, 1977; Nall et al., 1978; Schmid & Baldwin, 1979), it is strongly suggested that the slow-refolding species of the C_L fragment is produced by the introduction of wrong proline isomers. The possibility that the topology of the intrachain disulfide bonds of ribonuclease A is responsible for the presence of the two unfolded species has been suggested by Nall et al. (1978). As will be described in Chapter 5, however, the kinetics of unfolding and refolding of the reduced C_L fragment show that the slow-refolding species is produced irrespective of the presence of the intrachain disulfide bond and the equilibrium between the two unfolded species is not affected by the presence of the disulfide bond.

The following three distinguished features were observed for the kinetics of unfolding and refolding of the C_L fragment. (i) The proportion of the slow-refolding species is extremely high (about 90 % of the total unfolded protein). (ii) The apparent rate

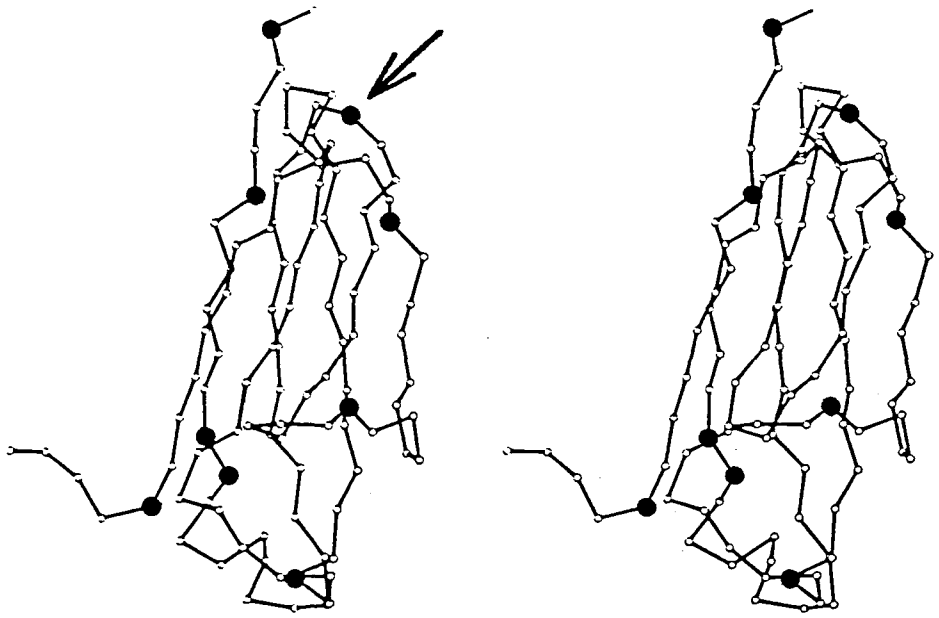

Fig. 4.14. Stereo drawing of the α-carbon backbone of the C_L fragment. Closed circles represent Pro residues. Arrow indicates Pro 143. Produced from the original drawing by Amzel & Poljak (1979).

constant of the slow phase (3×10^{-3} s^{-1}) is some ten times smaller than those for slow phases observed for other proteins with similar size (see for instance, Stellwagen, 1979). The rate constants of the slow phase determined by CD, fluorescence, and ultraviolet absorption are all the same. (iii) The apparent rate constant of the slow phase is independent of GuHCl concentration in the conditions where the kinetic intermediate with wrong proline isomers is formed. Contrary to the folding reaction of ribonuclease A (Nall et al., 1978; Schmid, 1981; Cook et al., 1979) and bovine pancreatic trypsin inhibitor (Jullien & Baldwin, 1981), the rate of proline isomerization in the intermediate is not enhanced and the activation energy determined far below the transition zone (0.1 M GuHCl) is 20 kcal mol^{-1}.

Here I refer to the refolding kinetics of other domains of immunoglobulin G1 (Table 4.1). The kinetics of refolding of the pFc' fragment, which closely corresponds to the C_H3 domain and has nine proline residues, from the unfolded state in 4 M GuHCl shows a slow phase with an apparent rate constant of 3×10^{-3} s^{-1} (Isenman et al., 1979), a value very similar to the rate for the C_L fragment observed here. The $V_L(\lambda)$ domains have four to seven proline residues depending on specimens. As will be described in Chapter 6, however, refolding of the $V_L(\lambda)$ fragments is fast and is complete within 30 sec. The kinetics of refolding of the Fc fragment, which consists of the C_H2 and C_H3 domains, from the unfolded state in 4 M GuHCl have been explained in terms of independent folding of the two domains and the C_H3 domain refolds much faster (a half time of about 5 sec) (Sumi & Hamaguchi, in preparation). The C_H2 domain contains nine proline residues.

TABLE 4.I. Proline residues of immunoglobulin (IgG1) domains.

Domains	Pro contents	Pro which corresponds to Pro(143) of $C_L(\lambda)$	Other cis-Pro	Refolding	Pro-Pro sequence
$C_L(\lambda)$	9[a]	cis-Pro(143)[d]	no[d]	slow[g]	Pro(121)-Pro(122)[a]
$C_L(\kappa)$	5[b]	Pro(141)[b] Cis-trans is unknown.	unknown	unknown	Pro(119)-Pro(120)[b]
C_H1	9[a]	cis-Pro(152)[e]	cis-Pro(154)[e]	unknown	no[a]
C_H2	9[a]	no[e]	no[e]	fast[h]	Pro(244)-Pro(245)[a]
C_H3	9[a]	cis-Pro(374)[e]	no[e]	slow[i]	Pro(352)-Pro(353)[a] Pro(395)-Pro(396)
$V_L(\lambda)$	4 - 7[b]	no[b]	not reported	fast[g]	One Pro-Pro sequence is generally found.[b]
$V_L(\kappa)$	5 - 8[b]	no[b]	cis-Pro(8)[f] cis-Pro(95)[f]	unknown	no[b]
β_2-microglobulin	5[c]	Pro(32)[c] Cis-trans is unknown.	unknown	unknown	no[c]

a) From Beale & Feinstein, 1976. b) From Fasman, 1976.
c) From Cunningham, 1976. d) From Marquart et al., 1980.
e) From Deisenhofer, 1981. f) From Huber and Steigemann, 1974.
g) From the present work, h) From Sumin & Hamaguchi, in preparation.
i) From Isenman et al., 1979.

Each domain of the immunoglobulin molecule has a very similar conformation called immunoglobulin-fold (Amzel & Poljak, 1979; Beale & Feinstein, 1976) (Figure 4.14) and the proline content of each domain is relatively high compared with other proteins with similar size. However, the C_L and C_H3 domains refold slowly and the $V_L(\lambda)$ and C_H2 domains refold fast. The extremely slow rate observed for the C_L fragment cannot be explained only by its high prolyl content. It is suggested that the role of each proline residue in the refolding is different and that there are the limited number of proline resiudes that are critical for refolding. Jullien and Baldwin (1981) have suggested that the presence of an interior Pro-Pro bond retards refolding greatly. The C_L domain contains Pro 124 - Pro 125 bond and the C_H3 domain contains two Pro-Pro bonds (Table 4.1). The C_H2 domain and most of the $V_L(\lambda)$ domains also contain one Pro-Pro bond (Table 4.1) but they refold very fast. Thus the extremely slow phase observed for the C_L and C_H3 domains is not due entirely to the presence of the Pro-Pro bond.

X-ray crystallographic studies on the fragments of immunoglobulin G1 show that Pro 374 in the C_H3 domain, Pro 152 and Pro 154 in the C_H1 domain, which contains nine proline residues, and Pro 143 in the $C_L(\lambda)$ domain are in cis configuration (Table 4.1). These proline residues (Pro 152 in the case of the C_H1 domain) occupy a corresponding position in each domain and are located in a β-turn. The corresponding proline residue is not present in the $V_L(\lambda)$ and C_H2 domains (Table 4.1). I have no information on the refolding of the C_H1 domain at present, but it is strongly suggested that these homologous cis-proline residues

are responsible for the slow refolding of the C_L and C_H3 domains. The proportion of trans configuration about X-Pro peptide bond is estimated to be 0.7 - 0.9 (Brandts et al., 1975; Granthwohl & Wüthrich, 1976). This value is in fair agreement with the proportion of U_1 for the C_L fragment (about 0.9). The residue that precedes the cis-proline residue is tyrosine for both C_L and C_H3 domains (Beale & Feinstein, 1976). The extremely slow rates observed for the refolding of these domains are compatible with the observation that a bulky residue that precedes proline residue retards the rate of cis-trans isomerization (Brandts et al., 1975). As described above, the slow phase of the refolding of the C_L fragment is well explained in terms of the cis-trans isomerism of one proline residue that is in cis in native protein. The other proline residues that are in trans in native protein may interfere little with folding or the cis to trans isomerization steps of the wrong isomers of these proline residues may not be rate-limiting owing to the trans to cis isomerization of Pro 143 being extremely slow. The role of each proline residue may be related with its location in the immunoglobulin-fold. As described above, they are located in the loops and at the ends of the β-strands. Therefore, the proline residues at the ends of the β-strands may not interfere the formation of the β-strands and the proline residues in the external loops may easily be accomodated by neighboring external residues even if they are in wrong configuration. However, the cis-proline residue (Pro 143) is located in a sharp and probably rigid turn and thus the cis-trans isomerism may play an important role in refolding; the unfolded species in which this proline residue is in

trans may not refold to the native molecule. Below the transiton zone, however, an intermediate with β-structure similar to that of the native protein molecule will be formed owing to strong interactions between the β-strands, even if the cis-proline is in trans. If these considerations are correct, it is expected that the refolding of the C_H1 domain is slow, because it has a homologous cis-proline residue and the residue that precedes it is bulky (Phe) (Beale & Feinstein, 1976).

As will be described in Chapter 6, the refolding processes of type κ light chains are as slow as those of type λ light chains and the $C_L(\lambda)$ fragment. The $C_L(\kappa)$ domain contains five proline residues, one of which occupies a position corresponding to the cis-proline in $C_L(\lambda)$ domain (Table 4.1). Although its configuration is not known, the above consideration leads to a suggestion that this proline residue in the $C_L(\kappa)$ domain is in cis and retards its refolding. The conservative two proline residue in the V_L fragment of a type κ light chain (Rei) have been reported to be in cis (Huber & Steigemann, 1974), but neither of these residues corresponds to the cis-proline in the $C_L(\lambda)$ domain. Thus the refolding experiment on the isolated $C_L(\kappa)$ fragment will be promising to clarify the cause of the slow refolding of the $C_L(\lambda)$ and C_H3 domains.

Chapter 5

Folding mechanism of reduced C_L fragment

5.A. Introduction

In the preceding Chapter, I described the kinetics of reversible denaturation of the intact C_L fragment by GuHCl. The kinetics were explained fundamentally on the basis of the three-species mechanism ($U_1 \leftrightarrow U_2 \leftrightarrow N$). The presence of the two forms of unfolded molecule was attributed to the cis-trans isomerization of the amino-terminal peptide bond of Pro 143. The reduced C_L fragment assumes a conformation very similar to the intact C_L fragment in the absence of denaturant, although the stability of the former is lower than that of the latter (Chapter 3). The decreased stability on reduction of the disulfide bond is almost entirely explained in terms of the larger entropy in the denatured state.

In the present Chapter, I describe the kinetics of unfolding and refolding of the reduced C_L fragment. Because the conformations of the intact and reduced C_L fragments are very similar and the C_L fragment contains only one intrachain disulfide bond, I expected that the comparison of the kinetics of unfolding and refolding of both proteins will give us useful and distinct information of the kinetic role of the intrachain disulfide bond in the folding of the C_L fragment. The results obtained not only demonstrated the kinetic role of the disulfide bond but also suggested the location of the rate-limiting step of folding and unfolding of the C_L fragment.

5.B. Results

5.B.1. Unfolding kinetics of reduced C_L fragment

The reduced C_L fragment begins to unfold at a very low concentration of GuHCl at pH 7.5 and 25°C, and the midpoint of the equilibrium transition for unfolding is 0.4 M GuHCl (Figure 5.1, see also Chapter 3). The kinetics of unfolding of the reduced C_L fragment were measured by fluorescence at 400 nm using manual mixing below 0.8 M GuHCl and by fluorescence at wavelengths longer than 330 nm using stopped-flow mixing above 0.7 M GuHCl. The overall process of the unfolding follows first-order kinetics above 1.5 M GuHCl. Below 1.2 M GuHCl, however, the kinetics were described by two exponential decay terms,

$$F(t) - F(\infty) = F_1 \exp(-\lambda_1 t) + F_2 \exp(-\lambda_2 t) , \qquad (5.1)$$

where $F(t)$ is the fluorescence at time t, $F(\infty)$ is the fluorescence after equilibration, λ_1 and λ_2 are the apparent rate constants of the slow and fast phases, respectively, and F_1 and F_2 are the amplitudes of the respective phases. I denote the amplitudes of the slow and fast phases relative to the total change as α_1 and α_2, respectively, where $\alpha_1 + \alpha_2 = 1$.

Figure 5.2 shows the dependence on GuHCl concentration of the apparent rate constants (λ_1 and λ_2) of the slow and fast phases and the amplitude (α_2) of the fast phase. The initial points of the fast and slow phases, which were obtained by extrapolation to time zero of the respective phases, are shown in Figure 5.1. As can be seen, the initial points of the fast phase fell on a line expected for the dependence on GuHCl concentration of the fluorescence of

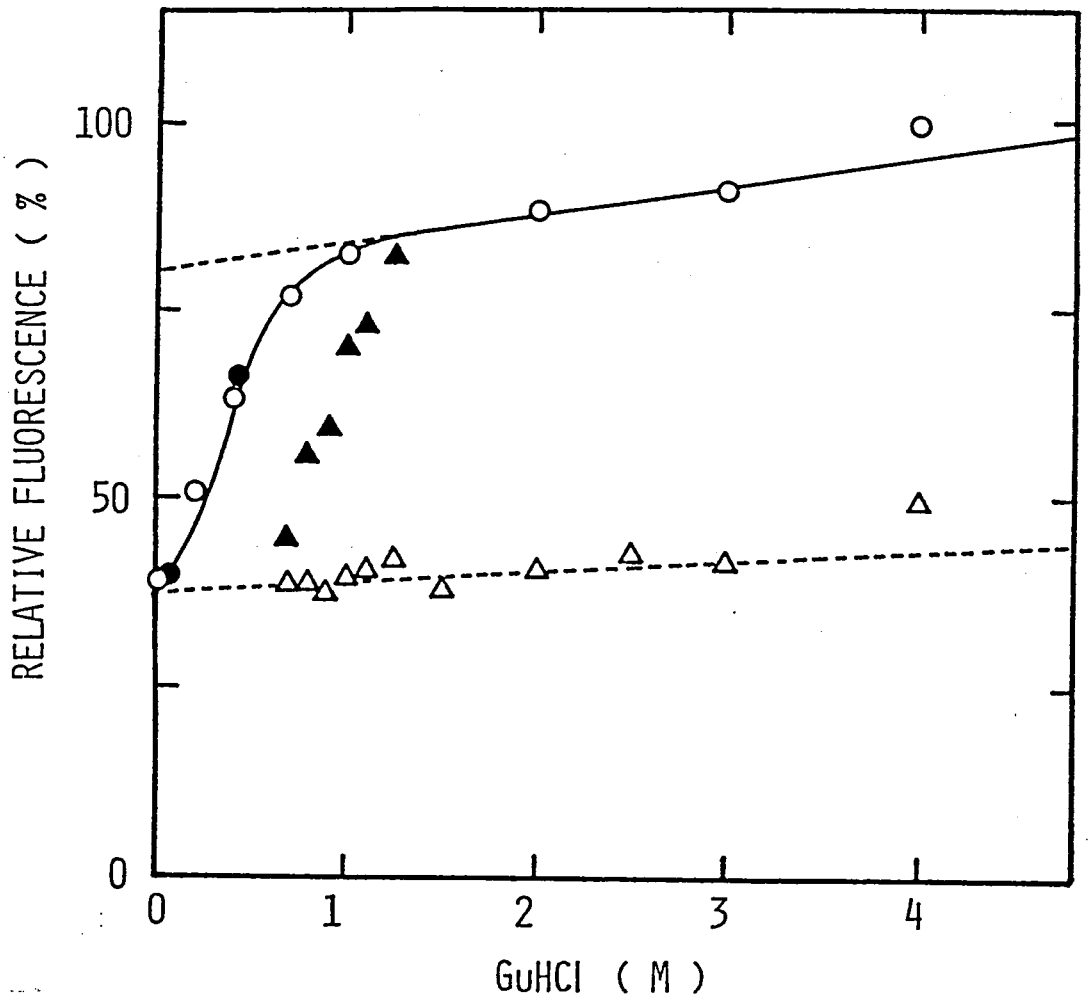

Fig. 5.1. Equilibrium and kinetic data for the denaturation of the reduced C_L fragment by GuHCl. pH 7.5, 25°C. Measurements were carried out by fluorescence using a stopped-flow apparatus at a protein concentration of 0.02 mg/ml. The initial concentrations of GuHCl for unfolding (○) and refolding (●) equilibria were 0 M and 4 M, respectively. The initial points of the slow and fast phases of unfolding kinetics are shown by ▲ and △, respectively. They were obtained by extrapolating the respective phases to time zero. Initial conditions for unfolding kinetics: 0 M GuHCl, protein concentration, 0.04 mg/ml. The solid line indicates the theoretical curve constructed using Eqs. (3.1) and (3.2) and the values of Δn and $\Delta G_D^{H_2O}$ obtained on the basis of k = 0.6 (Table 3.II) (see Chapter 3).

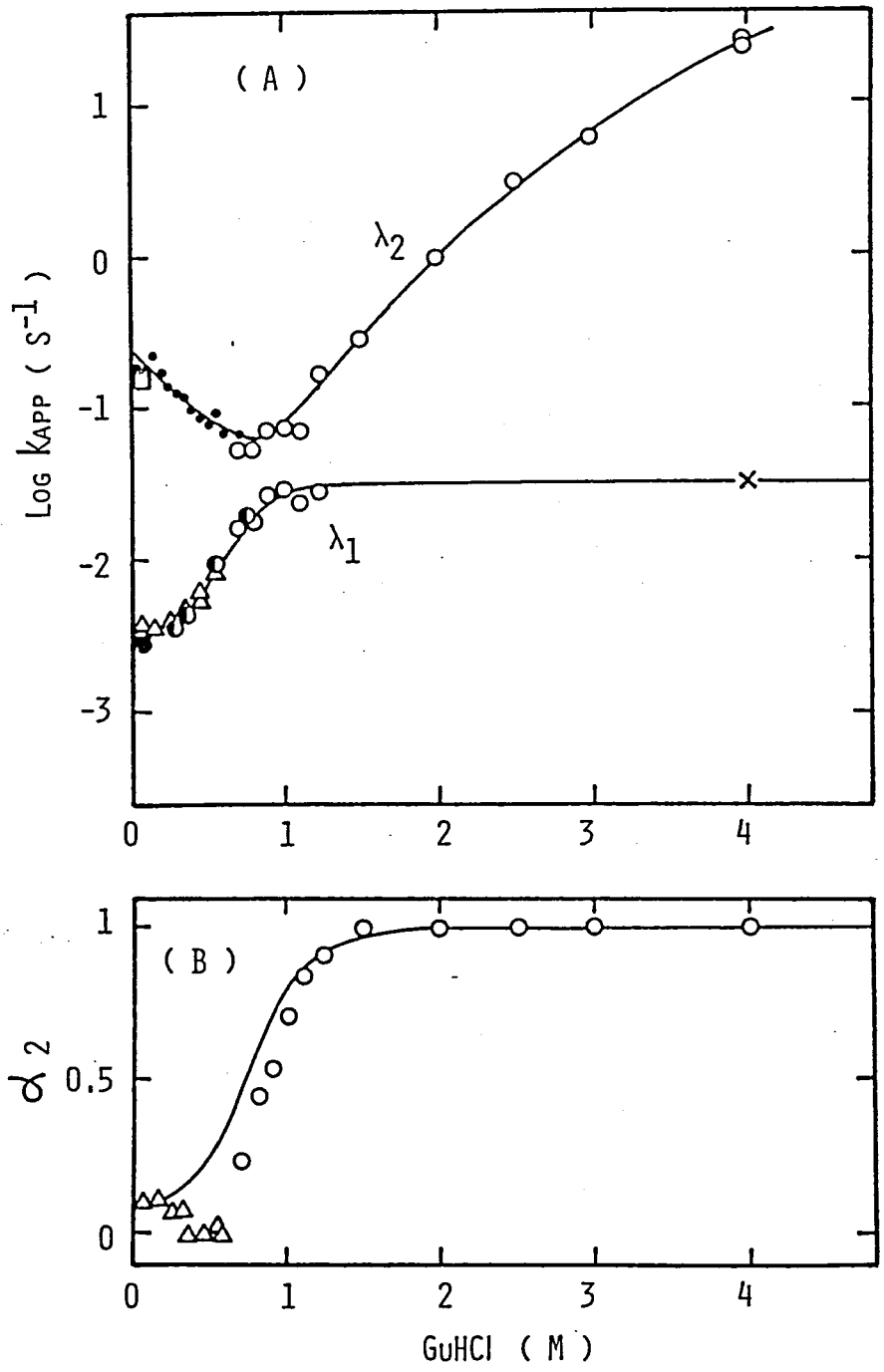

Fig. 5.2. See the next page.

Fig. 5.2. The dependence on GuHCl concentration of the apparent rate constnats (λ_1 and λ_2) (a) and the relative amplitude (α_2) of the fast phase (b) for unfolding and refolding kinetics of the reduced C_L fragment. pH 7.5, 25°C. (○), from unfolding kinetics obtained by stopped-flow fluorescence measurements. The conditions are as deacribed in the legend to Fig. 5.1; (◐), from unfolding kinetics measured by fluorescence at 400 nm using manual mixing. Initial conditions: protein concentration, 1 mg/ml, 0 M GuHCl. Final conditions: protein concentration, 0.02 mg/ml, the indicated concentration of GuHCl; (△), from refolding kinetics measured by fluorescence at 400 nm using manual mixing. Initial conditions: protein concentration, 1 mg/ml, 4 M GuHCl. Final conditions: protein concentration, 0.02 mg/ml, the indicated concentration of GuHCl; (●), from refolding kinetics measured by CD at 218 nm. Initial conditions: protein concentration, 7 mg/ml, 4 M GuHCl. Final condition: protein concentration, 0.2 mg/ml, 0.1 M GuHCl; (X), the apparent rate constant of the isomerization process of U_2 to U_1 in mechanism 5.1 after unfolding measured by double-jump experiments. The conditions are as described in the legend to Fig. 5.3. The dots below 0.7 M GuHCl show the values of λ_2 calculated using the microscopic rate constants in Fig. 5.7 (see the text). The square shows the value of λ_2 calculated using the result of double-jump experiment (see the text). The solid line in (b) indicates the value of α_2 calculated using $K_{21} = 10$ and the value of f_N obtained from the equilibrium measurement (see the text).

native protein. This shows that the total unfolding process was seen in these experiments. The apparent rate constants obtained using manual mixing agreed with those of the slow phases obtained using stopped-flow mixing.

As shown in Figure 5.2, the apparent rate constant (λ_1) of the slow phase increased with an increase in GuHCl concentration and tended to level off above 1 M GuHCl. The apparent rate constant (λ_2) of the fast phase, though I determined it only above 0.7 M GuHCl, increased with an increase in GuHCl concentration. The amplitude (α_2) of the fast phase increased from about 0.2 at 0.7 M GuHCl to 1.0 above 1.5 M GuHCl. The values of λ_1 and its dependence on GuHCl concentration were very similar to those for the intact C_L fragment, except that the curve for the reduced C_L fragment shifts by about 1 M to a lower concentration region of GuHCl (see Figure 4.3(a) in Chapter 4). As explained for the unfolding of the intact C_L fragment in Chapter 4, the results of Figure 5.2 suggest that the unfolding kinetics of the reduced C_L fragment also follows the three-species mechanism,

$$U_1 \underset{k_{21}}{\overset{k_{12}}{\rightleftharpoons}} U_2 \underset{k_{32}}{\overset{k_{23}}{\rightleftharpoons}} N \qquad \text{(Mechanism 5.1)}$$

where N is native protein, U_1 and U_2 are the two forms of unfolded protein, and k_{12}, k_{21}, k_{23}, and k_{32} are the rate constants for the respective processes.

For the intact C_L fragment, I have demonstrated the presence of two forms of the unfolded C_L fragment by double-jump method

(Brandts et al., 1975; Nall et al., 1978). This method was also used here to confirm whether two forms are present in the unfolded molecule of the reduced C_L fragment. The result is shown in Figure 5.3. The reduced C_L fragment was first denatured by 4 M GuHCl, and then refolding was initiated at 0.06 M at various times in the denaturing conditions. Unfolding of the reduced C_L fragment in 4 M GuHCl was complete within 1 sec. As shown in Figure 5.3, the amplitude of the slow phase of refolding was dependent on the time of exposure of the protein to 4 M GuHCl. This indicates that there exist the fast-refolding species (U_2) and slow-refolding species (U_1) in the unfolded reduced C_L molecule and that the former converts slowly to the latter in 4 M GuHCl. The apparent rate constant for the interconversion between U_1 and U_2 was estimated to be 3×10^{-2} s^{-1}, which is very similar to that for the intact C_L fragment. As shown in Figure 5.3, however, the slow phase did not disappear and amounted to 20 % of the total amplitude even at time zero. This will be discussed later (section 5.C.1). As in the case of the intact C_L fragment, the rate of the interconversion estimated from the double-jump experiments agreed well with the values of λ_1 obtained from the unfolding experiments at high concentrations of GuHCl. These results obtained by double-jump experiments strongly suggest that the unfolding kinetics of the reduced C_L fragment follow the three-species mechanism, in which the equilibrium constant K_{21} ($= k_{21}/k_{12}$) is independent of GuHCl concentration.

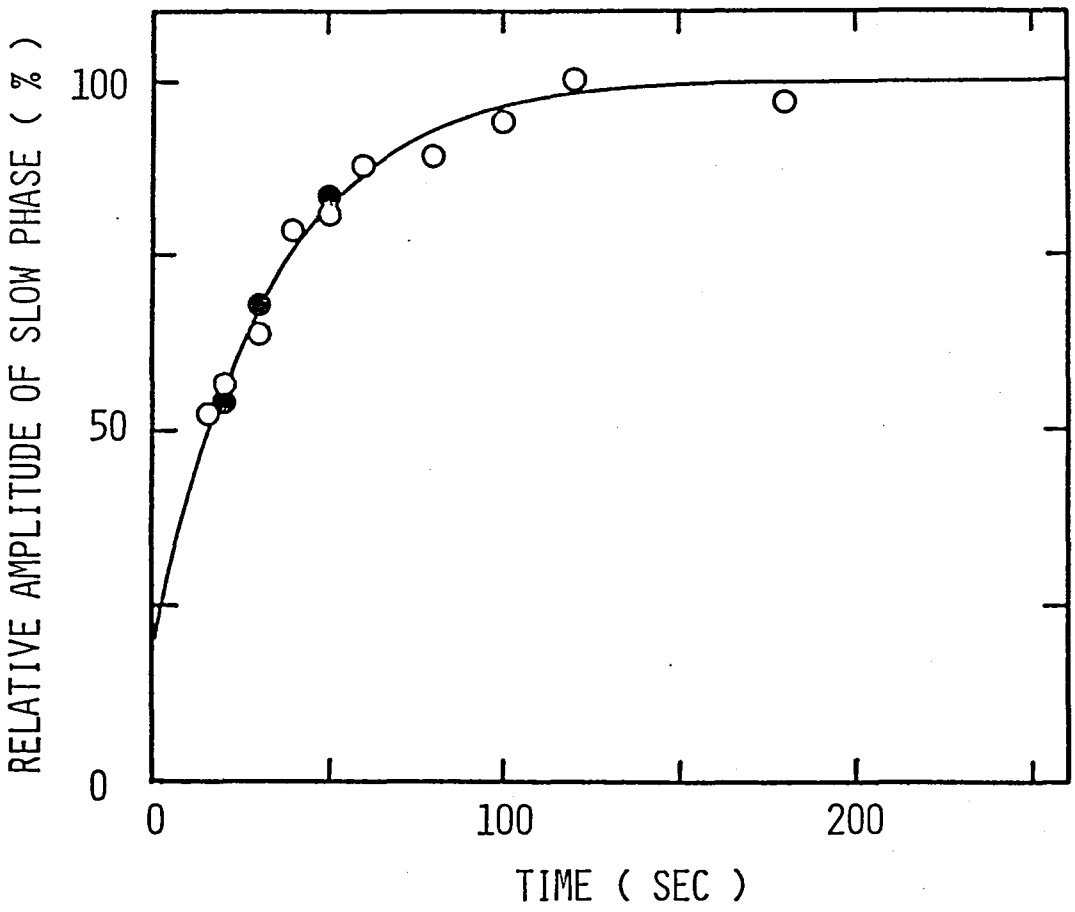

Fig. 5.3. A double-jump experiment measuring the process of U_2 to U_1 in mechanism 5.1 after unfolding. pH 7.5, 25°C. Formation of the U_1 species was monitored by taking samples at the indicated times of unfolding and measuring the refolding kinetics by fluorescence at 400 nm (○) or at 350 nm (●). All the mixing procedures were made manually. The ordinate shows the fluorescence change for the slow phase observed in refolding process relative to the maximum fluorescence change obtained at infinite time in the unfolding conditions. Initial conditions: 0 M GuHCl, protein concentration, 2.5 mg/ml. Unfolding conditions: 4 M GuHCl, protein concentration, 1.2 mg/ml. Refolding conditions: 0.07 M GuHCl, protein concentration, 0.02 mg/ml. The solid line indicates the theoretical curve with a rate constant of 3×10^{-2} s^{-1}.

5.B.2. Refolding kinetics of reduced C_L fragment

Refolding kinetics of the reduced C_L fragment from 4 M GuHCl measured by fluorescences at 330, 350, and 400 nm were all the same. The kinetics were very slow and the observable process (more than 90 % of the total change) followed first-order kinetics. The amplitudes of the fast phases at 400 nm estimated assuming that the kinetics consists of two phases are included in Figure 5.2(b). The apparent rate constants determined by fluorescence at 400 nm are shown in Figure 5.2(a). They agreed well with the apparent rate constants of the slow phases determined by the unfolding experiments. The agreement of the kinetic parameters obtained from unfolding kinetics with those from refolding kinetics establishes the kinetic reversibility of the folding transition of the reduced C_L fragment.

The kinetics of refolding of the reduced C_L fragment at 0.1 M GuHCl from 2 M GuHCl were also studied by circular dichroism at 218 and 230 nm. The refolding was very slow and the apparent rate constant was found to be 3×10^{-3} s^{-1}, which is independent of the wavelength used and is the same as the rate constant determined by fluorescence measurement (Figure 5.2(a)). The amplitude of the slow phase determined by CD at 218 and 230 nm was about 90 % of the total change of the CD estimated by extending to lower concentrations the linear portion corresponding to the unfolded state in the transition curve. This relative amplitude was the same as that estimated by fluorescence measurement (Figure 5.2(b)). The agreement of the refolding kinetics obtained by fluorescence and CD measurements suggests that there is no intermediate in the refolding process. This is consistent with

the three-species mechanism. The large amplitude of the slow phase at very low concentrations of GuHCl and the low values of λ_1 at very low concentrations of GuHCl compared with the rate constant of isomerization from U_2 to U_1 obtained by the double-jump experiments suggest that the proportion of U_1 to the total unfolded molecule is large.

5.B.3. Titration of SH groups of reduced C_L fragment

Reduced C_L fragment has two SH groups. As described in Chapter 3, these SH groups are buried in the interior of the molecule and the rate of reaction with DTNB is very slow. I studied the reactivities of the SH groups of the reduced C_L fragment toward DTNB at various concentrations of GuHCl. Titration of the SH groups with DTNB at various concentrations was first examined in the absence of denaturant. Between 0.1 and 2.5 mM DTNB, all the titration processes gave the same kinetics; five percent of the total SH groups first reacted rapidly and the remaining 95 % reacted slowly. This shows that the intramolecular process of the reduced C_L fragment is rate-limiting and not the reaction of the exposed SH groups with DTNB.

The titration of the SH groups with 0.5 mM DTNB was carried out at various concentrations of GuHCl. All the titration processes consisted of two phases but the rate constant and the amplitude of the slow phase changed markedly depending on GuHCl concentration. At the highest concentration of GuHCl used (0.7 M), the titration of the SH groups was examined by changing DTNB concentration three times, but the kinetics was independent of DTNB concentration,

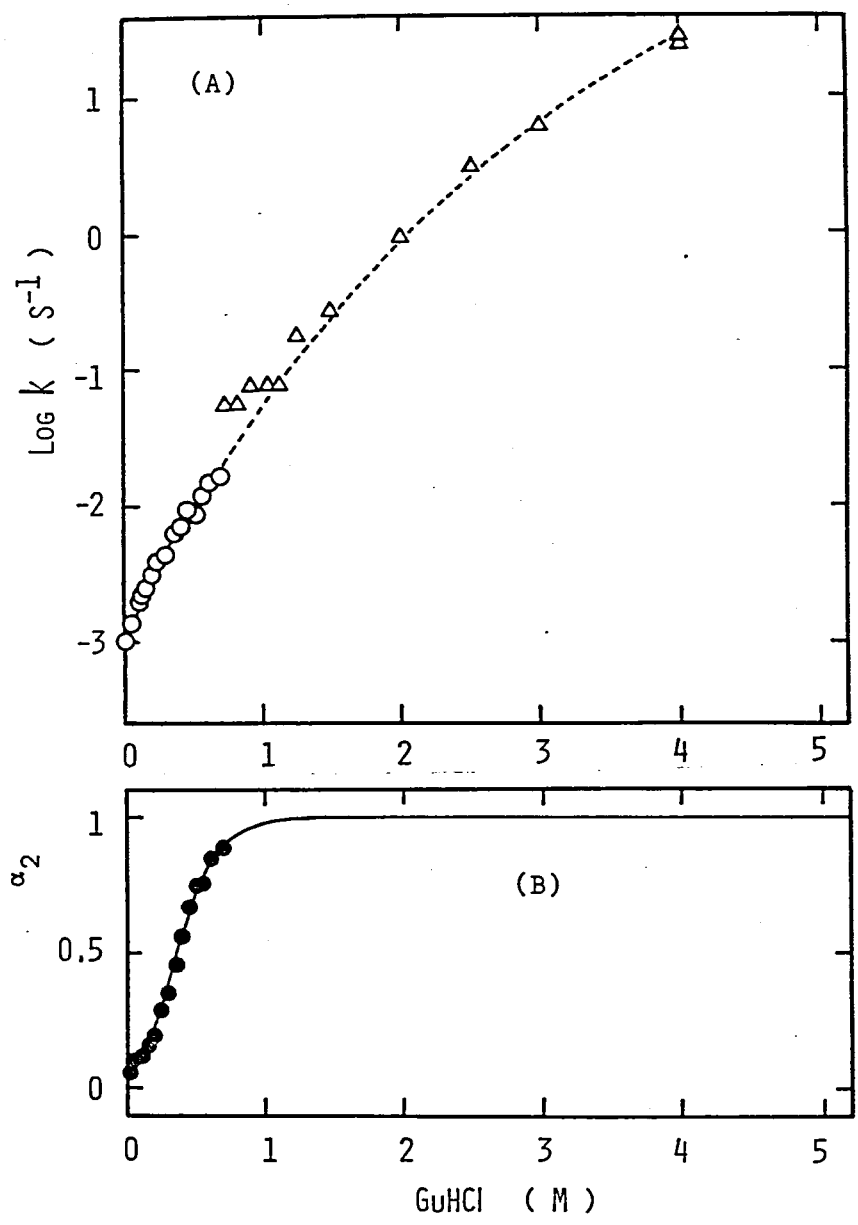

Fig. 5.4. The dependence on GuHCl concentration of the apparent rate constant (○) for the slow phase (A) and the relative amplitude of the fast phase (B) determined by SH titration of the reduced C_L fragment by DTNB. pH 7.5, 25°C. The SH groups of the reduced C_L fragment at a protein concentration of 0.06 mg/ml were titrated with 0.5 mM DTNB and the reaction was monitored by the absorbance change at 412 nm. The triangles in (A) represent the values of λ_2 shown in Fig 5.2(A).

indicating that even at 0.7 M GuHCl the intramolecular process of the reduced C_L fragment is rate limiting in the titration of the SH groups. The dependence on GuHCl concentration of the rate constant of the slow phase and the amplitude of the fast phase are shown in Figures 5.4(a) and (b), respectively. The rate constant of the slow phase increased markedly with increasing GuHCl concentration. These rate constants are on a line obtained by extending the values of λ_2 determined at higher concentrations of GuHCl. The amplitude of the fast phase increased sharply with increasing GuHCl concentration (Figure 5.4(b)). This change is the same as the equilibrium transition curve for unfolding obtained by fluorescence or CD measurement (Figure 5.1, see also Chapter 3). These results are explained in terms of mechanism 5.1. Because the reaction of the exposed SH groups with DTNB is very fast in the presence of excess DTNB (Whitesides et al., 1977), the amplitude of the fast phase should correspond to the proportion of the total amount of the unfolded species (U_1 + U_2) and the amplitude of the slow phase should correspond to the proportion of the folded species (N). Therefore the change with GuHCl concentration in the amplitude of the fast phase should represent the unfolding transition of the molecule. The titration of the buried SH groups of the native molecule is thus rate-limited by the unfolding process and the rate of titration is equal to the rate of the unfolding of the reduced C_L fragment (k_{32}). The value of λ_2 at a high GuHCl concentration represents the value of k_{32} (see section 5.C.1), and the rate constants obtained by SH titration are on a line extending the values of λ_2 at higher

concentrations of GuHCl. This confirms further that the rate constant obtained by SH titration represents the value of k_{32} in mechanism 5.1.

I then studied the reactivities of the SH groups of reduced C_L fragment toward DTNB at various temperatures. The titration process of the SH groups with 0.5 mM DTNB in the absence of denaturnat changed markedly depending on the temperature. With increasing the temperautre, the rate constant of the slow phase increased markedly (Figure 5.5) and the amplitude of the fast phase increased gradually below 30°C and sharply above 35°C (Figure 5.6). It was established from the SH titration of reduced C_L fragment at various GuHCl concentrations that the relative amplitude of the fast phase corresponds to the proportion of unfolded molecule and the rate constant for slow process corresponds to the rate of unfolding of the native molecule. Thus, although I did not examine the thermal unfolding of the reduced C_L fragment by other methods, the transition curve in Figure 5.6 should represent the thermal unfolding of the reduced C_L fragment and the dependence on temperature of the rate constant of slow phase should represent the temperature dependence of the unfolding rate (k_{32}) of the reduced C_L fragment. The apparent midpoint of thermal denaturation for the reduced C_L fragment estimated from Figure 5.6 was 43°C. The Arrhenius plot of the unfolding rate (k_{32}) fits a straight line over the wide temperature range of 15°C to 47°C and the slope gives an activation energy of 34.8 kcal mol^{-1}.

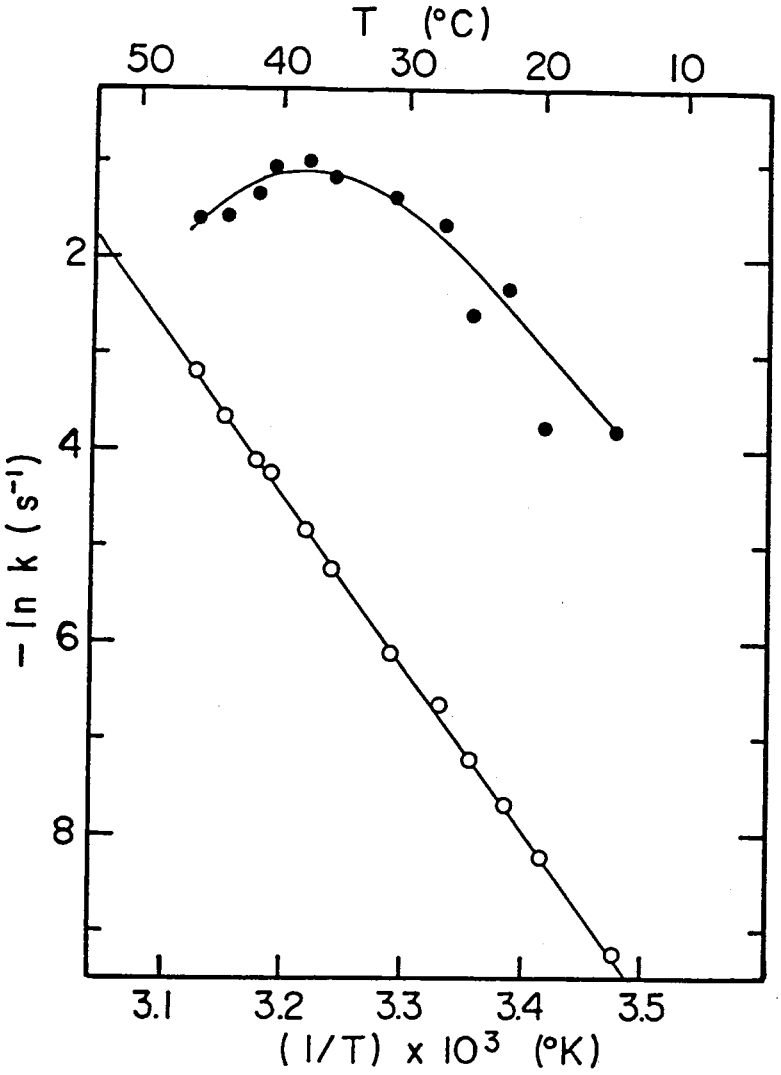

Fig. 5.5. The temperature-dependence of the apparent rate constant (O) for the slow phase determined by SH titration of the reduced C_L fragment by DTNB. The conditions are as described in the legend to Fig. 5.5. The closed circles represent the refolding rate (k_{23}) calculated with equation (5.2) and the values for K_{21} (= 10), f_D, and k_{23} (see the text).

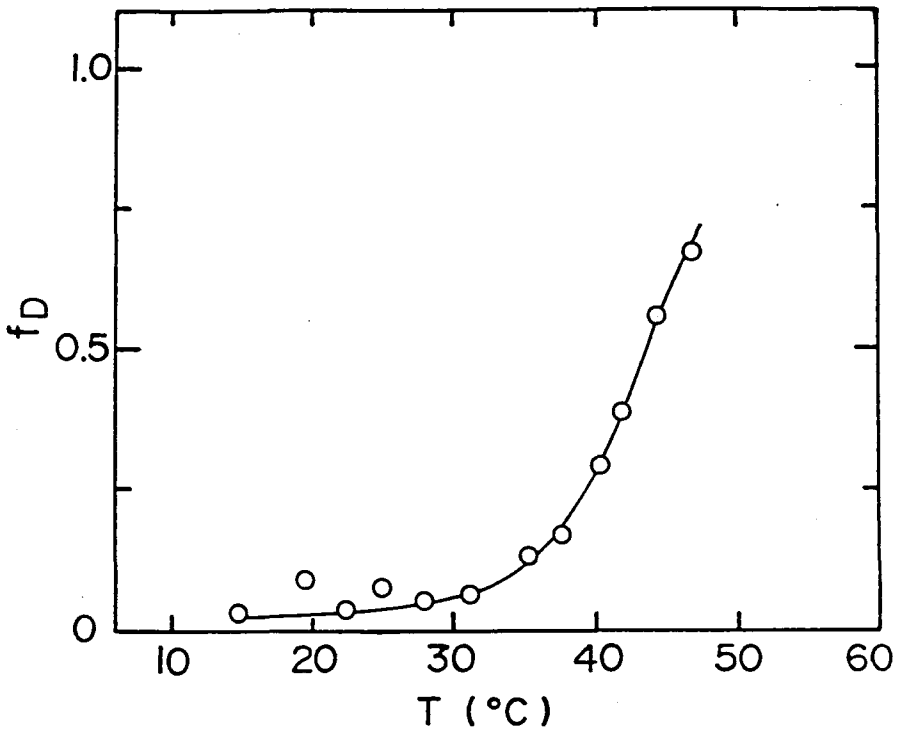

Fig. 5.6. The temperature-dependence of the relative amplitude of the slow phase determined by SH titration of the reduced C_L fragment by DTNB. pH 7.5. The SH groups of the reduced C_L fragment at a protein concentration of 0.06 mg/ml were titrated with 0.5 mM DTNB and the reaction was monitored by the absorbance change at 412 nm.

5.C. Discussion

5.C.1. Folding mechanism of reduced C_L fragment

I have described the kinetics of unfolding and refolding of the reduced C_L fragment as measured by tryptophyl fluorescence, CD and by reactivities of the SH groups toward DTNB. All the kinetic data obtained here are found to be consistent with the three-species mechanism, $U_1 \leftrightarrow U_2 \leftrightarrow N$. As described in Chapter 4, an intermediate is formed during the refolding process of the intact C_L fragment below the transition zone but not inside the zone. In the refolding of the reduced C_L fragment, however, I did not observe any intermediate. As shown in Figure 5.1 (see also Chapter 3), the unfolding transition of the reduced C_L fragment begins at a very low GuHCl concentration and thus I could study the refolding only in the transition zone. If I could study the refolding of the reduced C_L fragment far below the transition zone, I might have found an intermediate during the refolding process.

The rate constants in mechanism 5.1 can be determined essentially by the same way as described for the intact C_L fragment (Chapter 4). The value of $(k_{12} + k_{21})$ for the interconversion between U_1 and U_2 was determined to be 3×10^{-2} s^{-1} by the double-jump experiment. If the value of λ_1 at a very low concentration is assumed to be equal to k_{12}, the value of K_{21} $(= k_{21}/k_{12})$ is estimated to be about 10. Since the unfolding transition of the reduced C_L fragment begins at a very low GuHCl concentration, it is uncertain whether the value of λ_1 at a low GuHCl concentration is exactly the same as the value of k_{12}. However, I tentatively assumed the value of K_{21} to be 10.

This value is the same as the value of K_{21} for the intact C_L fragment. The value of k_{32} below 0.7 M GuHCl was directly obtained from the titration of the SH groups with DTNB (Figure 5.4(a)). The value of k_{23} is obtained by the relation,

$$k_{23} = k_{32} (1 + K_{21}) (1 - f_D)/f_D \ , \qquad (5.2)$$

using the values of f_D (the proportion of the total unfolded molecule) determined by the titration of the SH groups with DTNB (Figure 5.4(b)).

Although only the values of λ_1 are availabel below 0.7 M GuHCl, the values of k_{12} and k_{21} can be calculated with equation (4.3) and (4.4) (Chapter 4) and the known values of k_{23}, k_{32}, f_D, and λ_1 and the assumed value of K_{21}. Between 0.7 and 1.2 M GuHCl, the values of λ_1, λ_2, and α_2 are available and thus the four microscopic rate constants in mechanism 5.1 can be determined with equations (4.3) to (4.6) in Chapter 4. In the region far above the transition zone, the value of λ_2 equals the k_{32}, because k_{23} should be small.

The four microscopic rate constants thus obtained at various concentrations of GuHCl are shown in Figure 5.7(a). In Figure 5.7(b) the values of f_D in the region of 0.7 to 1.2 M GuHCl calculated using the kinetic parameters are shown. It can be seen that they fall on the equilibrium curve obtained by fluorescence or CD measurement. With increasing concentration of GuHCl, k_{23} decreases and k_{32} increases sharply. This is expected for the rates of conformational transition of proteins. The values of k_{23} and k_{32} are the same at 0.8 M GuHCl, which is higher by 0.4 M GuHCl than the apparent midpoint of the equilibrium transition. This difference is due to the presence of the two forms of the unfolded species and has been discussed for the intact

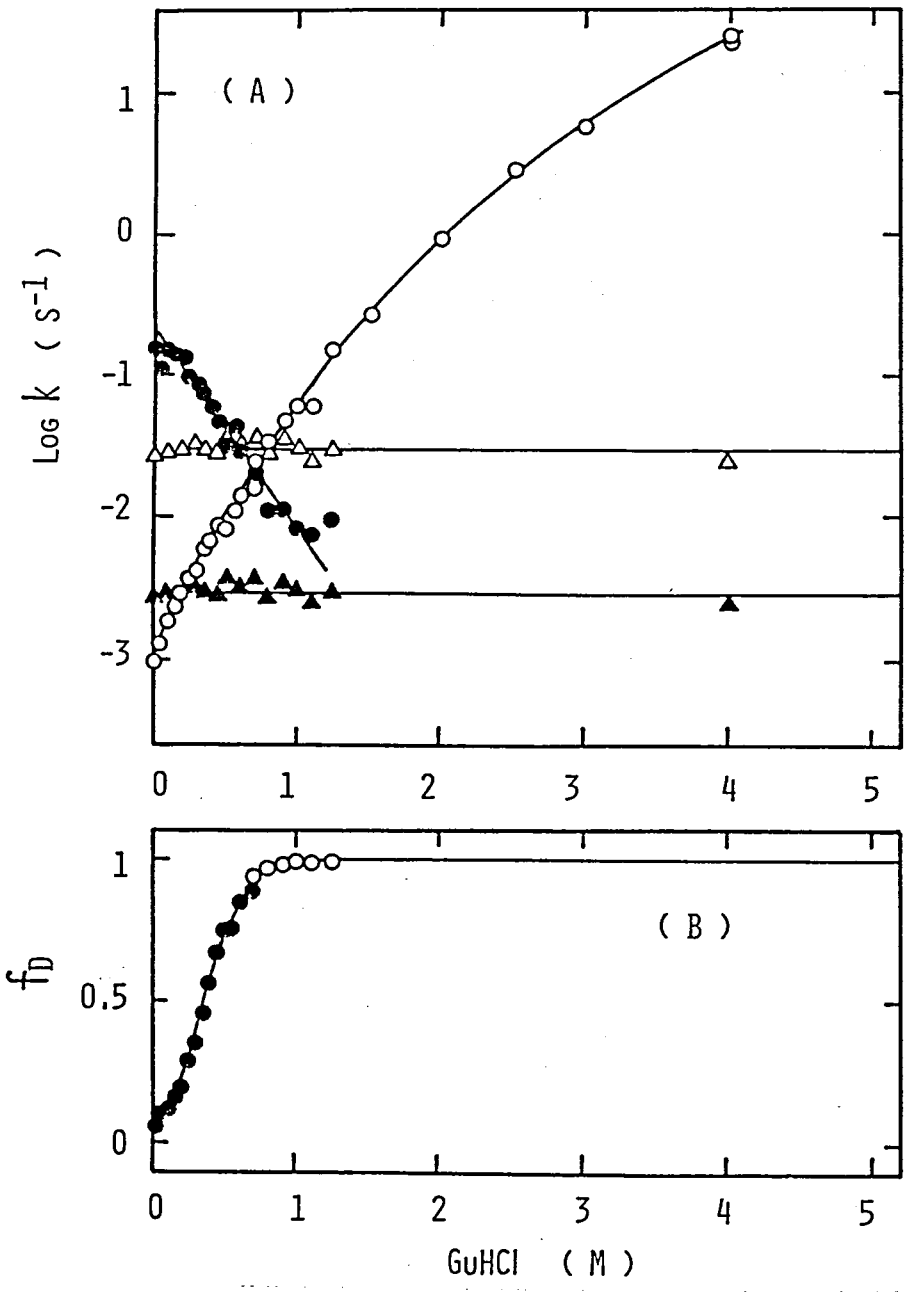

Fig. 5.7. The dependence on GuHCl concentration of the microscopic rate constants estimated based on mechanism 5.1 for folding of the reduced C_L fragment (A) and the transition curve for unfolding obtained from kinetic measurements (B). pH 7.5, 25°C. (A) (○), k_{32}; (○), k_{23}; (△), k_{21}; (▲), k_{12}. (B) (●), the amplitude of the fast phase determined by SH titration shown in Fig. 5.4(B); (○), the fraction of the unfolded species calculated using the four microscopic rate constants. The solid line indicates the transition curve for unfolding obtained from equilibrium measurement.

C_L fragment in Chapter 4. The rates of the isomerization process (k_{12} and k_{21}) are independent of GuHCl concentration. These results confirm the validity of the above assumption that K_{21} equals to 10 and is independent of GuHCl concentration.

The values of λ_2 below 0.6 M GuHCl, where the values of λ_2 could not be measured directly by our procedure, can be calculated using the above microscopic rate constants (see equation 4.2 in Chapter 4). The values of λ_2 thus calculated are given in Figure 5.2. The calculated λ_2 values agreed well with the value obtained experimentally at 0.7 M GuHCl and increases with decreasing GuHCl concentration. The dependence of λ_2 on GuHCl concentration has a minimum at about 0.8 M GuHCl. The appearance of the minimum is expected from mechanism 5.1 (see Chapter 4). The solid line in Figure 5.2(b) shows the values of α_2 expected under the limiting conditions where $\lambda_2/\lambda_1 \gg 1$ (see equation 4.9). The observed values of α_2 inside the transiton zone are smaller than these values in the limiting conditions. Similar observation has been reported for ribonuclease A (Brandts et al., 1975; Hagerman & Baldwin, 1976). Hagerman (1977) has discussed the amplitude of the fast phase in mechanism 5.1 which is expressed as a function of the ratio of the two apparent rate constants (λ_1/λ_2) at a fixed values of f_N and K_{21} and shown that under the conditions where the ratio of λ_2/λ_1 is not so large, α_2 is expected to be smaller than the value of α_2 under the limiting conditions. As can be seen from Figure 5.2, the separation of λ_2 and λ_1 at about 1 M GuHCl is actually not so large. In the case of the intact C_L fragment (Figure 4.3 in Chapter 4), λ_2 is well separeted from λ_1 at all the concentra-

tions of GuHCl studied and the observed values of α_2, except below the transiton zone where an intermediate emerges, are nearly equal to the values of α_2 under the limiting conditions.

In the double-jump experiments (Figure 5.3), the slow phase of refolding did not disappear and amounted to about 20 % of the total change at time zero. The relation between the relative amplitude and the ratio of the two apparent rate constants (λ_2/λ_1) is extended to the analysis of the results obtained by the double-jump experiments. The relative amplitude of the fast phase at time zero obtained by the double-jump experiment is expressed as a function of λ_2/λ_1 by

$$\alpha_2 = \left\{ 1 - (\lambda_2/\lambda_1) \frac{a - (1 + 2K_{21}f_N^s) + (\lambda_2/\lambda_1)}{a - (\lambda_2/\lambda_1)(1 + 2K_{21}f_N^s) + 1} \right\}^{-1}, \quad (5.3)$$

where

$$a = -\left\{ \left[(\lambda_2/\lambda_1) - 1 \right]^2 - 4(\lambda_2/\lambda_1)K_{21}f_N^f \right\}^{1/2} .$$

In equation (5.3), f_N^s is the proportion of the native molecule at the start of unfolding and f_N^f is the proportion of the native molecule when refolding is complete under specified conditions. This equation can be applied to the case where the unfolding of N to U_2 is complete and refolding is initiated prior to conversion from U_2 to U_1. This equation predicts that, in the refolding condition where f_N^f is nearly equal to f_N^s, α_2 approaches 1 when the ratio of λ_2/λ_1 is extremely high and α_2 becomes smaller than 1, i.e., the slow phase does not disappear at time zero when λ_2 is not so large compared with λ_1.

I analyzed the result of the double-jump experiment using equation (5.3) and estimated the apparent rate constant of the fast phase (λ_2) in the refolding conditions where the value of λ_2 was difficult to determine experimentally. Using $K_{21} = 10$, $f_N^s = 0.95$, $f_N^f = 0.90$, and $\alpha_2 = 0.8$ in equation (5.3), a value of about 50 is obtained for (λ_2/λ_1). When a value of 3×10^{-3} s^{-1}, which was obtained directly from the refolding experiments, is used for λ_1, we obtain a value of 0.15 s^{-1} as the value of λ_2. This value agrees quite well with the value obtained using the microscopic rate constants (Figure 5.2).

From the titration of the SH groups of the reduced C_L fragment, I obtained the temperature dependences of f_D and k_{32} (Figure 5.5 and 5.6). The equilibrium constant for cis-trans isomerization of prolyl residue is relatively insensitive to the temperature change (Chang & Bovey, 1977; Roques et al., 1977). Thus assuming that K_{21} in mechanism 5.1, which probably represents the cis-trans isomerization of Pro 143 (Chapter 4.C.2), is constant ($K_{21} = 10$) between 15°C and 47°C, I obtained the refolding rate (k_{23}) by equation (5.2) and using f_D and k_{32} obtained by the SH titration (Figure 5.5). Contrary to the unfolding rate (k_{32}), the refolding rate (k_{23}) thus estimated showed a maximum at about 35°C. This indicates that, while the unfolding is an elemetary reaction with a usual positive activation energy, the refolding rate consists of at least two component. Similar obsevations for the rates of unfolding and refolding have been reported on lysozyme (Segawa et al., 1973) and chymotrypsinogen A (Pohl, 1976) and it may be a common property of proteins. Although

these thermal property of rates for conformational transiton should be closely correlated with a rate limiting step of protein folding (see section 5.C.2). it is yet difficult to interpret them with present data alone.

5.C.2. Kinetic role of intrachain disulfide bond

I now obtained the four microscopic rate constsnts in the three-species mechanism for the folding kinetics of the reduced C_L fragment. As described in Chapter 4, I also obtained the microscopic rate constants for the intact C_L fragment under the conditions where the kinetics follow the three-species mechanism. I compare the rate constants for the reduced C_L fragment (Figure 5.7(a)) with those for the intact C_L fragment (Figure 4.13(a) in Chapter 4) and consider the role of the intrachain disulfide bond in the folding of the C_L fragment.

The rate constants of the isomerization in the unfolded state (k_{12} and k_{21}) are the same for both proteins and the slow-refolding species amounts to about 90 % of the total unfolded species for both proteins. This indicates that the two forms of the unfolded species are formed irrespective of the presence of the intrachain disulfide bond. The two forms of the unfolded species must have been formed by the isomerization of proline residues, and the isomerization process for the reduced C_L fragment is the same as that for the intact C_L fragment. The role of a particular proline residue (Pro 143) in the folding of the intact C_L fragment has been discussed in detail in Chapter 4.C.

The rate constant (k_{32}) of unfolding of the reduced C_L fragment is only slightly greater than that of the intact C_L fragment. Only the rate constant (k_{23}) of folding from the fast-folding species to native protein differs greatly between the two proteins.

Although the rate constants k_{23} for both proteins were obtained in different concentration ranges of GuHCl because of their different stabilities, the marked difference of k_{23} is apparent. When we compare the values of k_{23} at 1.0 M GuHCl, where the rate constants for both proteins were determined experimentally, the rate constant for the intact C_L fragment is about 100 times greater than that for the reduced C_L fragment. The large increase in the rate constant of refolding by the presence of the intrachain disulfide bond indicates the importance of the disulfide bond in the direct folding transition of the C_L fragment.

As described in Chapter 3, the stability of the C_L fragment decreases upon reduction of the intrachain disulfide bond. This is due mostly to the decreased rate constant (k_{23}) from U_2 to N for the reduced C_L fragment. The process from U_2 to N is important to understand the folding of the C_L fragment and I consider this process in detail. In Chapter 3, I estimated the free energy change of denaturation of the C_L fragment using a two-state approximation for the equilibrium transition. As described in Chapter 4, however, when two forms of the unfolded species (U_1 and U_2) are present, the apparent equilibrium constant (K_{app}) of native protein to the total unfolded protein may be expressed by

$$K_{app} = ((U_1) + (U_2))/(N) = K_{32}(1 + K_{21}), \qquad (5.4)$$

where

$$K_{32} = (U_2)/(N) = k_{32}/k_{23} .$$

Thus the apparent free energy change of denaturation ($- RT \cdot \ln K_{app}$) is smaller by $RT \cdot \ln(1 + K_{21})$ than the true free energy change ($- RT \cdot \ln K_{32}$). The term $RT \cdot \ln(1 + K_{21})$ is calculated to be 1.4 kcal mol^{-1} using $K_{21} = 10$ at 25°C for the intact and reduced C_L fragments.

I first constructed the free-energy diagrams of the folding and unfolding of the intact and reduced C_L fragment at 1.0 M GuHCl, where the rate constants of unfolding and refolding (k_{23} and k_{32}) were determined experimentally for both proteins. The transition state free energy, $\Delta G^{\ddagger}$, is calculated using the relation,

$$\Delta G^{\ddagger} = - RT \cdot \ln(kh/k_B T), \qquad (5.5)$$

where k is the rate constant, h is Planck's constant, k_B is Boltzmann's constant, T is the temperature in degrees Kelvin, and R is the gas constnat.

Figure 5.8(a) shows the profiles at 25°C constructed by setting the native states for both proteins at the same energy level. The free energy change of denaturation estimated using the rate constants of unfolding and refolding is 2.0 kcal mol^{-1} for the intact C_L fragment and - 1.2 kcal mol^{-1} for the reduced C_L fragment. These values are in good agreement with those calculated using equation (5.4) and the equilibrium transition data in Chapter 3.

Figure 5.8(b) shows the free-energy profiles in the absence of GuHCl. The profile for the reudced C_L fragment can be constructed directly using the values of k_{23} and k_{32}. Because the values of k_{23} and k_{32} for the intact C_L fragment in the absence of GuHCl were not determined, I constructed the profile assuming that the difference in k_{32} in the absence of GuHCl between the intact C_L fragment and

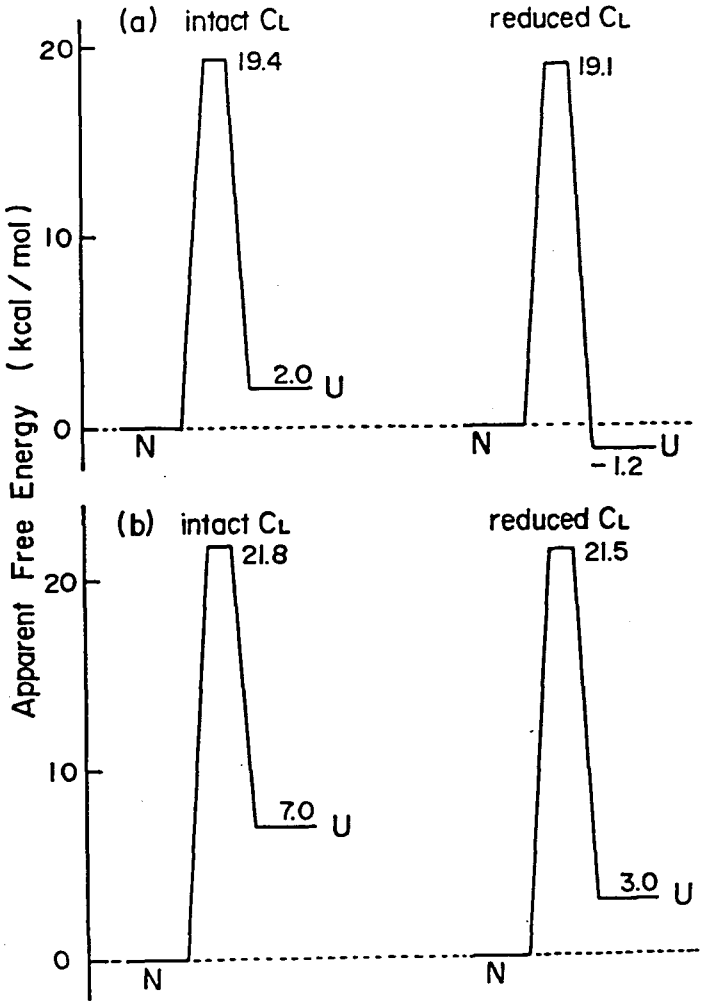

Fig. 5.8. Free-energy profiles for the unfolding and refolding of the intact and reduced C_L fragments in the presence of 1 M GuHCl (a) and in the absence of GuHCl (b). pH 7.5, 25°C. N and U represent the native and denatured states, respectively. The energy levels of the native states of the intact and reduced C_L fragments were set to zero (see the text).

reduced C_L fragment is the same as that in the presence of 1.0 M GuHCl and using the true free energy change of denaturation in the absence of GuHCl which is calculated with equation (5.4) and the equilibrium transition data described in Chapter 3. The rate constant of refolding of the intact C_L fragment is estimated to be about 80 s^{-1} from this energy profile.

When the free energies for the intact and reduced C_L fragments are assumed to be the same in the native state, the energy levels of the transition state for both proteins are very similar and only the energy levels in the denatured state are different between the two proteins. In Chapter 3, I showed that the decrease in the stability of the C_L fragment on reduction of the disulfide bond is consistently explained in terms of the increase in the entropy of the denatured state. Provided that this is the case, the free-energy profile shows that the change in the refolding rate is due entirely to the change in the entropy of the denatured state. By the presence of the disulfide bond, the energy level of the denatured state is increased by about 4 kcal mol^{-1}, which is due to the decreased entropy of the denatured state. This results in about 100 times increase in the refolding rate. The other contribution of the disulfide bond to the folding kinetics of the C_L fragment, if any, may be small compared with the entropic effect, and we may thus conclude that the kinetic role of the disulfide bond in the folding of the C_L fragment is largely entropic. This may be applicable to the folding of other proteins with several disulfide bonds.

The energy levels of the denatured states are different between the intact and reduced C_L fragment only because of the different entropies of the denatured proteins but the energy levels of the transition states are the same for both proteins. This means that the presence of the disulfide bond does not affect the rate-limiting step for the conformational transition of the C_L fragment. Several mechanisms have been proposed for protein folding (see, for instance, Baldwin, 1978, 1980). The problem as to the rate-limiting step in the folding pathway is still in controversy. The results obtained here suggest the location of the rate-limiting step when the folding process is measured by the compactness of the molecule. If the rate-limiting step of the folding of the C_L fragment is located near the denatured state, the transition states of the two proteins may be in different energy levels because the loop formed by the disulfide bond is large and thus the entropies of the two proteins in early stage of folding may be different. If we assume that the intact and reduced C_L fragments fold through the same folding pathway, the same energy level for the transition states may be realized only when a compact conformation, for which there is no difference in the conformational entropy between the intact and reduced C_L fragment, is formed at a later stage of folding. The unfolding rates for the intact and reduced C_L fragments are expected to be the same for the transition state with such a compact conformation.

On the basis of his detailed kinetic data of the reduction and oxidation of the three disulfide bonds in bovine pancreatic trypsin inhibitor, Creighton (1977, 1978, 1980a) has constructed the energy

profile of the entire intramolecular transition in the unfolding and refolding of the protein. He has shown that the transition is very cooperative and its rate-limiting step is very close to the native state. The kinetics of formation of the disulfide bonds in ribonuclease A obtained by a similar method (Creighton, 1979) and the results of unfolding and refolding of several proteins obtained by urea-gradient gel electrophoresis (Creighton, 1980b) are also consistent with this idea. Segawa et al. (1973) studied the kinetics of thermal unfolding of lysozyme and suggested that in the transition state the molecule folds tightly, though many intramolecular hydrogen bonds are broken. Although a further study is necessary to define the rate-limiting step in the folding of the C_L fragment, the results are consistent with these suggestions.

Chapter 6

Refolding of immunoglobuin light chain

6.A. Introduction

Immunoglobulin light chain consists of two structural units with molecular weight of about 12,000 each, the amino-terminal variable domain (V_L domain) and the carboxy-terminal constant domain (C_L domain) (Davies et al., 1975; Beale & Feinstein, 1976; Amzel & Poljak, 1979) (see Figure 1.2 in Chapter 1). Both V_L and C_L domains have very similar tertiary structure consisting of two β-sheets (immunoglobulin-fold). The structure of the isolated domains, V_L and C_L fragments, are essentially the same as those in whole light chain and an independent folding of the domains is indicated. Azuma et al. (1972) studied the equilibrium denaturation of type λ Bence Jones proteins (which correspond to the light chain) and showed that the two domains of light chain are denatured independently, i.e., the C_L domain was denatured first at low GuHCl concentrations, followed by denaturation of the V_L domain at higher GuHCl concentrations. Thus the results of the equilibrium denaturation supported the idea of independent folding of the two domains.

On the other hand, interactions between the domains may exist when the functions of immunoglobulin molecule are taken into account. Antigen bindings to the immunoglobulin molecules which occur at the amino-terminal variable domains (V_H and V_L domains) are transmitted to the constant domains which are located at the

carboxy-portion of the molecule and cause various subsequent events, e.g., a complement fixation. One way of exploring the interactions between domains which were not apparent in equilibrium measurements is to examine whether an independence of the domains is retained even during their folding process.

The mechanism of the folding of the C_L fragment has been interpreted in detail (Chapters 3 and 4). I could obtain some V_L fragments. Thus, I studied the refolding of several species of light chain and V_L fragment, and examined whether the refolding kinetics of light chains are explained by the independent folding of the two domains or there exist significant interactions between domains during refolding. The results should not only be important for the interpretation of the structure and function of the immunoglobulin molecule but also cast light on the folding mechanism of proteins with complicated domain structure.

6.B. Results

6.B.1. Structure of Bence Jones proteins and V_L fragments

The result of amino acid analysis showed that V_L fragment of Bence Jones protein Tod consists of 111 or 112 amino acid residues and contains two tryptophyl, six tyrosyl, and three phenylalanyl residues (Table I).

The CD spectrum of Bence Jones protein Nag is shown in Figure 6.1. As in the case of C_L fragment, there was a negative maximum at 218 nm, which is characteristic of β-sheet conformation.

The difference spectrum of Bence Jones protein Nag in 4 M GuHCl referred to the protein in the absence of denaturant is shown in Figure 6.2. The shape of the spectrum is similar to that of the C_L fragment (Figure 3.4), but the value of $\Delta\varepsilon$ at 292 nm (- 3,500 M^{-1} cm^{-1}) for Bence Jones protein Nag is two-fold of the value (- 1,700 M^{-1} cm^{-1}) for the C_L fragment. This value of Bence Jones protein Nag corresponds to the change in the molar extinction coefficient accompanying exposure of two tryptophyl residues from the interior of the molecule to the aqueous environment, one from V_L domain and the other from C_L domain. This is consistent with the presence of one interior tryptophyl residue in each immunoglobulin domain (Davies et al., 1975).

The fluorescence spectra of Bence Jones protein Tod and V_L fragment of Tod are shown in Figure 6.3 with that of the C_L fragment. The spectra of these proteins in 4 M GuHCl were similar and had a maximum at 350 nm. For the intact proteins, however, the maximum wavelength was below 340 nm and the intensity was much lower than

TABLE 6.I. Amino acid composition of type λ V_L(Tod) fragment. Results are based on 24 and 72 h hydrolysis time. The value for tryptophan was obtained after hydrolysis with 6 N HCl containing 4 % thioglycolic acid (Matsubara & Sasaki, 1969)

Amino acid	Residue per molecule
Lysine	3
Histidine	1
Arginine	2
Aspartic acid Asparagine	9
Threonine	12
Serine	17
Glutamic acid Glutamine	10
Proline	6 or 7
Glycine	13
Alanine	6
Cystein	2
Valine	7
Isoleucine	4
Leucine	8
Tyrosine	6
Phenylalanine	3
Tryptophan	2
Total	111 or 112

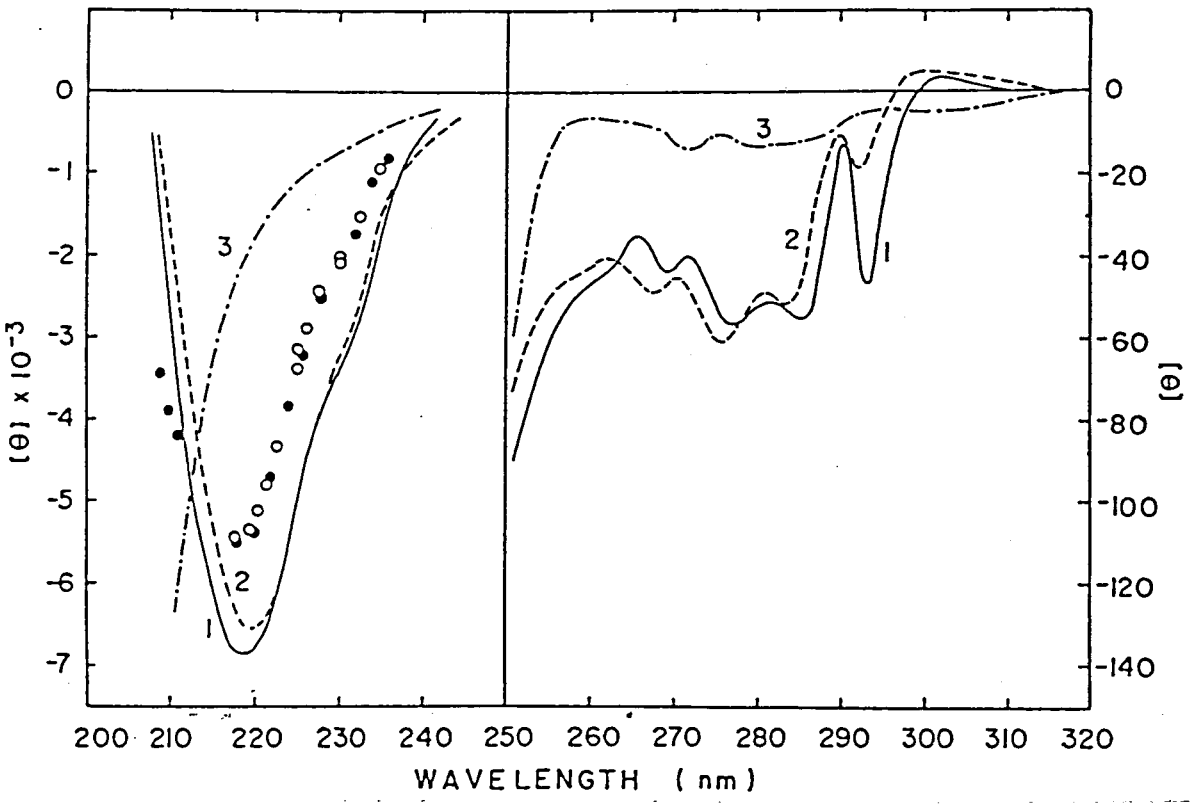

Fig. 6.1. CD spectra of C_L fragment (1) and Bence Jones protein Nag (2) in 0.05 M Tris-HCl buffer containing 0.15 M KCl at pH 7.3, 25°C. Curve 3 shows the spectrum of Bence Jones protein Nag in 4 M GuHCl at pH 7.3, 25°C. Closed and open circles represent zero-time ellipticities obtained by extrapolation of the slow phases in the refolding reactions of Bence Jones protein Nag and C_L fragment, respectively.

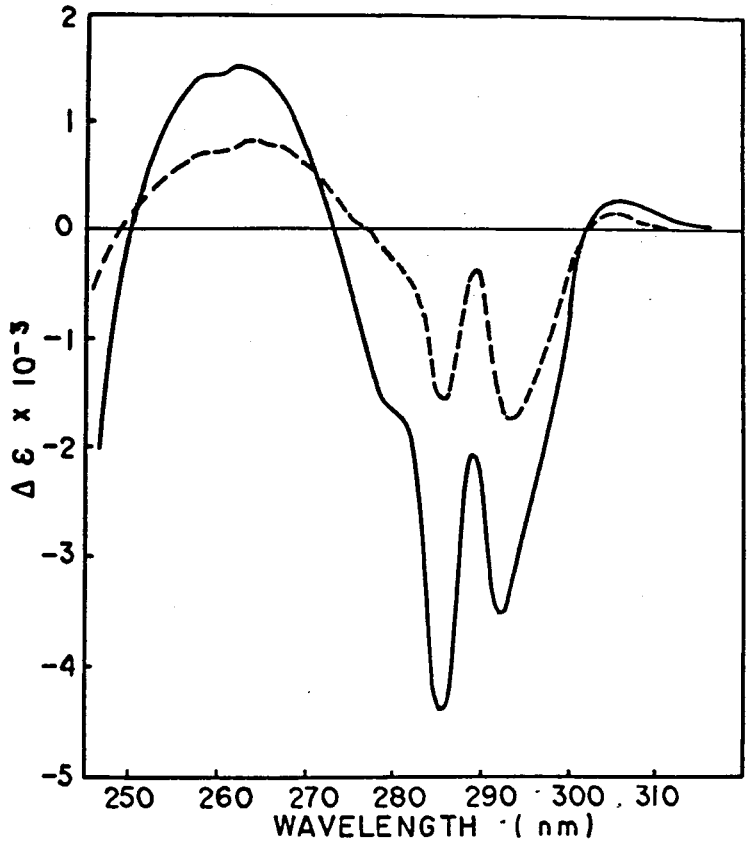

Fig. 6.2. Difference absorption spectra of Bence Jones protein Nag (solid line) and C_L fragment (dotted line) in 4 M GuHCl referred to the protein in Tris-HCl buffer at pH 7.5. 25°C.

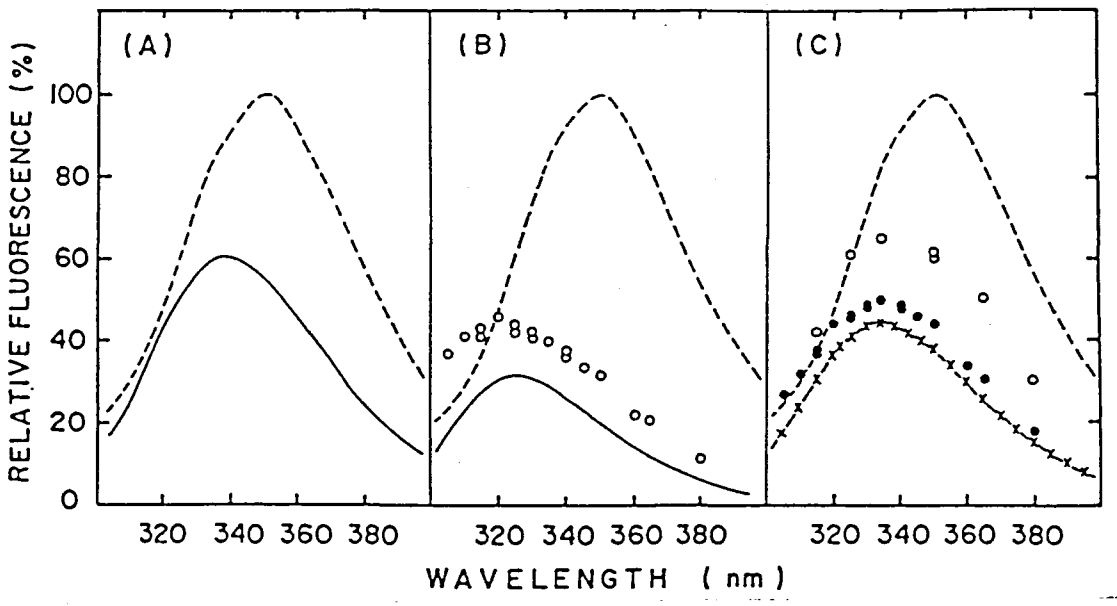

Fig. 6.3. Fluorescence spectra of V_L(Tod) fragment (A), C_L(Nag) fragment (B), and Bence Jones protein Tod (C) at 25°C. The ordinate represents the fluorescence relative to that in the presence of 4 M GuHCl. Solid and broken lines indicate the fluorescences of intact proteins in 0.05 M Tris-HCl buffer containing 0.15 M KCl at pH 7.3 and those of denatured proteins in 4 M GuHCl at pH 7.3, respectively. The excitation wavelength was 280 nm. Concentrations of Bence Jones protein Tod, V_L(Tod) fragment, and C_L(Nag) fragment were 0.05, 0.05, and 0.06 mg/ml, respectively. ×, Fluorescence spectrum of Bence Jones protein Tod calculated using the spectra of V_L(Tod) fragment and C_L(Nag) fragment (see the text); O, zero-time fluorescence obtained by extrapolation of slow phases; ●, the sum of the zero-time fluorescence for C_L(Nag) fragment and fluroescence for intact V_L(Tod) fragment.

in the case of the denatured proteins. The maximum emission wavelength and the maximum intensity were different depending on the protein studied (Table 6.II). This shows that the environment of tryptophyl residues is different in the different proteins and that the tryptophyl fluorescence is greatly quenched in the native state. Similar results were also reported by Pollet et al. (1972). As can be seen from Table 6.II, the shorter the maximum wavelength, the lower the maximum intensity. Since the results of amino aicd analysis show that V_L fragment of Tod contains two tryptophyl residues and that of the C_L domains of type λ Bence Jones protein Nag contain two tryptophyl residues (Table 3.I), four tryptophyl residues exist in Bence Jones protein Tod. Assuming that the fluorescence intensity of denatured protein is proportional to the tryptophyl content, I calculated the fluorescence spectrum of Bence Jones protein Tod using the observed spectra of V_L(Tod) fragment and C_L(Nag) fragment. As shown in Figure 6.3, the calculated spectrum agreed well with the observed spectrum of Bence Jones protein Tod. This shows definitely that the conformations of isolated domains are the same as those in whole light chain and confirmed the structural independence of the two domains. Similar obsevation was also reported by Karlsson et al. (1972b).

Figure 6.4 shows the denaturation curves of Bence Jones protein Nag constructed from the CD measurements at 218 and 257 nm, ultraviolet absorption at 292 nm, and fluorescence at 350 nm. The ordinate of this figure represents the formal degree of unfolding (f_D) calculated as

TABLE 6.II. Fluorescences of type λ Bence Jones proteins, and V_L and C_L fragments in 0.05 M Tris-HCl buffer containing 0.15 M KCl at pH 7.5, 25°C. Excitation wavelength, 280 nm.

Proteins	Maximum emisson wavelength (nm)	Fluorescence intensity[a]
Bence Jones protein Sh	320	0.21
Bence Jones protein Nag	320	0.23
Bence Jones protein Kob	318	0.25
Bence Jones protein Tod	335	0.45
Bence Jones protein Ni	340	0.52
Bence Jones protein Fu	338	0.56
C_L(Nag) fragment	325	0.31
V_L(Tod) fragment	338	0.61
V_L(Fu) fragment	342	0.71

a Relative to the fluorescence intensity of denatured protein in 4 M GuHCl.

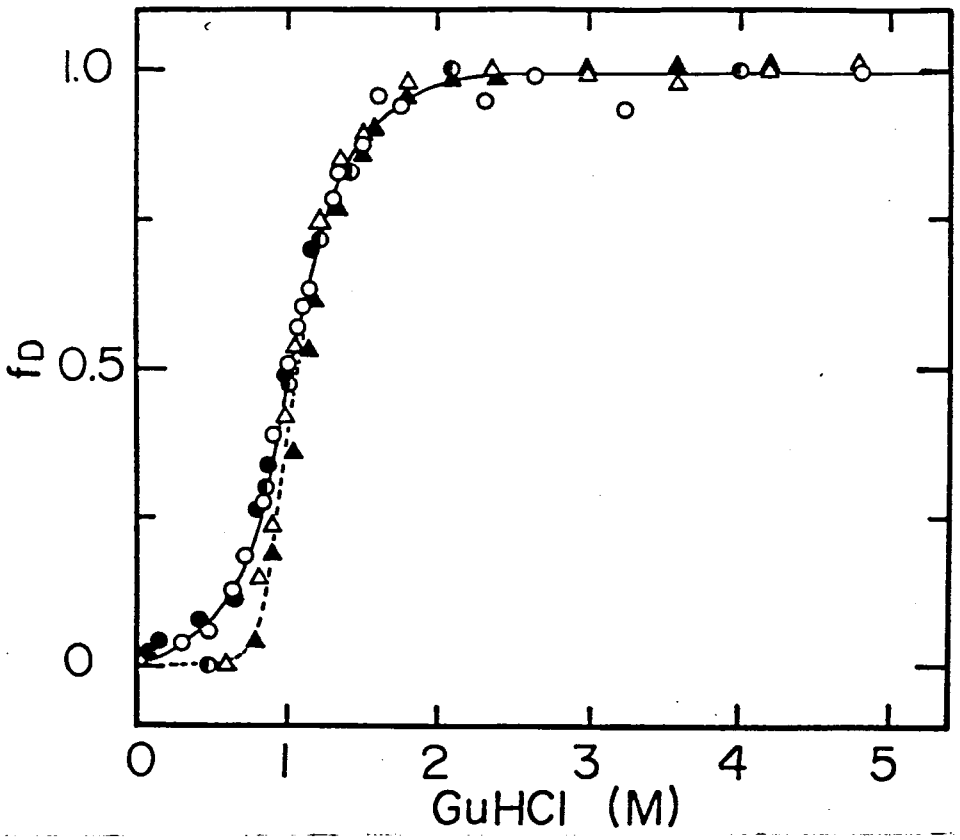

Fig. 6.4. Various physical parameters of Bence Jones protein Nag as functions of GuHCl concentration. 25°C, pH 7.3. The ordinate represents the formal degree of unfolding (f_D) (see the text). ▲, CD at 218 nm; △, CD at 257 nm; ◐, Δε at 292 nm; ○, fluorescence intensity at 350 nm. Closed circles represent the fluorescence intensities at 350 nm obtained by dilution from 4.8 M GuHCl.

$$f_D = (y - y_N)/(y_D - y_N) \qquad (6.1)$$

where y_N and y_D represent the initial and final values of a physical parameter and y the value at any intermediate GuHCl concentration. The denaturation curve obtained by measurement of fluorescence at 350 nm was different from those obtained by ultraviolet absorption at 292 nm and CD at 218 nm and 257 nm. The fluorescence increased gradually below 0.8 M GuHCl, where the other parameters did not change. This indicates that the two-state approximation cannot be applied to the unfolding process of Bence Jones protein Nag. Azuma et al. (1972) reported the denaturation by GuHCl of several Bence Jones proteins by CD measurement. The denaturation curve for Bence Jones protein Nag obtained by CD measurement at 218 nm is different from the curves for Tod and Ni proteins without reduction and alkylation of the interchain disulfide bond and is similar to the curve for Fu protein. As shown by closed circles, the denaturation of Bence Jones protein Nag measured in terms of fluorescence was reversible.

The effect of GuHCl concentration on the fluorescence spectrum of Bence Jones protein Nag is shown in Figure 6.5. While there were no appreciable changes in the CD at 218 nm or 257 nm, or in the value of $\Delta\varepsilon$ at 292 nm in the concentration range of 0 to 0.7 M GuHCl (Figure 6.4), a gradual increase in the fluorescence intensity and a shift of the emission maximum to longer wavelength were observed in the concentration range. The difference spectrum obtained by subtracting the fluorescence spectrum of native Bence Jones protein Nag from the spectrum at a fixed GuHCl concentration below 0.7 M had a

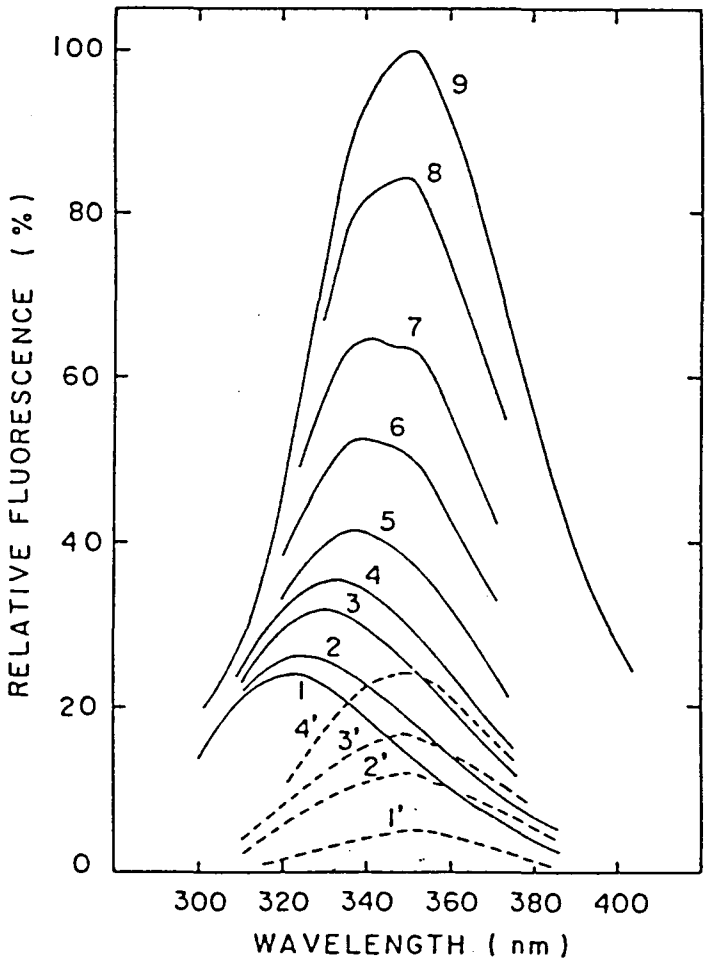

Fig. 6.5. Fluorescence spectra of Bence Jones protein Nag at various GuHCl concentrations. pH 7.5, 25°C. Excitation wavelength, 280 nm; protein concentration, 0.03 mg/ml. 1, 0 M; 2, 0.48 M; 3, 0.64 M; 4, 0.72 M; 5, 0.84 M; 6, 0.95 M; 7, 1.05 M; 8, 1.48 M; 9, 4 M GuHCl. Difference spectra obtained by subtraction of the fluorescence spectrum of Bence Jones protein Nag in the absence of GuHCl from the spectra in the presence of 0.48 M, 0.64 M, 0.72 M, and 0.84 M are shown by curves 1', 2', 3', and 4', respectively.

maximum at 350 nm, which is identical to the maximum emission wavelength of denatured protein. I studied quenching of the tryptophyl fluorescence of Bence Jones protein Nag by I^- ion (Leher, 1971). The quenching was analyzed by the Stern-Volmer equation (Stern & Volmer, 1919),

$$F_0/F = 1 + K_q[Q] , \qquad (6.2)$$

where F_0 is the fluorescence intensity when the concentration of quencher [Q] is zero, F is the fluorescence intensity in the presence of the quencher, and K_q is the Stern-Volmer constant. Figure 6.6 shows the Stern-Volmer plots in the presence and absence of 4 M GuHCl. In the presence of 4 M GuHCl fluorescence of all the tryptophyl residues was quenched by I^- ion with a K_q of 3.0 M^{-1}. On the other hand no quenching was observed in the native state (K_q = 0). These results show that the fluorescence of all the tryptophyl residues in the intact Bence Jones protein Nag molecule is strongly quenched in the absence of denaturant and that the change in the fluorescence in the presence of GuHCl below 0.7 M is due to a small conformational change which causes dequenching of the fluorescence of tryptophyl residues that are located near or on the surface of the protein molecule.

6.B.2. Refolding of V_L fragments

Refolding of the V_L fragments of Tod and Fu proteins was studied by fluorescenc and ultraviolet absorption measurements. Mixing for starting the reaction was made manually. Refolding of both the V_L(Tod) and V_L(Fu) fragments in 0.1 to 0.5 M GuHCl from 4 M GuHCl at 25°C was fast and was completed within the dead time (30 sec).

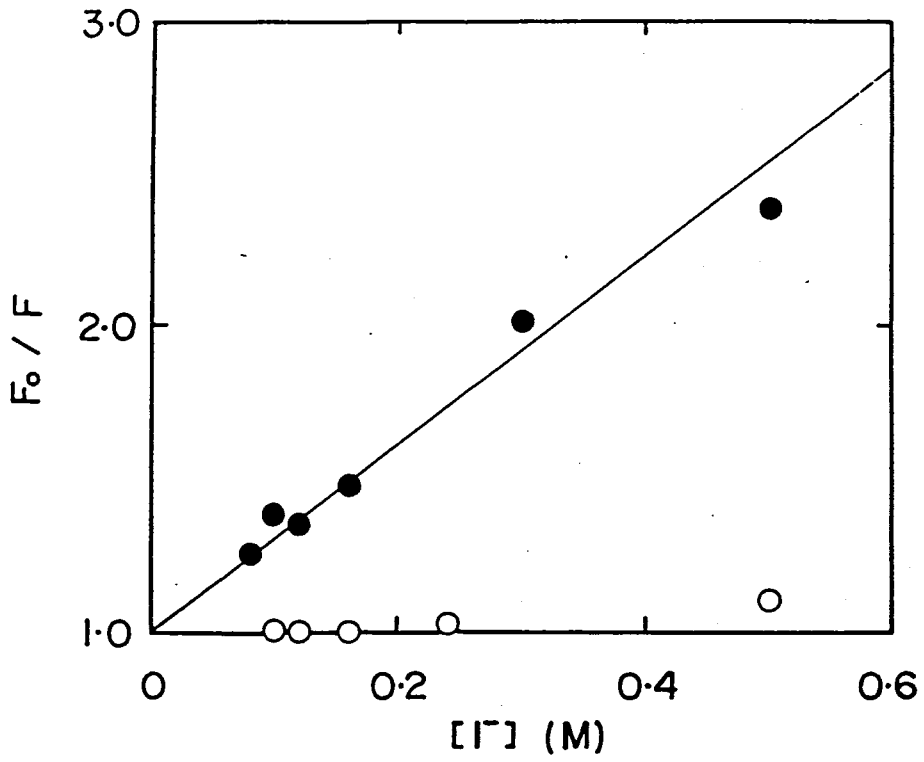

Fig. 6.6. Stern-Volmer plots of the quenching of tryptophyl fluorescence of Bence Jones protein Nag by iodide in the presence (●) and absence (○) of 4 M GuHCl. pH 7.5, 25°C. A small amount of $Na_2S_2O_3$ (0.1 mM) was added to the iodide solution to prevent I_3^- formation. Excitation wavelength, 280 nm; emission wavelength, 350 nm.

6.B.3. Refolding of type λ Bence Jones proteins

The kinetics of refolding of six specimens of type λ Bence Jones proteins in 0.1 M GuHCl from 4 M GuHCl were studied by CD, ultraviolet absorption, and fluorescence spectrometry. All the refolding reactions were started using manual mixing. In Chapter 4, I showed that the refolding kinetics of the C_L fragment in 0.1 M GuHCl contained a very slow phase with an apparent rate constant of $3 \times 10^{-3} s^{-1}$. This phase was a main process observable by manual mixing. As described above, the refolding of type λ V_L fragments was fast and was completed within the dead time of the measurement (30 sec). Thus if the refolding of whole light chain is a sum of the independent folding of the two domains, only a very slow phase similar to that observed for the C_L fragment was expected to be observable for the refolding of Bence Jones proteins.

Figure 6.7 shows the changes with time in the CD signal at 225 nm. In these CD measurements, the fast reaction within about 1 min of dilution could not be followed. The observable process followed first-order kinetics, but a slight deviation from linearity in the semilog plot was observed at an early stage for all the proteins studied except Bence Jones protein Tod (Figure 6.8). While the amplitude of the CD change in the process that follows first-order kinetics was different for different specimens (from 30 to 50 % of the total change), the rate constants among all the proteins studied were very similar. And these rates are also very similar to that of the C_L fragment ($3 \times 10^{-3} s^{-1}$) (Table 6.III).

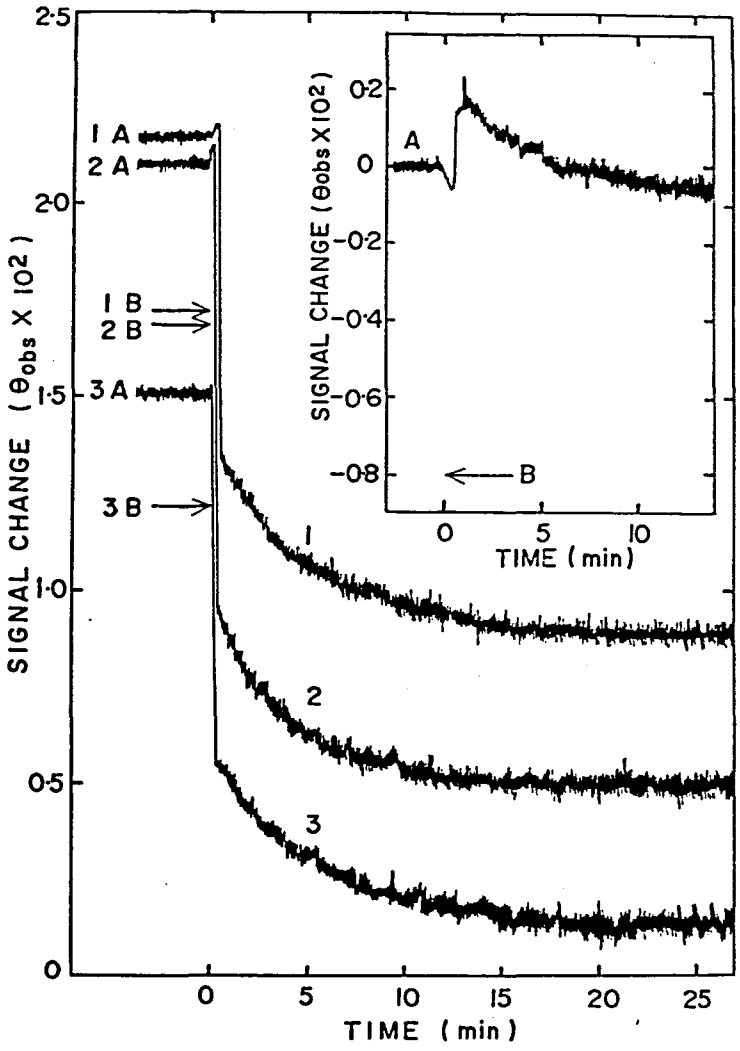

Fig. 6.7. Tracings of the CD signal changes with time. 1, Bence Jones protein Sh at 225 nm; 2, Bence Jones protein Nag at 224 nm; 3, C_L(Nag) fragment at 225 nm. The inset shows a tracing of the CD signal at 235 nm for Bence Jones protein Ni. A represents the base line and B represents the CD signal of the corresponding proteins in 4 M GuHCl. Refolding was carried out in 0.07 M GuHCl at pH 7.5 from 4 M GuHCl at pH 7.5. The protein concentration was 0.1 mg/ml.

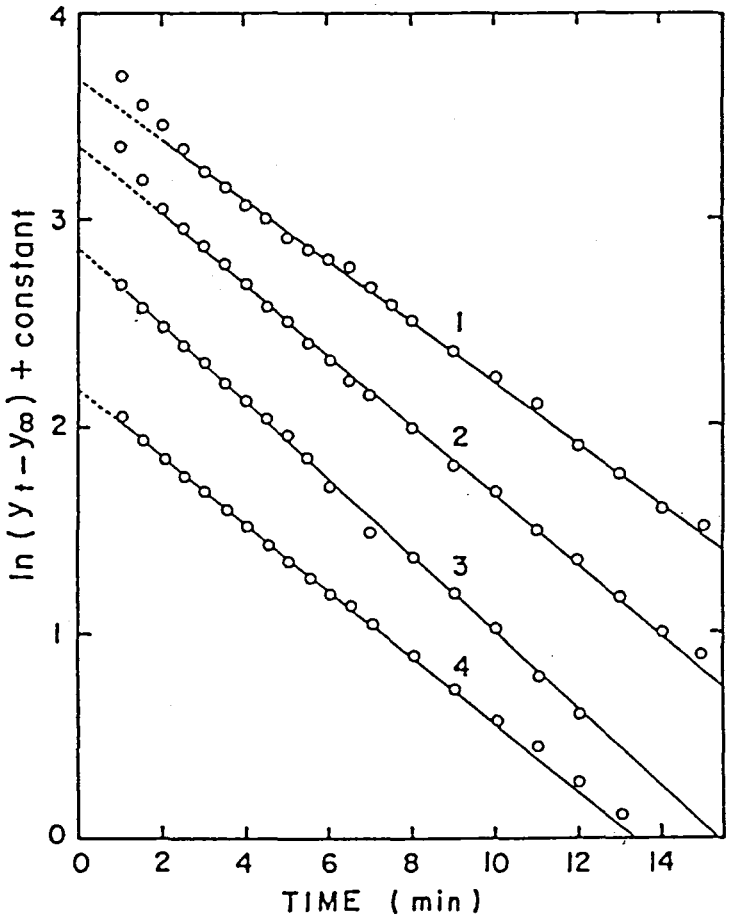

Fig. 6.8. First-order plots for the slow phases in the refolding reactions of Bence Jones protein Sh (1), Bence Jones protein Nag (2), Bence Jones protein Tod (3), and C_L(Nag) fragment (4) measured by CD. The conditions were as described in the legend to Fig. 6.7.

TABLE 6.III. The apparent rate constants for the slow phases in the refolding reactions of type λ Bence Jones proteins, and V_L and C_L fragment in 0.1 M GuHCl at pH 7.5, 25°C.

Proteins	Apparent rate constants (x 10^3 s^{-1})			
	CD[a]	Tryptophyl fluorescence[b]	Ultraviolet absorption[c]	ANS fluorescence[d]
Bence Jones protein Nag	3.1	3.1	2.9	2.5
Bence Jones protein Tod	3.3	3.2	-	2.9
Bence Jones protein Kob	2.4	2.6	-	-
Bence Jones protein Sh	2.4	3.0	-	-
Bence Jones protein Fu	3.0	2.8	-	-
C_L(Nag) fragment	2.4	2.7	3.3	not detected
V_L(Tod) fragment	not detected	not detected	not detected	not detected
V_L(Fu) fragment	-	not detected	-	not detected

[a] The conditions were as described in the legend to Fig. 6.7. Values are averages of several determinations. [b] The conditions were as described in the legends to Fig. 6.9. Values are averages of several determinations. [c] The conditions were as described in the legends to Fig. 6.9. [d] The conditions were as described in the legend to Fig. 6.13. Values are average of several determinations at different ANS concentrations.

The refolding reaction was also studied by fluorescence and absorption measurements. The first-order plots of the observable process in the refolding reactions of Bence Jones protein Nag and Tod are shown in Figures 6.9 and 6.10, respectively. Deviation from linearity in the semilog plot was observed at an early stage for the refolding process of Bence Jones protein Nag but was less marked for Tod protein. Such deviation was also observed for the other proteins studied and differed depending on the specimen. The early part of the reaction of Bence Jones protein Nag measured by fluorescence, i.e., the part that showed deviation from the first-order plot, gave a linear semilog plot when replotted after subtraction of the slower first-order phase. The rate constant obtained from this plot was about 2×10^{-2} s^{-1} (Figure 6.9, inset). The sum of zero-time fluorescence amplitudes obtained by extrapolation of the fast portion (about 50 % of the total) and that obtained by extrapolation of the slow portion (about 30 % of the total) in the refolding kinetics of Bence Jones protein Nag could not account for the total fluorescence change that was expected on the basis of the equilibrium study. Therefore, the refolding kinetics of Bence Jones protein consist of at least three phases. Small but distinct deviation from the first-order plots obtained by CD and ultraviolet absorption may correspond to the detectable fast phase obtained by fluorescence. The first-order rate constant for the slow phase determined by fluorescence and absorption measurements was in agreement with that determined by CD measurement. The first-order rate constants for the slow phase in the refolding reactions of the six specimens of Bence Jones proteins are summarized in Table 6.III.

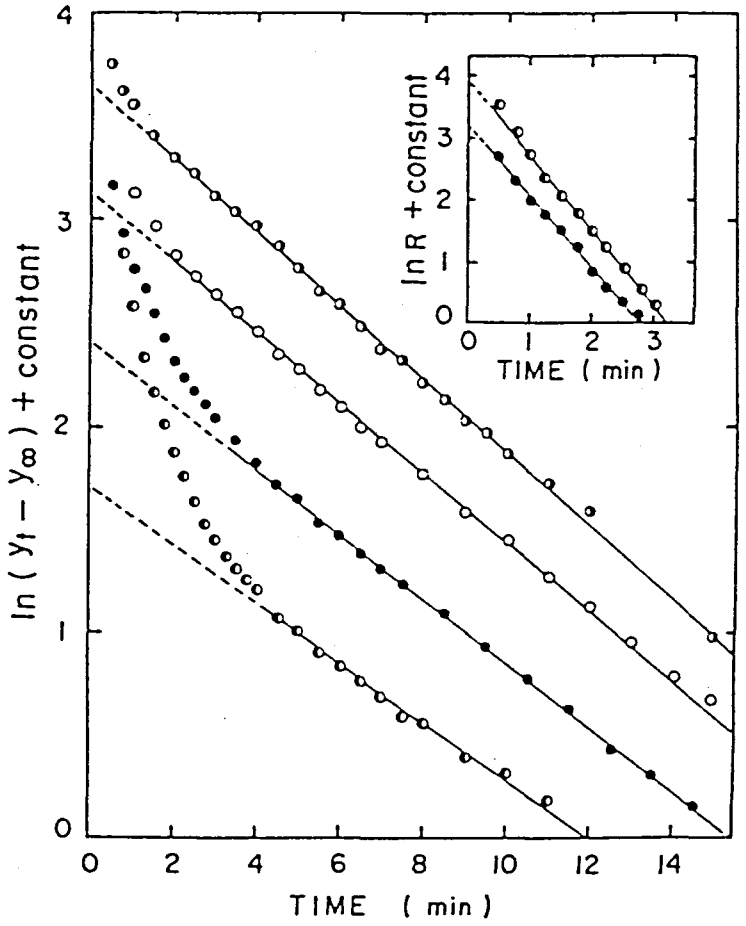

Fig. 6.9. First-order plots of the refolding reactions of Bence Jones protein Nag measured in terms of ultraviolet absorption at 292 nm (◑), CD at 224 nm (○), tryptophyl fluorescence at 350 nm (●), and ANS fluorescence at 470 nm (◐). The conditions for CD measurement were as described in the legend to Fig 6.7. For ultraviolet absorption measurements, the protein concentration was 0.43 mg/ml and the final GuHCl concentration was 0.08 M. For tryptophyl fluorescence measurements, the protein concentration was 0.02 mg/ml and the final GuHCl concentration was 0.03 M. Excitation was at 280 nm. ANS fluorescence was measured in the presence of 0.01 mM ANS and at a protein concentration of 0.16 mg/ml. The final GuHCl concentration was 0.07 M. Excitation was at 365 nm. The inset shows the first-order plots for the detectable fast phase. The fluorescence change in the first-order slow phase is subtracted from the observed fluorescence change, and the logarithm of the residue R is plotted against time. ○, Tryptophyl fluorescence; ◐, ANS fluorescence.

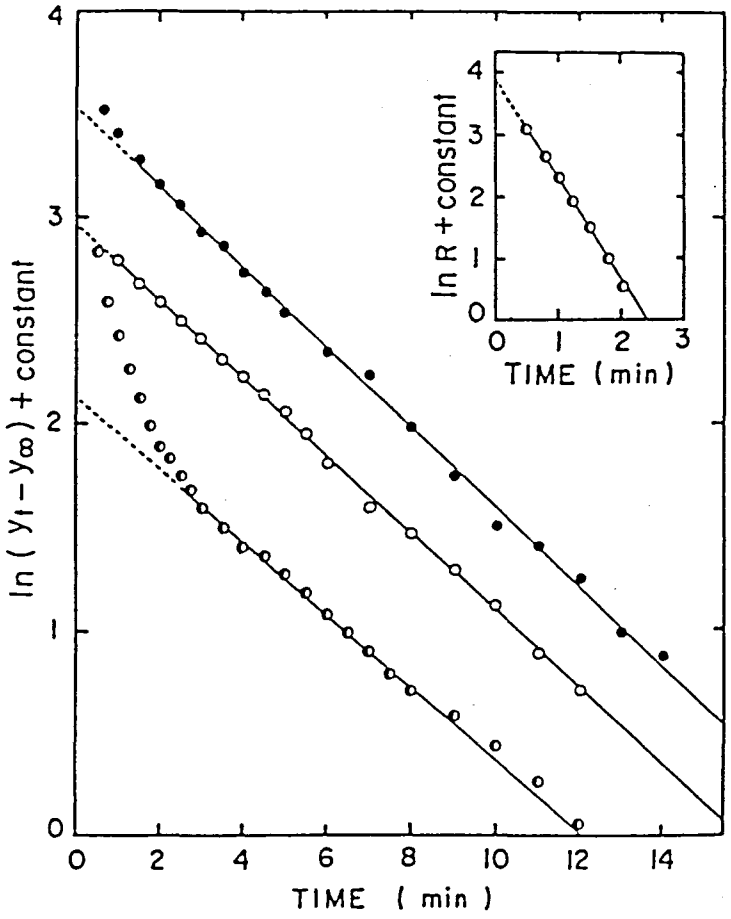

Fig. 6.10. First-order plots of the refolding reaction of Bence Jones protein Tod measured in terms of tryptophyl fluorescence at 350 nm (●), CD at 225 nm (○), and ANS fluorescence at 470 nm (◐). The conditions for CD measurement were as described in the legend to Fig. 6.7. For tryptophyl fluorescence measurements, the protein concentration was 0.043 mg/ml and the final GuHCl concentration was 0.03 M. Excitation was at 280 nm. ANS fluorescence was measured in the presence of 0.01 mM ANS and at a protein concentration of 0.14 mg/ml. The final GuHCl concentration was 0.1 M. Excitation was at 365 nm. The inset shows a first-order plot of the detectable fast phase measured in the presence of ANS.

Azuma et al. (1972) studied the denaturation of type λ Bence Jones proteins by GuHCl and showed that the C_L domain was denatured first at low GuHCl concentrations, followed by denaturation of the V_L domain at higher GuHCl concentrations. The ellipticity at 235 nm of Bence Jones protein Ni in the absence of GuHCl was nearly zero. The ellipticity at 235 nm increased from about zero to + 300 degrees $cm^2\ dmol^{-1}$ in the presence of 1.5 M GuHCl and then decreased to about -400 in the presence of 4 M GuHCl. Azuma et al. (1972) also showed that the CD band at 235 nm originated from a tryptophyl or tyrosyl residue in the V_L domain of Bence Jones protein Ni and that a stable intermediate in which the V_L domain remains intact and the C_L domain is denatured completely, existed at 1.5 M GuHCl. I studied the refolding kinetics of Bence Jones protein Ni in terms of the CD band at 235 nm (Figure 6.7, inset). On dilution of Bence Jones protein Ni in 4 M GuHCl with Tris-HCl buffer at pH 7.5, the ellipticity at 235 nm rapidly increased from - 400 to + 100 within the dead time of the measurement and then slowly decreased to about zero. The rate constant for the slow phase was $3 \times 10^{-3}\ s^{-1}$, which is the same as the rate constant for the slow phase of C_L fragment. This is as expected if refolding of the V_L domain precedes refolding of the C_L domain.

Bence Jones proteins whose interchain diuslfide bonds are reduced and alkylated are known to be in an equilibrium between the dimer and the monomer (Azuma et al., 1974, 1978). In order to determine whether the monomer-dimer equilibrium affects the refolding kinetics, I measured the refolding of Bence Jones protein Nag at various protein concentrations in terms of the CD change at 225 nm. In the concentration range from 5.7×10^{-3} to 4.8×10^{-1} mg protein/ml, where the monomer fraction was estimated to be 62 to 10% by weight on the basis

of a dimerization constant of 2×10^6 M^{-1} for reduced and alkylated Bence Jones protein Nag (Azuma et al., 1974), the rate constant and the amplitude of the slow phase showed little dependence on the protein concentration. This indicates that the refolding process is not affected by dimerization of the native protein.

I also compared the refolding kinetics of reduced and alkylated Bence Jones protein Nag with those of the unmodified protein. No difference was observed in kinetic behavior between these proteins. Furthermore, as shown in Table 6.III, the rate constant of the slow phase in the refolding reaction of Bence Jones protein Kob, which is a disulfide-bonded dimer, and that of Bence Jones protein Sh, which contains dimers with an interchain disulfide and monomers, were similar to those of the reduced and alkylated Nag, Tod, Ni, and Fu proteins. Only Bence Jones protein Ni with an intact disulfide bond was not completely renatured to intact protein from 4 M GuHCl. These findings indicate that the interchain disulfide bond has nothing to do with the refolding process of Bence Jones proteins.

The first-order rate constant for the slow phase of refolding of Bence Jones protein Nag was determined at various temperatures and compared with that of the C_L fragment (Figure 6.11). Although the rate constant for Bence Jones protein Nag was slightly higher than that for the C_L fragment, the activation energies for the refolding reaction of Bence Jones protein Nag was the same as that of the C_L fragment (20 kcal mol^{-1}). This indicates that the slow phase of refolding observed for Bence Jones protein Nag and the C_L fragment reflects the same process. The cis-trans isomerization of the prolyl residue as a cause of the marked slow phase was discussed in detail in Chapter 4.

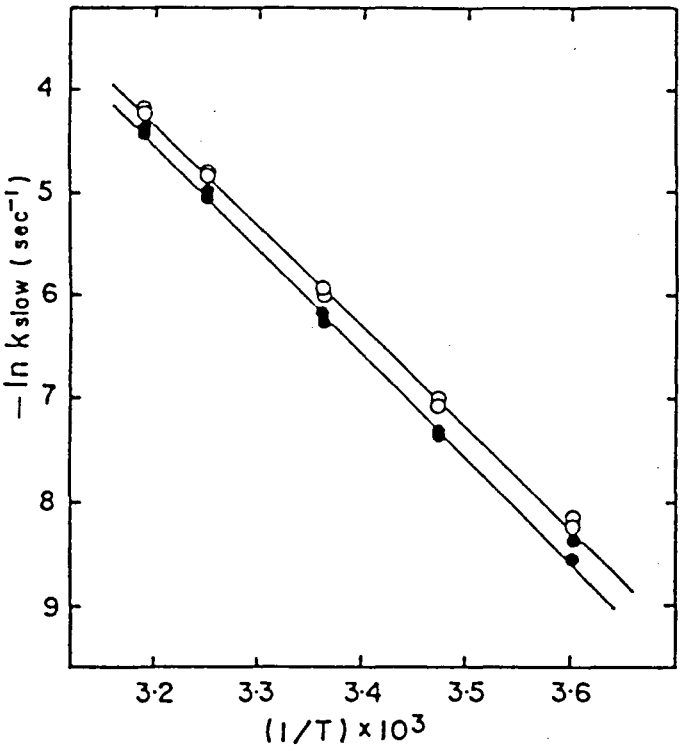

Fig. 6.11. Arrhenius plots of the first-order rate constants for the slow phases in the refolding reactions of Bence Jones protein Nag (○) and C_L(Nag) fragment (●).

I measured the refolding kinetics of Bence Jones protein Nag in terms of CD changes at various wavelengths and calculated the zero-time values of [θ] by extrapolation of the slow phase. The results are shown in Figure 6.1. The extrapolated spectrum was similar in shape to that of the C_L fragment. In the same way, zero-time values of fluorescence intensity of Bence Jones protein Tod was calculated by extrapolation of the slow phase observed in terms of fluorescence changes at various emission wavelengths (Figure 6.3) (see Discussion, 6.C).

6.B.4. Refolding of Bence Jones proteins, and C_L and V_L fragments in the presence of ANS

The fluorescence of ANS is known to increase when the dye binds to hydrophobic regions of a protein (Stryer, 1965). A small ANS fluorescence increase was observed for Bence Jones proteins, and C_L fragment in the native states, but not in the denatured states (Figure 6.12). In the unfolding process of Bence Jones protein Nag by GuHCl, ANS fluorescence reached a maximum at 1 - 1.2 M GuHCl but no change in the ANS fluorescence was observed for C_L fragment (Figure 6.12). Because of the limited amount of sample available, I did not measure the change in ANS fluorescence with GuHCl concentration for V_L(Tod) fragment. Ghose (1973) found that the increase in ANS fluorescence was small for intact Bence Jones proteins, and V_L and C_L fragments, and that the ANS fluorescences for Bence Jones proteins and V_L fragment increased considerably with increasing temperature, reaching a maximum at around 56°C, but no such increase

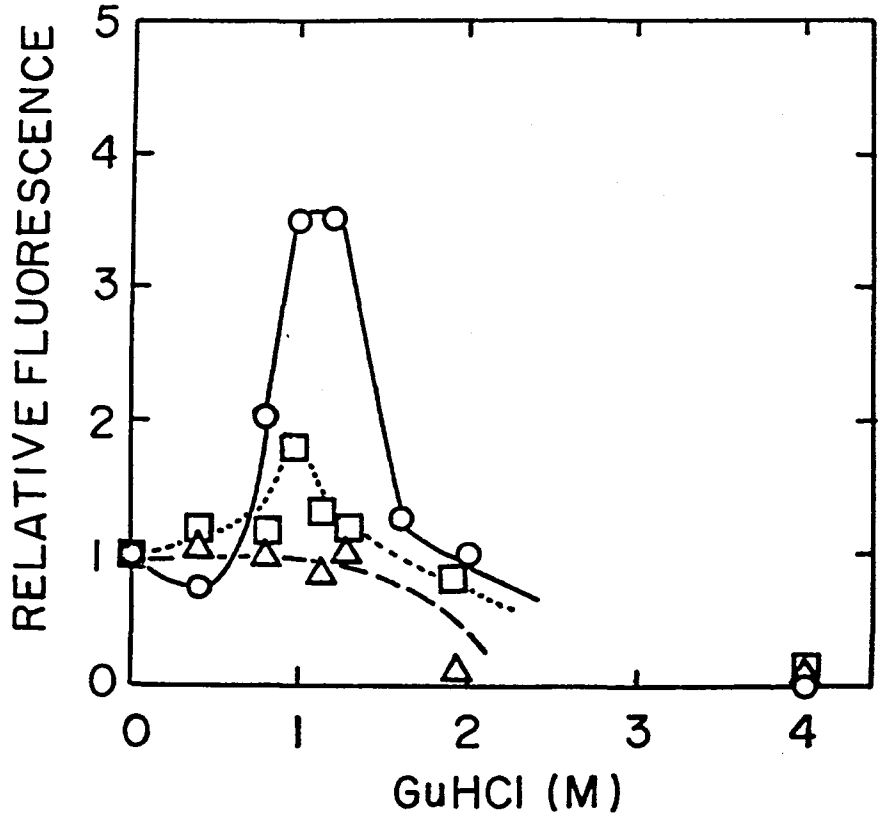

Fig. 6.12. Dependence on GuHCl concentration of the ANS binding ability of Bence Jones protein Nag (○), Bence Jones protein Tod (□), and C_L(Nag) fragment (△) in the presence of 0.01 mM ANS. pH 7.5, 25°C. Excitation wavelength, 365 nm; emission wavelength, 470 nm; protein concentration, 0.2 mg/ml.

were observed for C_L fragment.

I studied ANS binding during the refolding of Bence Jones proteins, and V_L and C_L fragments after dilution of protein solutions in 4 M GuHCl with Tris-HCl buffer, pH 7.5, containing ANS. When refolding of Bence Jones protein Nag was initiated in 0.1 M GuHCl containing 0.01 mM ANS, a large increase in ANS fluorescence was observed within the dead time of the measurement and the fluorescence then decreased slowly (Figure 6.13). The same result was also obtained for Bence Jones protein Tod. The first-order plots of the slow phases for Bence Jones protein Nag and Tod are shown in Figures 6.9 and 6.10, respectively. Although considerable deviations from the first-order plots were observed in the early stages, the rate constants obtained from the slow phase were similar to those obtained by other methods (Table 6.III). Deviation from the linear portion of the semilog plot also followed first-order kinetics with a rate constant of about 2×10^{-2} s^{-1} (Figures 6.9 and 6.10), which is the same as the rate constant for the detectable fast phase obtained from the tryptophyl fluorescence (Figure 6.9). These findings suggest that ANS binds to an intermediate which is produced during the refolding process and does not affect the refolding kinetics of Bence Jones proteins.

The initial rapid increase of ANS fluorescence occurred linearly with increase in ANS concentration up to 1 mM, but the rate constants for the detectable fast phase and slow phase were not affected by ANS concentration (Figure 6.14). However, the fluorescence change with time after dilution with buffer containing 3 mM ANS was very

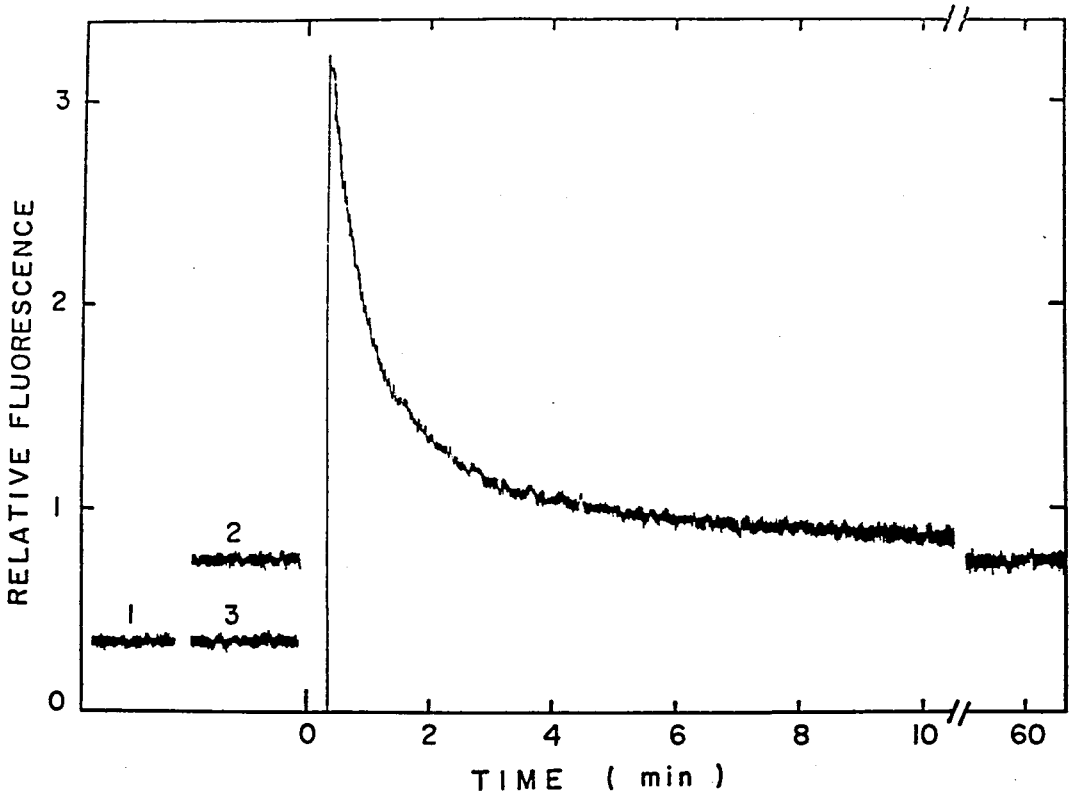

Fig. 6.13. Tracing of the change with time in the fluorescence intensity at 470 nm of an ANS solution containing Bence Jones protein Nag. pH 7.3, 25°C. 1, ANS fluorescence in the absence of Bence Jones protein Nag; 2, ANS fluorescence in the presence of native Bence Jones protein Nag; 3, ANS fluorescence in the presence of denatured Bence Jones protein Nag in 4 M GuHCl. ANS fluorescence was measured in the presence of 0.01 mM ANS and at a protein concentration of 0.16 mg/ml. The final GuHCl concentration was 0.07 M. Excitation was at 365 nm.

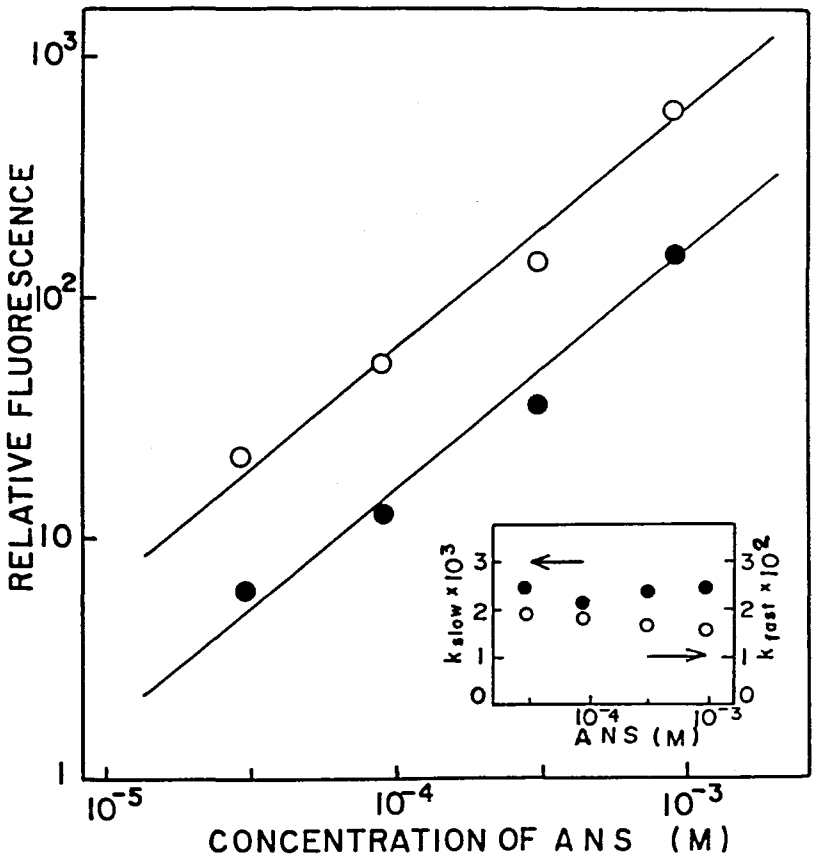

Fig. 6.14. Dependence on ANS concentration of the amplitude of ANS fluorescence change of fast (○) and slow (●) phases during the refolding of Bence Jones protein Nag. The inset shows the dependence on ANS concentration of the apparent rate constant of fast (○) and slow (●) phases. pH 7.5, 25°C. The protein concentration was 0.16 mg/ml and the final GuHCl concentration was 0.07 M. Excitation wavelength was 440 nm and emission wavelength was 470 nm.

slow, and the intensity did not decrease to that of the native value. Thus, although I could not elucidate the mode of binding of ANS to the refolding intermediate, ANS does appear to be useful to follow the refolding porcess of Bence Jones proteins.

I also studied the refolding kinetics of C_L fragment and V_L (Tod) fragment in the presnece of ANS. In contrast to the case of refolding of Bence Jones proteins, no ANS fluorescence changes were observed during refolding of these fragmens.

6.B.5. Refolding of type κ Bence Jones proteins

I studied the refolding of type κ Bence Jones proteins under conditions used for type λ proteins. Although the solutions became turbid on dilution of Bence Jones proteins Ta and Ham in 4 M GuHCl with Tris-HCl buffer at pH 7.5 and 25°C, the refolding reactions of these proteins seemed to be as slow as the reaction of type λ proteins.

The refolding process of type κ V_L(Ta) fragment could not be followed owing to turbidity.

6.C. Discussion

I have described here the kinetics of the refolding of type λ Bence Jones proteins and type λ V_L fragments in 0.1 M GuHCl from 4 M GuHCl. The refolding process of Bence Jones proteins is complicated and consists of at least three phases, a very fast phase which completes within the dead time of the measurement (30 sec), a detectable fast phase, and a slow phase. Because I did not measure the rate of the first undetectable fast phase in the present experiment, the exact mechanism of the entire refolding process of Bence Jones protein was not characterized. However, comparison of the refolding process of Bence Jones proteins with those of V_L and C_L fragments makes it possible to deduce some important features of the refolding mechanism of the Bence Jones protein molecule.

The apparent first-order rate constants for the slow phases in the refolding reaction were all very similar (Table 6.III). Refolding of the V_L fragments was very fast, and was completed within the dead time of the measurement using manual mixing. The activation energy of the slow phase of Bence Jones protein Nag was the same as that for C_L fragment (Figure 6.11). The CD band at 235 nm of Bence Jones protein Ni, which originates from a tryptophyl or tyrosyl residue in the V_L domain (Azuma et al., 1972), first increased within the dead time of the measurement and then decreased during refolding (Figure 6.7, inset). This indicates that the rapid increase in ellipticity corresponds to the fast processes of refolding of the V_L and C_L domains and the slow decrease corresponds to the slow process of

refolding of the V_L and C_L domains and the slow decrease corresponds to the slow process of refolding of the C_L domain. All these observations are consistent with the view that refolding of the V_L domain of the Bence Jones protein molecule occurs much faster than that of the C_L domain and that refolding of the C_L domain of the Bence Jones protein molecule is similar to refolding of the isolated C_L fragment. Thus the refolding of the Bence Jones protein is explained to a great extent by the sum of the refolding of the two constituent fragments and I conclude that the folding of Bence Jones protein is approximately the independent folding of the two domains.

Although the independent folding of the two domains of Bence Jones protein seems to be a good approximation, there are some differences in the refolding process between the C_L domain and the isolated C_L fragment and between the V_L domain and the isolated V_L fragment. If we assume that the refolding of the V_L domain of the Bence Jones protein molecule is as fast as that of the isolated V_L fragment and the rate of refolding of the C_L domain is the same as that of C_L fragment, the zero-time fluorescence spectrum of Bence Jones protein Tod should be expressed by the sum of the zero-time spectrum of C_L fragment and the spectrum of Bence Jones protein Tod. As shown in Figure 6.3, however, the zero-time spectrum thus calculated is different from the zero-time fluorescence spectrum of Bence Jones protein Tod. The amplitude of the detectable fast phase was different, depending on the specimen of the proteins. For instance, the fluorescence amplitude of this fast phase was relatively large for Bence Jones protein Nag but not for Bence Jones protein Tod

(Figures 6.9 and 6.10). The corresponding fast phase was less significant for C_L fragment (Chapter 4). This may indicate that the detectable fast phase reflects a part of the refolding process of the V_L domain of the Bence Jones protein molecule. An extremely large increase in ANS fluorescence was observed at an early stage of refolding of the Bence Jones protein molecule, but this was not the case for isolated C_L fragment. This indicates that an intermediate which can bind ANS is produced in the course of refolding of the Bence Jones protein molecule, but not during that of the C_L fragment. These observations suggest that refolding of the V_L domain may be retarded to some extent by the presence of the C_L domain in the Bence Jones protein molecule. Although X-ray crystallographic studies (Davies et al., 1975; Beale & Feinstein, 1976; Amzel & Poljak, 1979) show that the Bence Jones protein molecule consists of structurally independent domains, there may be subtle interactions between the V_L and C_L domains in the course of refolding. Similar subtle interactions were also found between C_H2 and C_H3 domains during the refolding process of Fc fragment from the denatured state by 4 M GuHCl (Sumi & Hamaguchi, in preparation).

Chapter 7

Formation of intrachain disulfide bond in reduced C_L fragment

7.A. Introduction

The exact mechanism *in vivo* of formation of the disulfide bonds for proteins is unknown. One of the candidates is a thiol-disulfide interchange reaction between protein SH groups and small-molecule thiol compounds such as glutathione and cystein. Nowadays, this system is frequently employed for *in vitro* reformation of disulfide bonds because of its quantitative high efficiency (Creighton, 1978). Two SH groups of the reduced C_L fragment are buried in the interior of the molecule and the reactivity of the SH groups toward DTNB is rate-limited by the unfolding process of the protein molecule (Chapter 5). Such buried SH groups are the first case as far as I know. The mechanism of disulfide formation for such SH groups mediated by thiol-disulfide interchange reaction was suggested to be different from the generally assumed mechanism in which the proximity of two SH groups always accelerate the disulfide formation. Intermediates with such buried SH groups may occur during the reoxidation process of the disulfide bonds of other proteins, although such a case has not yet been reported. How the disulfide bond is formed in the reduced C_L fragment is, thus, a very important problem for an interpretation of the protein folding which accompanies the formation of intrachain disulfide bonds.

In this Chapter, I describe the mechanism of formation of the disulfide bond in the reduced C_L fragment. The main interest is a relation between the disulfide bond formation and the conformational transition of the C_L fragment. Although it was shown that the unfolding and refolding of the C_L fragment follow the three-species mechanism ($U_1 \longleftrightarrow U_2 \longleftrightarrow N$) (Chapter 4 and 5), I analyzed the reaction by a two-state mechanism ($U \longleftrightarrow N$). The relation between the rate constants of conformational transition estimated by the two-state mechanism and those by the three-species mechanism will be described in the Discussion (7.C).

For the easy representation of the different species of C_L fragment which appear during the reaction, abbreviations for C_L fragments (C_{LS}^{S}, C_{LSH}^{SH}, C_{LSH}^{SSG}, C_{LSSG}^{SSG}, C_{LSCAM}^{SCAM}, and C_{LSCM}^{SCM}) will be frequently used.

7.B. Results

7.B.1. Separation of molecular species formed on oxidation of C_{LSH}^{SH} with GSSG

Oxidation of C_{LSH}^{SH} with GSSG yields four molecular species, C_{LSH}^{SH}, C_{LSH}^{SSG}, C_{LSSG}^{SSG}, and C_{LS}^{S}. Strictly speaking, there are two species depending on which of the two SH groups of C_{LSH}^{SH} forms a mixed disulfide (C_{LSH}^{SSG} and C_{LSSG}^{SH}). As described later, however, these two species were not discriminated in the present analysis. When the reaction is stopped by the addition of iodoacetamide, C_{LSH}^{SSG} and C_{LSH}^{SH} convert to C_{LSCAM}^{SSG} and C_{LSCAM}^{SCAM}, respectively, and the quenched solution contains four molecular species, C_{LSCAM}^{SCAM}, C_{LSCAM}^{SSG}, C_{LSSG}^{SSG}, and C_{LS}^{S}. I found that these four molecular species can be well separated on 15 % polyacrylamide gel electrophoresis at pH 9.5 on the basis of the differences in the hydrodynamic volume and the net charge of the protein molecule. Glutathione has two carboxyl groups with pK_as of 2.1 and 3.6 and one amino group with a pK_a of about 9 (Edsall and wyman, 1958). Therefore, the negative net charge on the protein molecule increases in the order of $C_{LS}^{S} = C_{LSCAM}^{SCAM} < C_{LSCAM}^{SSG} < C_{LSSG}^{SSG}$ at pH 9.5. Although C_{LS}^{S} and C_{LSCAM}^{SCAM} have the same net charge, the C_{LSCAM}^{SCAM} molecule is unfolded to a greater extent and its hydrodynamic volume is larger than that of the intact C_L fragment (Chapter 3). Thus these two species can be separated on the basis of the sieving effect of 15 % polyacrylamide gel. Since C_{LSCAM}^{SSG} and C_{LSSG}^{SSG} may have an unfolded conformation similar to C_{LSCAM}^{SCAM}, these three species can be separated on the basis of their net charges. This method was also applied to the reactions starting from various species of the C_L fragment.

In the kinetic analysis of thiol-disulfide interchange reaction, the reaction should be stopped immediately. This was performed by alkylation of free thiol groups with 0.1 M iodoacetamide in the presence of 4 M urea at pH 7, because a high concentration of iodoacetamide is needed to alkylate thiol groups immediately as reported by Creighton (1978) and because burial of the cysteinyl residues in the interior of the C_{LSH}^{SH} molecule in the absence of urea will prevent their thiol groups from immediate alkylation.

Figures 7.1 and 7.2 show typical results of electrophoretic separation of the four species appearing during the reaction of C_{LSH}^{SH} with GSSG in the absence and presence of 8 M urea. It can be seen that the four trapped species were clearly separated; C_{LSCAM}^{SCAM}, C_{LSCAM}^{SSG}, and C_{LSSG}^{SSG} were distributed with the same distance from cathode to anode depending on the charge difference produced by mixed disulfide with glutathione, and the migration of C_{LS}^{S} was the fastest owing to its compact molecular shape.

7.B.2. Reaction of C_{LSH}^{SH} with GSSG

Figure 7.3(a) and (b) shows the changes with time in the concentrations of species trapped with iodoacetamide during reaction of C_{LSH}^{SH} with GSSG in 8 M urea at pH 8.1 and 25°C. In 8 M urea, the protein molecule is denatured (Chapter 3) and the thiol-disulfide interchange reaction may proceed without any restriction of ordered conformations. Thus the results of Figure 7.3(a) and (b) may serve as the reference when reactions involving effects of protein conformation are considered. As shown in Figure 7.3(a) and (b), following the disappearance of C_{LSH}^{SH},

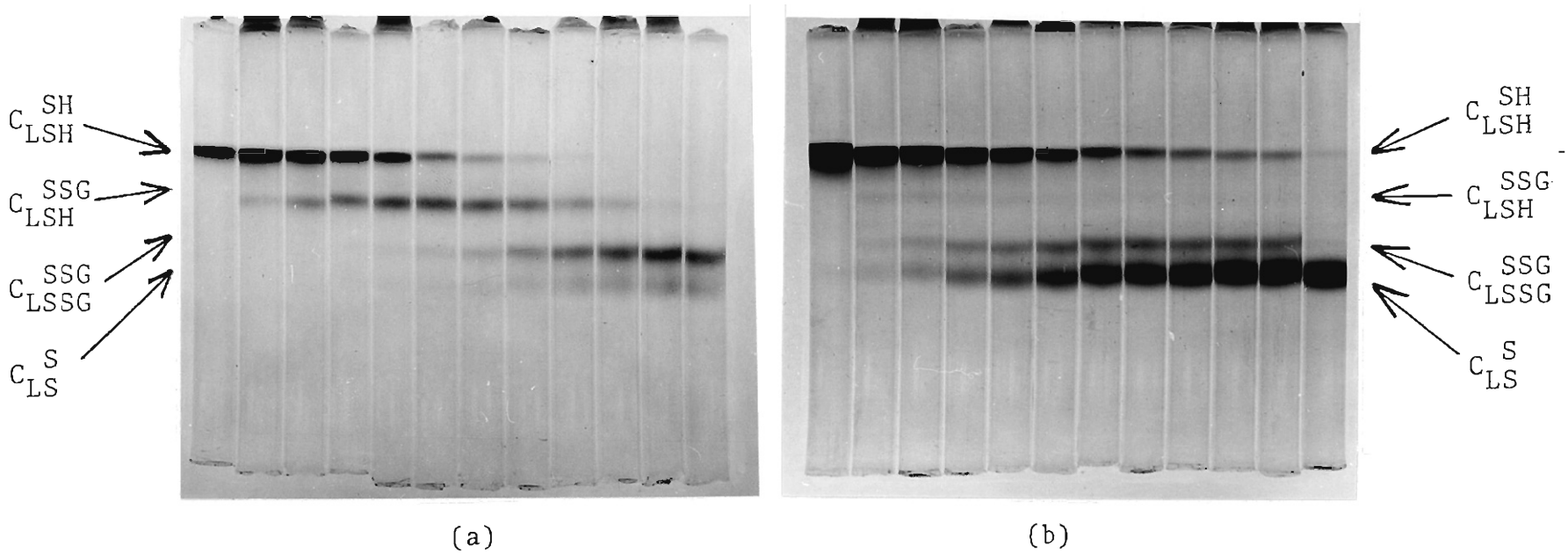

Fig. 7.1. Separation by gel electrophoresis in 15 % polyacrylamide at pH 9.5 of the species trapped during regeneration of reduced C_L fragment by 3 mM GSSG in the presence (a) and absence of 8 M urea (b). Reduced C_L fragment (0.03 mM) was regenerated at 25°C and at pH 8.1 for various times, when the reaction was quenched by addition of iodoacetamide to 0.1 M. Left to right: (a) 0, 0.5, 1, 1.5, 2, 3, 4, 5.5, 7.5, 10, 15 and 20 min; (b) 0, 0.2, 0.4, 0.7, 1, 1.5, 2, 2.5, 3, 3.5, 4 and 20 h.

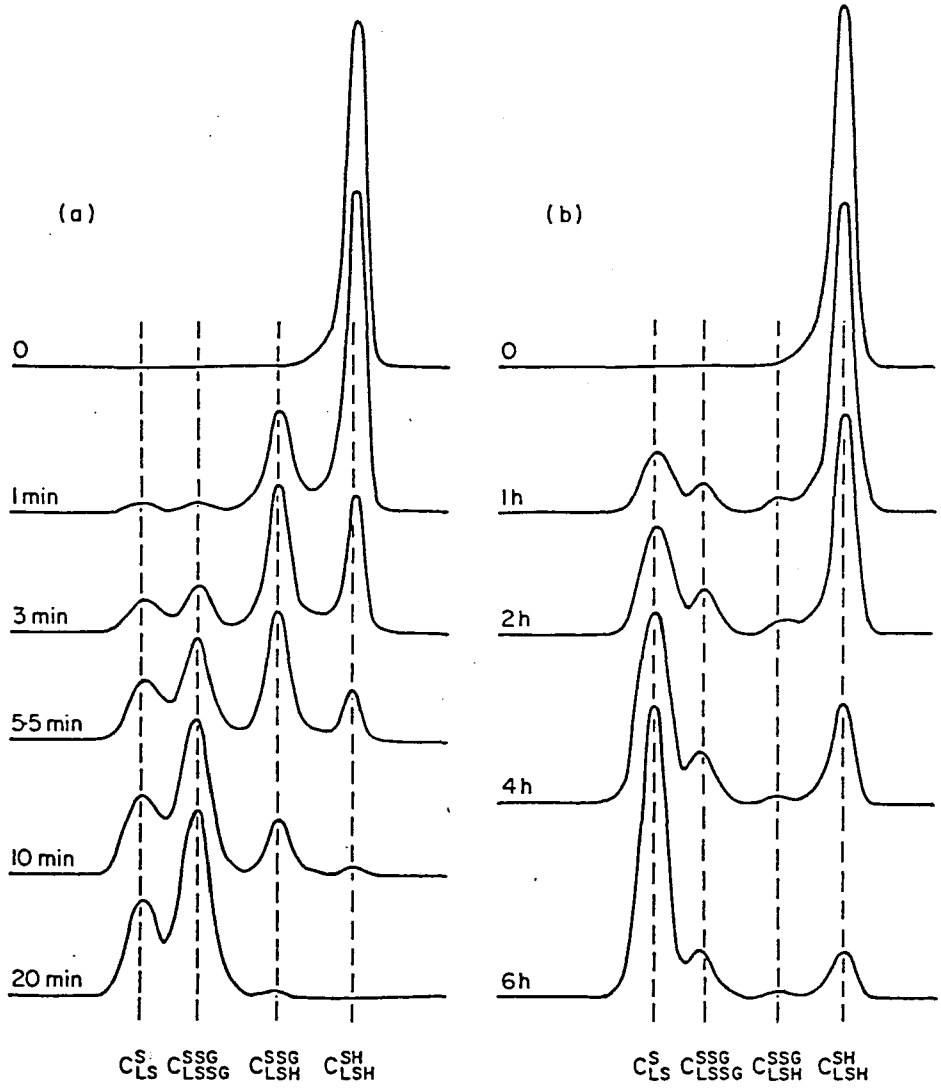

Fig. 7.2. Representative densitometer of the species trapped shown in Fig. 7.1. The experimental details were as described in the legend to Fig. 7.1. The top of the separating gel is at the right.

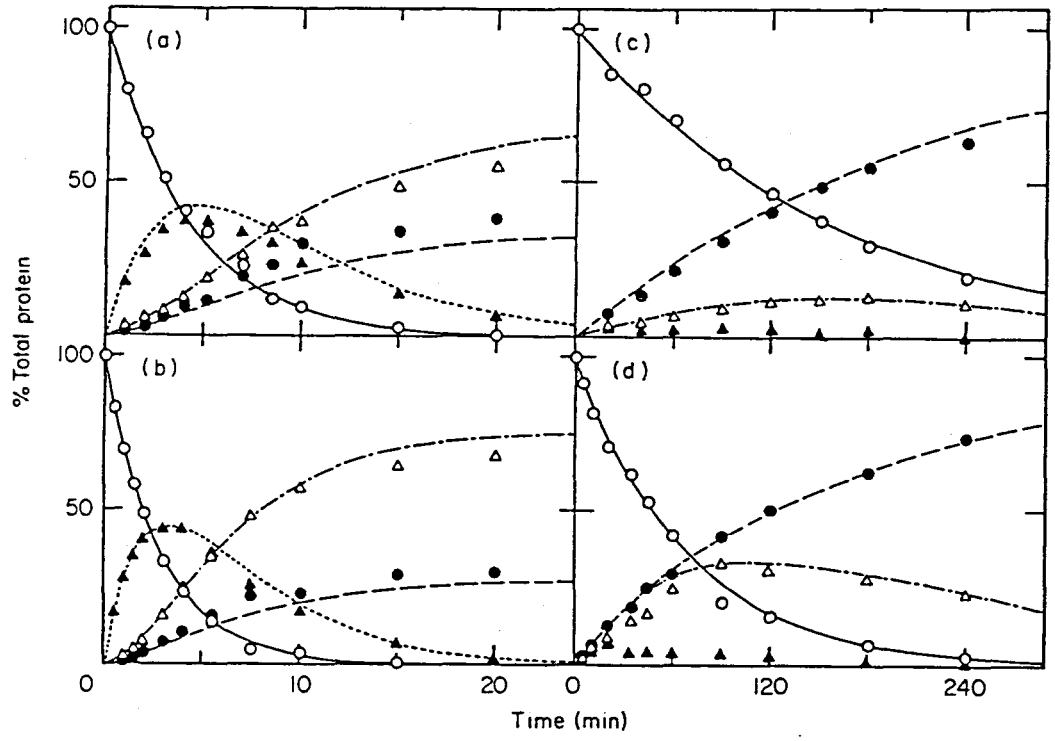

Fig. 7.3. Kinetics of the reaction of reduced C_L fragment with (a) 2 mM and (b) 3 mM GSSG in the presence of 8 M urea and with (c) 3 mM and (d) 9 mM GSSG in the absence of urea. Reduced C_L fragment (0.03 mM) was reacted with GSSG at pH 8.1 and 25°C, and the time-dependent concentrations of C_{LSH}^{SH} (○), C_{LSH}^{SSG} (▲), C_{LSSG}^{SSG} (△), and C_{LS}^{S} (●) were determined electrophoretically as in Fig. 7.2. The curves for (a) and (b) were calculated with kinetic mechanism 7.1 (see the text) and the values for the rate constants in Table 7.I, and the curves for (c) and (d) were calculated with kinetic mechanism 7.3 (see the text) and the values for the rate constants in Table 7.I.

C_{LSH}^{SSG} increased, attained a maximum level, and then decreased. Not only C_{LS}^{S} but also C_{LSSG}^{SSG} was produced with a lag phase under these conditions. Though the overall reaction was faster with 3 mM GSSG than with 2 mM GSSG, the formation of C_{LS}^{S} was more effective in the reaction with 2 mM GSSG.

The thiol-disulfide interchange reaction of C_L fragment with glutathione in the presence of 8 M urea may be expressed by mechanism 7.1.

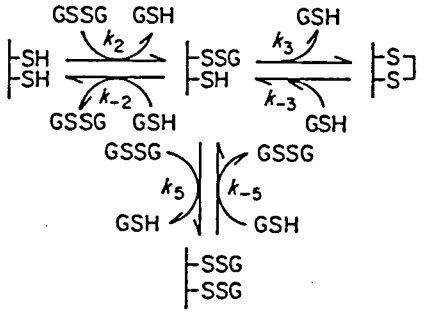

(Mechanism 7.1),

where k_2, k_{-2}, k_{-3}, k_5, and k_{-5} are the second-order rate constants for the thiol-disulfide interchange reactions and k_3 is the first-order rate constant for the formation of the intrachain disulfide bond. In this mechanism the reactivities of the two SH groups of C_{LSH}^{SH} toward GSSG were assumed to be the same in the denatured state and species C_{LSH}^{SSG} and C_{LSSG}^{SH} were not discriminated.

Since the concentration of C_{LSH}^{SH} was much lower than that of GSSG under the present experimental conditions, the concentration of GSH produced by the reaction may be negligible. Thus the results in Figure 7.3(a) and (b) may be explained on the basis of mechanism 7.2, and the thiol-disulfide interchange reaction of protein SH groups with GSSG may be treated as an irreversible reaction which follows pseudo-first-

order kinetics.

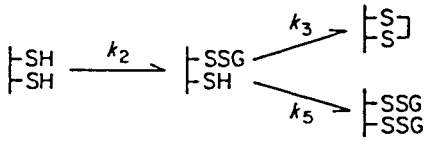

(Mechanism 7.2)†

The first-order plot for the decrease in the concentration of C_{LSH}^{SH} with time was linear and the k_2 value was determined to be 2.0 s^{-1} M^{-1} from this plot.

Figure 7.3(c) and (d) show the kinetics of the reaction of C_{LSH}^{SH} with GSSG in the absence of urea. Compared with the reaction kinetics in the presence of 8 M urea, the reaction in the absence of urea had the following three features. (i) The reaction was much slower in the absence of urea. With 3 mM GSSG, the reaction in the absence of urea continued for several hours, whereas the reaction in 8 M urea completed within 30 min. (ii) Accumulation of C_{LSH}^{SSG} was much lower in the absence of urea. In the reaction with 3 mM GSSG, accumulation of the intermediate attained to 40 % of the total protein at the maximum level in 8 M urea, whereas it accumulated only slightly in the absence of urea. (iii) Formation of the intrachain disulfide bond was more effective in the absence of urea. In the reaction with 3 mM GSSG, the yield of C_{LS}^{S} was about 80 % of the total protein in the absence of urea but only 30 % in the presence of 8 M urea.

---

† In this mechanism and mechanism 7.4 to 7.8, reactant GSSG or GSH is omitted.

As described in Chapter 3, in the absence of denaturant, C_{LSH}^{SH} has a conformation very similar to that of the intact C_L fragment and the two cysteinyl residues are buried in the interior of the protein molecule. Consequently, in order to react with GSSG in the absence of denaturant, the C_{LSH}^{SH} molecule must open and the SH groups must be exposed to solvent. The C_{LS}^{S} molecule may also have both opened and closed conformations. Thus the thiol-disulfide interchange reaction of C_L fragment with glutathione in the absence of denaturant may be expressed thus:

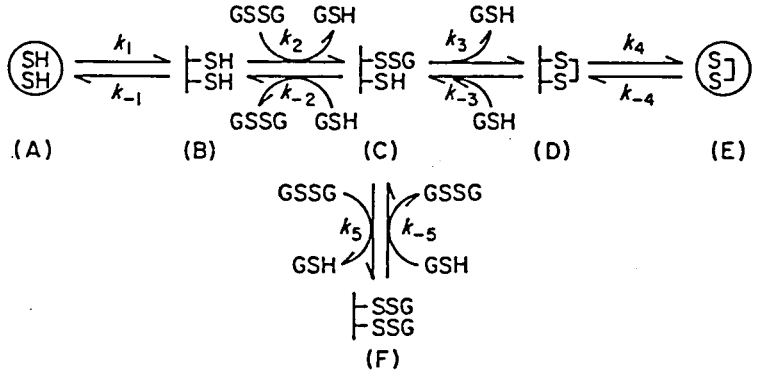

(Mechanism 7.3)

where k_2, k_{-2}, k_{-3}, k_5, and k_{-5} are the second-order rate constants for the thiol-disulfide interchange reactions and the others are the first-order rate constants for the intramolecular reactions. In this mechanism, the reactivities of the two SH groups of the opened form of C_{LSH}^{SH} (B) were assumed to be the same and species C_{LSH}^{SSG} and C_{LSSG}^{SH} were not discriminated. Under the present experimental conditions where the concentration of GSSG is much higher than that of C_{LSH}^{SH}, the reactions involving GSH may be assumed not to proceed significantly. Furthermore, the value of k_{-4} is much smaller than that of k_4 as will

be described later (see 7.B.5). Thus the results in Figure 7.3(c) and (d) may be explained on the basis of mechanism 4.

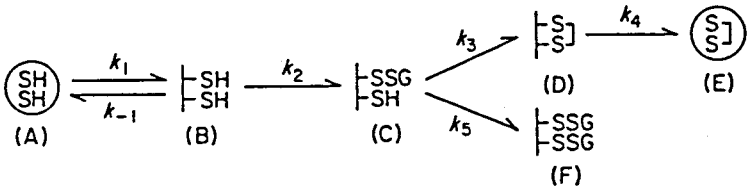

(Mechanism 7.4)

As can be seen from Figure 7.3(c) and (d), the amount of C_{LSSG}^{SSG} first increased and then decreased with time. One of the final products, C_{LSSG}^{SSG}, is readily reduced with GSH but the other product C_{LS}^{S} is not (see 7.B.3 and 7.B.5). The decrease in the amount of C_{LSSG}^{SSG} may be due to the reduction of C_{LSSG}^{SSG} with GSH produced by the reaction of protein SH groups with GSSG being significant at the late period of time. The results in Figure 7.3(c) and (d) at the early period of time may thus be explained on the basis of mechanism 7.4 but participation of GSH in the reactions cannot be neglected at the late period of time.

If the equilibrium between closed (A) and opened (B) forms of C_{LSH}^{SH} shifts to the closed form and is much faster compared with the rate $k_2[GSSG]$, the rate of disappearance of C_{LSH}^{SH} is given by $K \cdot k_2[GSSG]$, where $K = k_1/k_{-1}$. On the other hand, if the equilibrium between A and B shfts to A and the rate $k \cdot [GSSG]$ is much faster than k_1 and k_{-1}, the rate of disappearance of C_{LSH}^{SH} is given by k_1 and is independent of the concentration of GSSG. I studied the dependence of the GSSG concentration of the concentrations of the species trapped at a given time (Figure 7.4). The concentration of C_{LSH}^{SH} decreased steeply at low GSSG

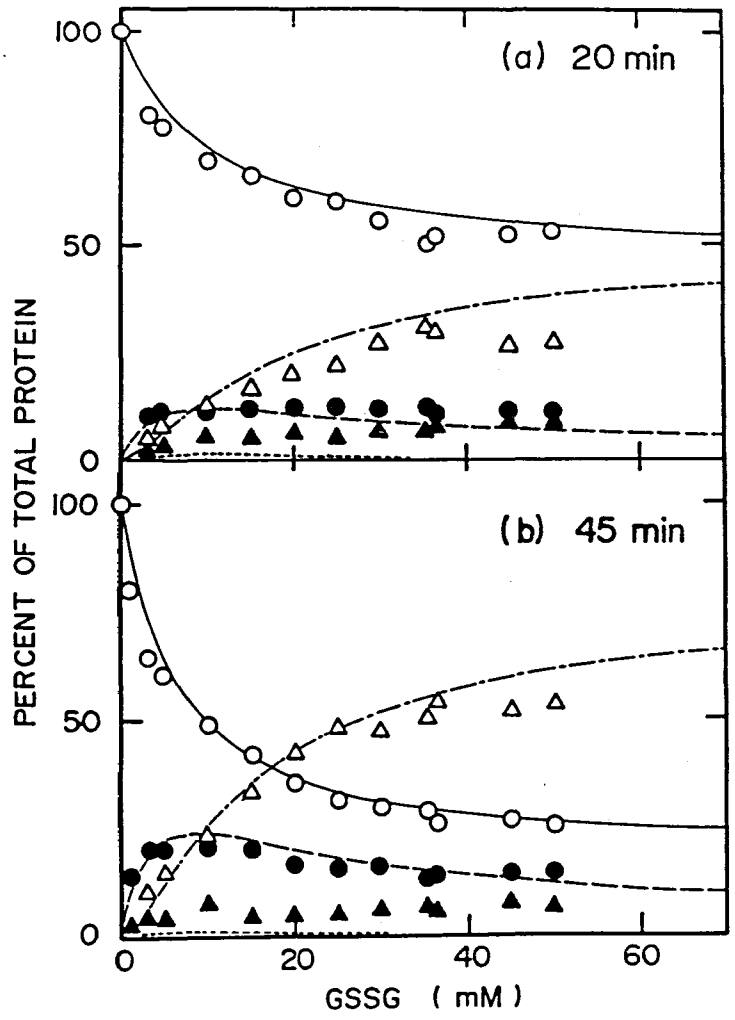

Fig. 7.4. Dependence on the GSSG concentration of the concentrations of species formed during regeneration of reduced C_L fragment. Reduced C_L fragment (0.03 mM) was reacted with various concentrations of GSSG for (a) 20 min and (b) 45 min, when the reaction was quenched by addition of iodoacetamide, and the concentrations of each species were determined electrophoretically. The symbols used are the same as for Fig. 7.3. The curves were calculated with kinetic mechanism 7.3 (see the text) and the values for the rate constants in Table 7.I.

concentrations and reached a constant value at higher GSSG concentrations; the rate of the disappearance being independent of the GSSG concentration. This as well as the kinetic data shown in Figure 7.3(c) and (d) demonstrates that there exists an equilibrium between the closed form and opened form of C_{LSH}^{SH}, only the latter form can react with GSSG, and the fraction of the latter form is very small. The value of $K \cdot k_2[GSSG]$ was thus estimated using the rate of disappearance of C_{LSH}^{SH} at the lowest GSSG concentration used and the value of k_1 was estimated from the rate of disappearance at the highest GSSG concentration. As will be described later, k_{-1} can also be determined as k_2 is estimated by other experiments.

As shown in Figure 7.4, the concentration of C_{LSSG}^{SSG} was higher than that of C_{LS}^{S} at low GSSG concentrations but this relation was reversed at higher GSSG concentrations. This may be explained in terms of mechanism7.4,in which the formation of C_{LSSG}^{SSG} from C_{LSH}^{SSG} is dependent on the GSSG concentration ($k_5[GSSG]$), but the formation of C_{LS}^{S} is independent of the GSSG concentration.

In order to establish mechanism 7.1 and 7.3 for the reactions of C_{LSH}^{SH} with GSSG in the presence and absence of urea, I studied the kinetics of the reactions starting from various species of the C_L fragment as will be described below.

7.B.3. Reaction of C_{LSSG}^{SSG} with GSH

The reaction of C_{LSSG}^{SSG} with GSH in 8 M urea was studied by gel electrophoresis (Figure 7.5(a) and (b)). In the reaction with 3.5 mM GSH, C_{LSSG}^{SSG} decreased exponentially, C_{LSH}^{SSG} accumulated transiently,

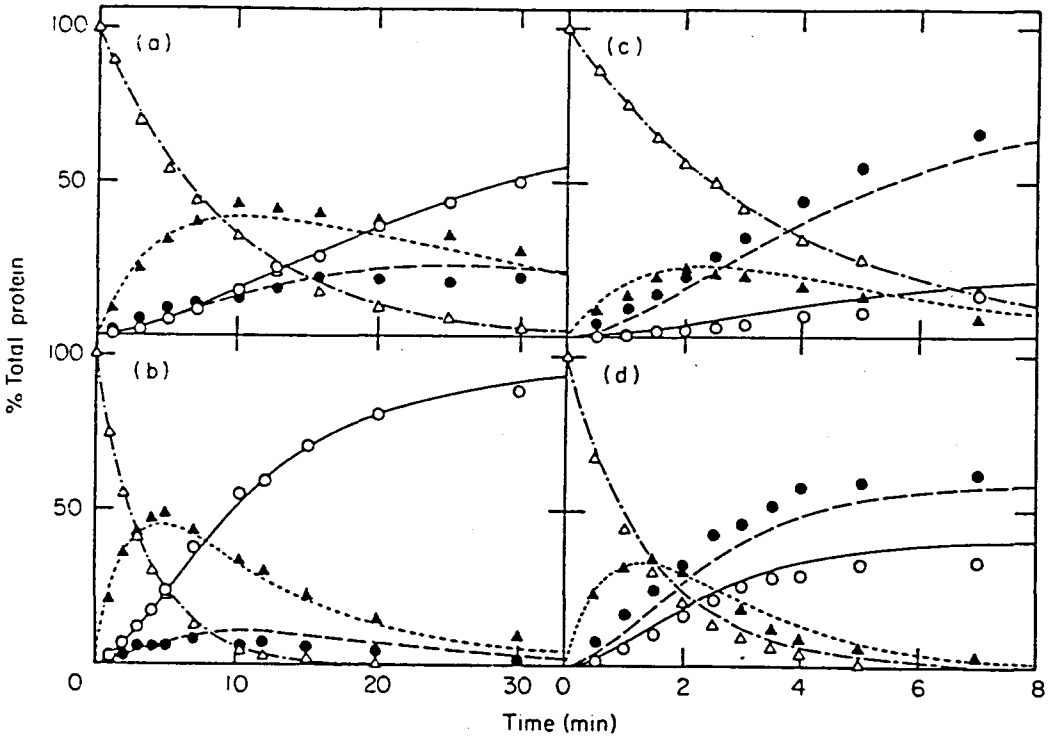

Fig. 7.5. Kinetics of the reaction of C_{LSSG}^{SSG} with (a) 1.4 mM and (b) 3.5 mM GSH in the presence of 8 M urea and with (c) 1.4 mM and (d) 3.5 mM GSH in the absence of urea. C_{LSSG}^{SSG} (0.03 mM) was reacted with GSH at pH 8.1 and 25°C and the time-dependent concentrations of each species were determined electrophoretically. The symbols used are the same as for Fig. 7.3. The curves for (a) and (b) were calculated with kinetic mechanism 7.1 (see the text) and the values for the rate constants in Table 7.I; the curves for (c) and (d) were calculated with kinetic mechanism 7.3 (see the text) and the values for the rate constants in Table 7.I.

and C_{LSH}^{SH} appeared with a lag phase. A small amount of C_{LS}^{S} also accumulated but this species slowly disappeared after it reached a maximum level (10 %). The overall reaction with 1.4 mM GSH was slower than that with 3.5 mM GSH but the accumulation of C_{LS}^{S} increased to 20 % at the maximum level.

In this experiment, I studied the reaction of C_{LSSG}^{SSG} with GSH in excess of the concentration of C_{LSSG}^{SSG}. Therefore, I may neglect the reaction in which GSSG participates in mechanism 7.1, and the reaction may be expressed by mechanism 7.5.

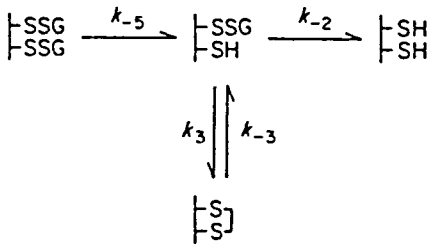

(Mechanism 7.5)

The slow decrease of C_{LS}^{S} after it reached a maximum level is due to the disulfide bond of C_{LS}^{S} being susceptible to reduction with GSH in its denatured state. On the basis of mechanism 7.5, the thiol-disulfide interchange reaction of C_{LSSG}^{SSG} should follow the pseudo-first-order kinetics. The disappearance of C_{LSSG}^{SSG} (Figure 7.5(a) and (b)) followed first-order kinetics and a value of 1.3 s^{-1} M^{-1} was obtained as the second-order rate constant k_{-5}.

The reaction of C_{LSSG}^{SSG} with GSH was also studied in the absence of urea (Figure 7.5(c) and (d)). The kinetics of the reaction in the absence and presence of urea were different in that C_{LS}^{S} was formed more effectively than C_{LSH}^{SH} as a final product in the absence of urea.

Both species appeared with a lag phase. The overall rate was slower but the yield of C_{LS}^{S} was higher in the reaction with 1.4 mM GSH than in the reaction with 3.5 mM GSH.

In this experiment, I studied the reaction under the conditions where the concentration of GSH is much higher than that of C_{LSSG}^{SSG}. Thus the reactions in which GSSG participates in mechanism 7.3 may be neglected. As will be described in 7.B.5, the disulfide bond of C_{LS}^{S} has essentially no reactivity toward GSH in the absence of denaturant. It is thus suggested that process D to E should be much faster than process D to C and process E to D scarcely occurs. In the absence of denaturant, C_{LSH}^{SH} has essentially a folded conformation and k_{-1} is much larger than k_1 (see mechanism 7.3 and Table 7.1). Thus we may neglect the reduction of C_{LS}^{S} with GSH and the unfolding processes of C_{LS}^{S} and C_{LSH}^{SH}. The results of Figure 7.5(c) and (d) may thus be explained on the basis of mechanism 7.6

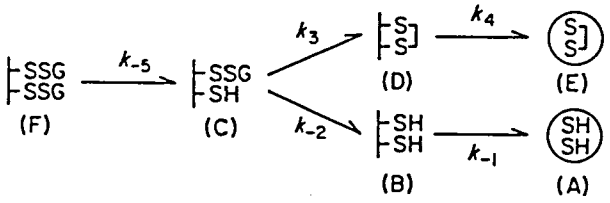

(Mechanism 7.6)

The disappearance of C_{LSSG}^{SSG} followed pseudo-first-order kinetics under the present experimental conditions and the k_{-5} value was determined to be 3.3 s^{-1} M^{-1}.

In mechanism 7.6, D and E, which are both disulfide-bonded species but are conformationally different, cannot be distinguished electro-

TABLE 7.I. Values for the rate constants for reaction of the C_L fragment with glutathione at pH 8.1 and 25°C as determined by gel electrophoresis,

	k_1 (s^{-1})	k_{-1} (s^{-1})	k_2 ($s^{-1}M^{-1}$)	k_{-2} ($s^{-1}M^{-1}$)	k_3 (s^{-1})	k_{-3} ($s^{-1}M^{-1}$)	k_4 (s^{-1})	k_{-4} (s^{-1})	k_5 ($s^{-1}M^{-1}$)	k_{-5} ($s^{-1}M^{-1}$)
In the absence of urea	$6{\cdot}3\times10^{-4}$	$2{\cdot}8\times10^{-2}$	2·0	1·7†	$8{\cdot}3\times10^{-3}$† $6{\cdot}2\times10^{-3}$‡	(2·1)§	Very fast	Very slow	1·0	3·3†
In the presence of 8 M-urea			2·0	$6{\cdot}7\times10^{-1}$	1×10^{-3}	$8{\cdot}3\times10^{-1}$			1·0	1·3

† These values were also obtained by fluorescence measurements for the reaction of C_{LSSG}^{SSG} with GSH.

‡ Determined by fluorescence and gel elctrophoresis measurements for the diuslfide formation in C_{LSH}^{SSG} by pH jump (see Fig. 7.7).

§ See the text for details.

phoretically. A and B, which are both disulfide-reduced species but are conformationally different, cannot be distinguished electrophoretically either. Since I had found that the fluorescence spectra of intact C_L, reduced C_L, and reduced and alkylated C_L fragment are different (Chapter 3), I expected that the reaction in mechanism 7.6 could be followed by fluorescence measurement. The fluorescence spectrum of C_{LSSG}^{SSG} was very similar to that of reduced and alkylated C_L fragment and had a maximum at 350 nm. This indicates that the C_{LSSG}^{SSG} molecule has an unfolded conformation. The fluorescence spectra of C_{LS}^{S} and C_{LSH}^{SH} had maxima at 325 and 328 nm, respectively. When compared at 350 nm, the fluorescence intensities of C_{LS}^{S}, C_{LSH}^{SH}, and C_{LSSG}^{SSG} were 23, 60, and 85 %, respectively, relative to that of the C_L fragment denatured in 4 M GuHCl.

As shown in Figure 7.6(a), the fluorescence of C_{LSSG}^{SSG} changed greatly with a lag phase on the addition of GSH. The final fluorescence spectrum obtained in the presence of 0.17 mM GSH was essentially the same as the spectrum of intact C_L fragment. The overall reaction proceeded faster and the final fluorescence intensity was higher in the presence of 1.25 mM GSH than in the presence of 0.17 mM GSH.

The fluorescence change shown in Figure 7.6(a) was analyzed assuming that the fluorescences of B and D are the same as the fluorescence of C_{LSSG}^{SSG} (F) and that the fluorescence changes appear in the processes D to E and B to A in mechanism 7.6. At the GSH concentrations used here, the value of k_{-1} is much greater than that of k_{-2}[GSH] and the value of k_4 is much greater than that of k_3 (see Table 7.1 and section 7.B.5). Under these conditions, the fluorescence at time t (F(t)) may be expressed

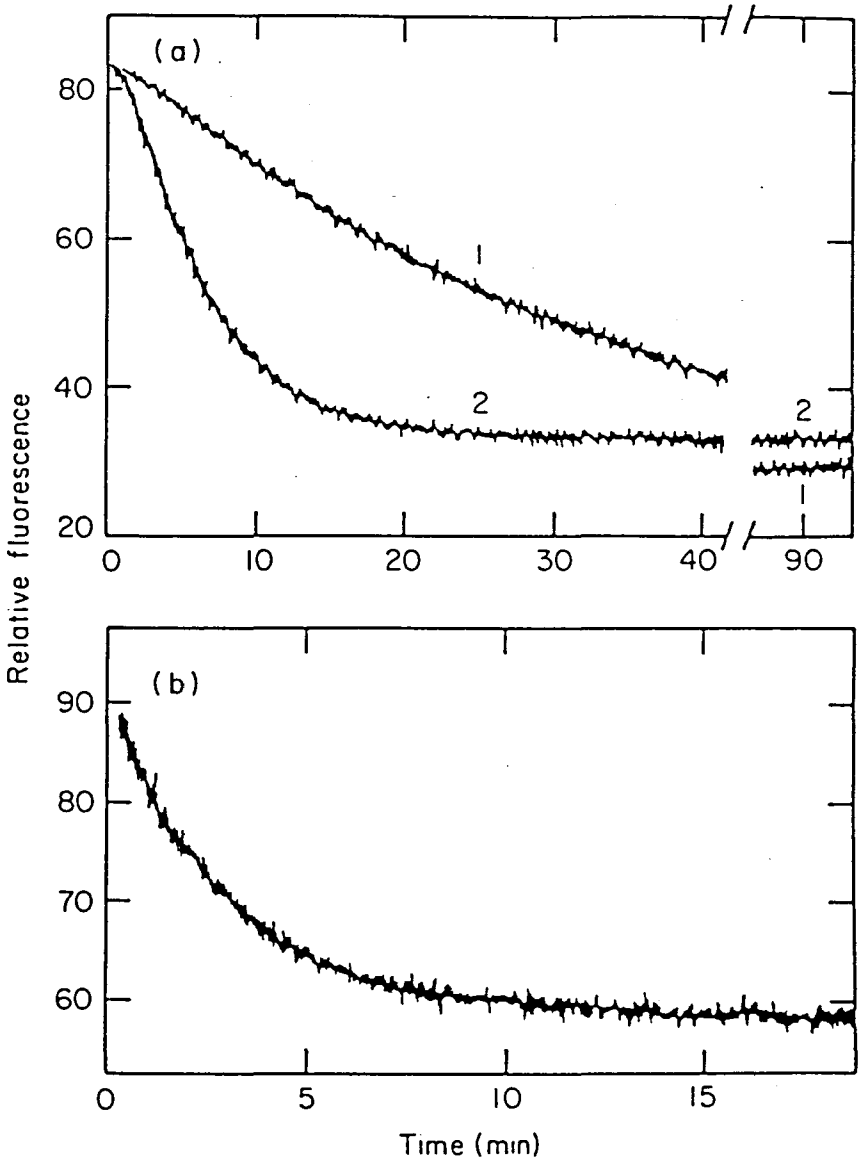

Fig. 7.6. (a) Kinetics of the reaction of C_{LSSG}^{SSG} with GSH obtained by fluorescence measurement. Change with time in the fluorescence intensity at 350 nm excited at 295 nm was measured after the addition of GSH to 0.17 mM (1) and 1.25 mM (2) to a solution of C_{LSSG}^{SSG} (0.03 mM) at pH 8.1 and 25°C. (b) Kinetics of the formation of disulfide bond in C_{LSH}^{SSG} by a pH jump from 5 to 8.1. Change in the fluorescence intensity at 350 nm excited at 295 nm of a solution that contains C_{LSH}^{SSG} was measured after the pH of the solution was raised from 5 to 8.1.

by the following equation:

$$F(t) = F(0) - \left(\frac{k_{-2}[GSH]\Delta F_1 + k_3 \Delta F_2}{k_{-2}[GSH] + k_3} \right) \left\{ 1 + \frac{(k_{-2}[GSH] + k_3)e^{-k_5[GSH]t} - k_{-5}[GSH]e^{-(k_{-2}[GSH] + k_3)t}}{k_{-5}[GSH] - k_{-3}[GSH] - k_3} \right\}, \quad (7.1)$$

where F(0) is the initial fluorescence intensity, and ΔF_1 and ΔF_2 are the differences in the fluorescence intensity between B and A and between D and E, respectively.

At a very low GSH concentration, equation (7.1) reduces to:

$$F(t) = F(0) - \Delta F_2(1 - e^{-k_{-5}[GSH]t}) . \quad (7.2)$$

The value of k_{-5} was estimated to be 3.3 s^{-1} M^{-1} using equation (7.2) on the basis of the results of the reaction with 0.17 mM GSH, where the lag phase was very small and the reaction followed first-order kinetics except at a very early stage. This value is the same as that determined electrophoretically.

7.B.4. Intramolecular thiol-disulfide interchange reaction in C_{LSH}^{SSG}

The species, C_{LSH}^{SSG}, is very important as the intermediate from which the intrachain disulfide bond is formed through intramolecular thiol-disulfide interchange reaction. Although it was difficult to isolate only this species, the intramolecular disulfide formation in this species was found to be followed fluorimetrically even in the

presence of the other species, C_{LSH}^{SH}, C_{LSSG}^{SSG}, and C_{LS}^{S}. In order to obtain reliable results, it is desirable to prepare a solution which contains a maximal amount of C_{LSH}^{SSG}. It can be easily shown that a solution containing 50 % C_{LSH}^{SSG}, 25 % C_{LSH}^{SH}, and 25 % C_{LSSG}^{SSG} can be prepared by the reaction of C_{LS}^{S} with an excess of glutathione at the molar ratio of [GSH]/[GSSG] = k_5/k_{-2} in the presence of 8 M urea (see mechanism 7.1 and Table 7.1). Experimentally such a solution was prepared as follows. The C_L fragment was dissolved in a solution of 8 M urea (pH 8.5) containing 20 mM GSSG, 30 mM GSH, and 1 mM EDTA, and the solution was allowed to stand for 30 min at 25°C. The concentration of the C_L fragment was about 0.1 mM. The reaction was stopped by lowering the pH to about 4 by the addition of acetic acid, and then the protein was separated from the residual reagents on a column of Sephadex G-25 equilibrated with 5 mM potassium acetate buffer at pH 5.0 containing 1 mM EDTA and 0.2 M KCl. It was shown by gel electrophoresis that the resulting solution contained about 50 % C_{LSH}^{SSG}, 25 % C_{LSH}^{SH}, 25 % C_{LSSG}^{SSG}, and 0 % C_{LS}^{S}.

When the pH of the solution is raised from 5 to higher values where the SH group is ionized, the disulfide will be formed only in C_{LSH}^{SSG} and not in the other species present in this solution. This reaction of C_{LSH}^{SSG}, whcih is a part of the reaction of mechanism 7.3, may be expressed by mechanism 7.7, if we assume that k_{-4} is negligible in the absence of denaturant.

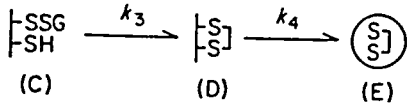

(Mechanism 7.7)

As shown in Figure 7.6(b), a large fluorescence change was observed on raising the pH from 5 to 8.1. This fluorescence change must have been caused by the disulfide formation in C_{LSH}^{SSG} and not by the other species. A small and rapid change in the fluorescence was also observed on the pH jump within the dead time of the measurement. This may be due to a change with pH in the fluorescence of all the species. Formation of C_{LS}^{S} from C_{LSH}^{SSG} consists of at least two steps, one is the intramolecular thiol-disulfide interchange with rate constant k_3 and the other the following conformational change with rate constant k_4. The fluorescence change followed first-order kinetics. This suggests that k_3 is much greater than k_4 or vice versa. The fluorescence changes were measured at pH's between 7 and 10. All these changes followed first-order kinetics, but at pH's higher than 8.5 a small deviation from the first-order plot was observed at the late period of time. This deviation is due probably to the reaction of C_{LSSG}^{SSG} with GSH produced by the intramolecular thiol-disulfide interchange reaction in C_{LSH}^{SSG}. Thus the rate constants at pH's above 8.5 were determined using the data at the early period of time.

The first-order rate constants are plotted against pH in Figure 7.7. This change was found to be expressed by the following equation:

$$k = k^{\circ} \frac{K_a}{K_a + (H^+)}, \qquad (7.3)$$

where k° is the maximum rate constant and (H^+) is the acitvity of hydrogen ions. This equation is obtained for the reaction in which a single ionizable group with ionization constant K_a is involved. The

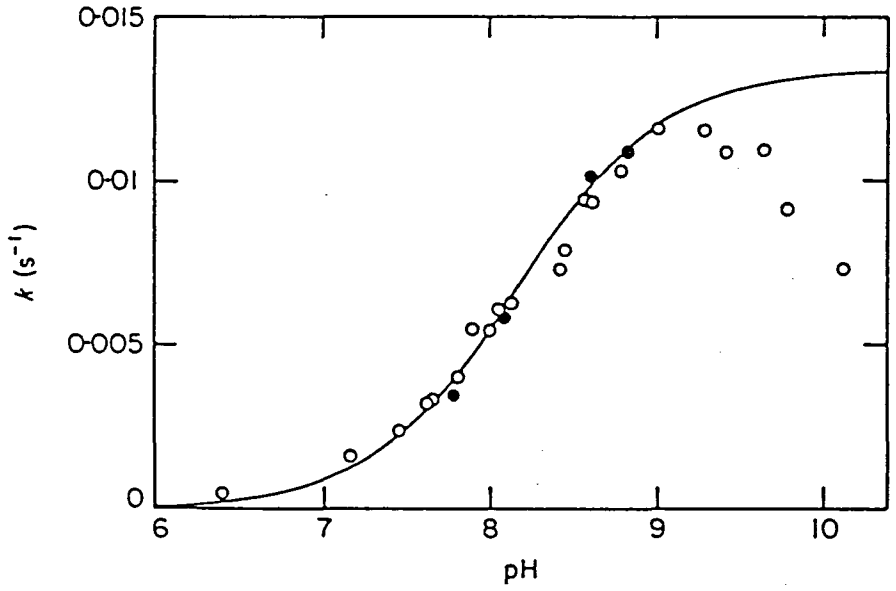

Fig. 7.7. Dependence of the value of k on pH. The values of k at various pH values were determined by fluorescence measurement (○) shown in Fig. 7.6(b) and by polyacrylamide gel electrophoresis (●) similar to the experiment shown in Fig. 7.2. The buffers used to raise the pH were Tris-HCl buffers (below pH 9) and glycine-KOH buffers (above pH 9). The unbroken line indicates the theoretical curve constructed using the maximum value of k (k°) = 1.3×10^{-2} s^{-1} and pKa = 8.2 (see equation (7.3)).

value of pH_a and k^o were determined to be 8.2 and 1.3×10^{-2} s^{-1}, respectively. However, the values of k^o and hence pK_a determined here are minimum values, because the value of k decreased above pH 9. Since the intramolecular thiol-disulfide interchange reaction occurs only for species C_{LSH}^{SSG} with the SH group ionized, the ionizable group with pK_s 8.2 should be assigned to this group. These findings indicate that the rate constant in equation (7.3) corresponds to k_3 and that the conformational change with rate constant k_4 occurs much faster compared with the reaction with rate constant k_3. It is also suggested that the SH group of C_{LSH}^{SSG} has a pK_a value similar to that of C_{LSSG}^{SH}. Formation of the disulfide in C_{LSH}^{SSG} on pH jump was also studied electrophoretically. As shown in Figure 7.7, these results were in good agreement with those determined electrophoretically. The decrease in the rate constant above pH 9 may be due to destabilization of the conformation of C_{LSH}^{SSG} (see section 7.C).

7.B.5. Reaction of C_{LS}^{S} with GSH

Although this reaction is the reverse of the disulfide formation, it is important to study this reaction in order to understand the overall reaction of the C_L fragment with glutathione. Figure 7.8 shows the kinetics of reduction of the intrachain disulfide bond of C_{LS}^{S} with GSH in 8 M urea. An exponential decrease in the amount of C_{LS}^{S}, a transient accumulation of C_{LSH}^{SSG}, and formation of the product, C_{LSH}^{SH}, with a lag phase were observed. An increase in GSH concentration from 4 to 8 mM accelerated the reaction as a whole. This reaction may be expressed by mechanism 7.8, because the reactions in which GSSG participates in

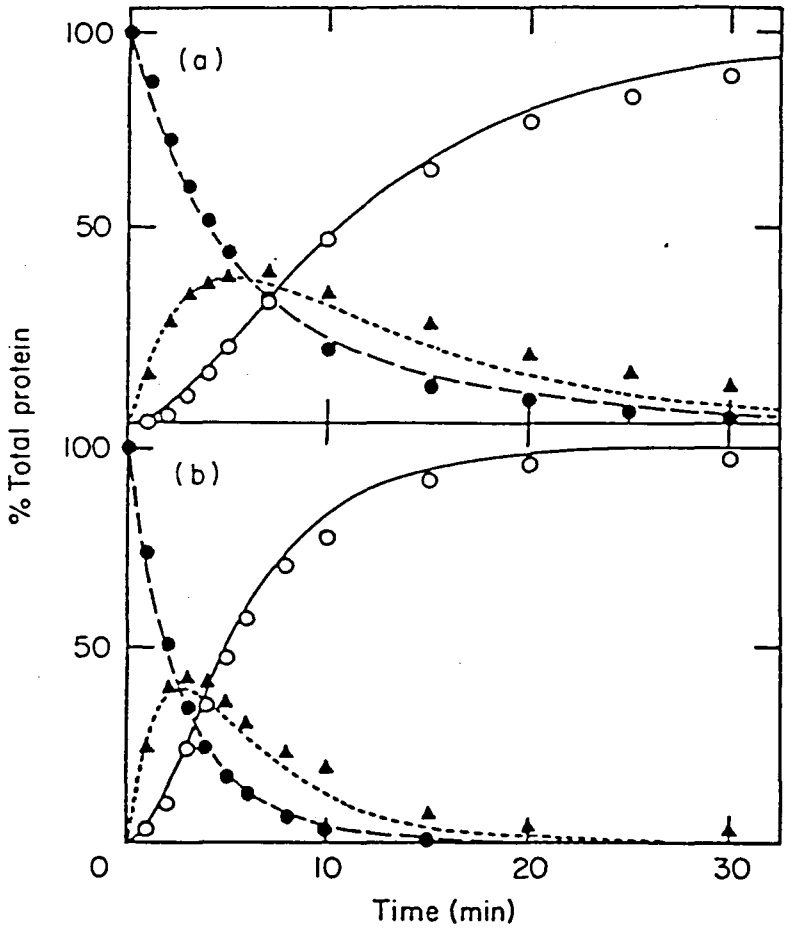

Fig. 7.8. Kinetics of the reduction of C_{LS}^{S} with (a) 4 mM and (b) 8 mM GSH in the presence of 8 M urea at pH 8.1 and 25°C. C_{LS}^{S} (0.03 mM) was reduced with GSH and the species formed were identified by polyacrylamide gel electrophoresis. The symbols used are the same as for Fig. 7.3. The curves were calculated with kinetic mechanism 7.1 (see the text) and the values for the rate constants in Table 7.I.

mechanism 7.1 can be neglected under the present experimental conditions.

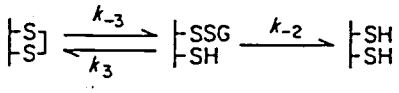

(Mechanism 7.8)

The reaction of C_{LS}^{S} with 25 mM GSH was carried out in a Tris-HCl buffer at pH 8.1 without urea. No significant amount of C_{LSH}^{SH} was formed after standing this solution for more than 10 hours at 25°C. This shows that in the absence of denaturant the intrachain disulfide bond of the C_L fragment is essentially buried in the interior of the molecule and cannot react with GSH.

7.B.6. Overall reaction of C_L fragment with glutathione

As the thiol-disulfide interchange reactions of the four different species of the C_L fragment were available, the mechanisms (7.1 and 7.3) for the overall reaction of the C_L fragment with glutathione can now be established.

(i) Reaction of C_L fragment with glutathione in 8 M urea (mechanism 7.1)

The values of k_2 and k_{-5} were described in sections 7.B.2 and 7.B.3. When the species involved are denatured and the SH groups have the same reactivity, the rate constant for the interchange reaction of protein SH groups with GSSG is assumed to be proportional to the number of the reactive site on the protein molecule. Since C_{LSH}^{SH} has two SH groups that react with GSSG and C_{LSH}^{SSG} has one, the rate constant k_2 is twice the rate constant k_5. The rate constant k_5 was thus estimated

to be 1.0 s^{-1} M^{-1} from the value of k_2 determined previously. Likewise the value of k_{-5} should be twice that of k_{-2}, and the value of k_{-2} was estimated to be 0.7 s^{-1} M^{-1}. In the reaction of C_{LSH}^{SH} with GSSG (mechanism 7.2), the ratio of the yields of the final products, C_{LS}^{S} and C_{LSSG}^{SSG}, is determined by the ratio of the two rate constants, k_3 and k_5[GSSG]. The value of k_3 was thus estimated using the data of Figure 7.3(a) and (b). Using the rate constants of k_{-2} and k_3 thus determined, the value of k_{-3} that fits the observed kinetic data shown in Figure 7.8 was estimated. The rate constants for mechanism 7.1 are summarized in Table 7.1. The theoretical curves constructed by the Runge-Kutta method (see for instanc Henrici (1962)) using mechanism 1 and the values for rate constants in Table 7.1 agreed quite well with the experimental data of Figures 7.3(a) and (b), 7.5(a) and (b), and 7.8.

(ii) Reaction of C_L fragment with glutathione in the absence of urea (mechanism 7.3)

The k_1 value estimated electrophoretically was described in section 7.B.2. The k_{-5} value determined electrophoretically was in good agreement with the value determined fluorimetrically as described in section 7.B.3. Since C_{LSSG}^{SSG} and C_{LSH}^{SSG} may have a similar unfolded conformation and C_{LSSG}^{SSG} has two mixed disulfides and C_{LSH}^{SSG} has one, the rate constant for the reaction of the former with GSH should be twice the rate constant for the reaction of the latter. The value of k_{-2} was thus estimated to be 1.7 s^{-1} M^{-1} from the value of k_{-5}. The value of k_3 was determined by the following three methods.

(i) As described in section 7.B.4, analysis of the change in the fluorescence on pH jump of a solution which contains C_{LSH}^{SSG} gave the value of k_3. (ii) Since the concentration ratio of C_{LSH}^{SH} to C_{LS}^{S} is determined by the ratio of $k_{-2}[GSH]$ to k_3 in mechanism 7.6 and k_{-2} is known, the value of k_3 can be determined using the data of Figure 7.5(c) and (d). (iii) Since the value of k_{-5} and k_{-2} are available, the value of k_3 can be determined so that the fluorescence changes with time of C_{LSSG}^{SSG} on the addition of GSH at various concentrations fit equation (7.1). The values of k_3 determined by these methods were in good agreement with one another. The value of k_5 was estimated from the value of k_3 using the data of Figure 7.3(c) and (d), since the concentration ratio of C_{LS}^{S} to C_{LSSG}^{SSG} at the early time of period is determined by the ratio of k_3 to $k_5[GSSG]$. In mechanism 7.3, the rate constant for the reaction of the opened form of C_{LSH}^{SH} (species B) with GSSG should be twice that for the reaction of C_{LSH}^{SSG} with GSSG. The value of k_2 was thus estimated from the value of k_5. As described in section 7.B.2, I estimated the value of $k_2[GSSG] \cdot k_1/k_{-1}$ using the data of Figure 7.4. Since the values of k_2 and k_1 are now available, k_{-1} can be estimated. The values for the rate constants in mechanism 7.3 are summarized in Table 7.I. The theoretical curves constructed by the Runge-Kutta method using mechanism 7.3 and the rate constants in Table 7.1 and assuming that $k_4 \gg k_{-4}$ and $k_4 \gg k_{-3}[GSH]$ are in good agreement with the experimental data (see Figure 7.3(c) and (d), 7.4, and 7.5(c) and (d)). In this calculation I set the value of k_{-3} equal to 2.0 s^{-1} M^{-1}. This value was estimated assuming that the k_{-3} value in the absence of urea is 2.5 times greater than that in the presence

of 8 M urea (k_{-3} = 0.8 s^{-1} M^{-1}), since the rate constant of the reduction of the mixed disulfide with GSH (k_{-5} or k_{-2}) are 2.5 times greater in the absence of urea than in its presence (see Table 7.1).

Compared with the rate constants in 8 M urea, the value of k_3 is about ten times larger in the absence of urea. The values of k_{-2} and k_{-5} are also larger in the absence of urea.

7.C. Discussion

I have described the formation of the intrachain disulfide bond of the C_L fragment from its reduced state in the absence and presence of urea. One of the most important findings is that the reaction is much slower but the yield of C_{LS}^{S} is much higher in the absence of urea than in its presence when compared at the same GSSG concentration. The slowness of the formation of C_{LS}^{S} in the absence of urea is due to the two cysteinyl residues of the C_{LSH}^{SH} molecule being buried in the interior and the higher yield of C_{LS}^{S} is due to higher efficiency of the intramolecular thiol-disulfide interchange in C_{LSH}^{SSG}.

In the absence of denaturant, the C_{LSH}^{SH} molecule has a folded conformation very similar to intact C_L fragment (Chapter 3). In order to react with GSSG, therefore, the C_{LSH}^{SH} molecule must open. The values of k_1 and k_{-1} in mechanism 7.3 were determined to be 6×10^{-4} s^{-1} and 2.8×10^{-2} s^{-1}, respectively (Table 7.1). The value of k_1 is comparable with that obtained from the titration of the SH groups with DTNB (1×10^{-3} s^{-1})(Chapters 3 and 5). The free energy change for this fluctuation is estimated to be -2.3 kcal mol^{-1} based on two-state approximation. This value is also comparable with that obtained from the analysis of the denaturation equilibrium of reduced C_L fragment by GuHCl (about - 2 kcal mol^{-1})(Chapter 3).

Compared with the reaction of C_{LSH}^{SH} with GSSG in 8 M urea, the accumulation of C_{LSH}^{SSG} was much lower and the yield of C_{LS}^{S} was much higher in the absence of urea (see Figure 7.5). In Chapter 3, I showed that reduced and alkylated C_L fragment in the absence of denaturant is completely unfolded with respect to the states of its two tryptophyl

residues but not with respect to the conformation of the polypeptide backbone. The amplitude of the fluorescence change on a pH jump from 5 to 8.1 (Figure 7.6(b)) was about 35 % of the initial fluorescence intensity. If the fluorescence intensity of C_{LSH}^{SSG} is the same as that of C_{LSSG}^{SSG}, a 38 % decrease in the fluorescence intensity is expected for the formation of disulfide in C_{LSH}^{SSG} from the fluorescence intensities and the fractional amounts of the molecular species present in this solution. This value is in good agreement with the observed value and it is shown that C_{LSH}^{SSG} has an opened conformation with respect to the states of tryptophyl residues. The C_{LSH}^{SSG} molecule thus seems to have a conformation very similar to reduced and alkylated C_L fragment and the presence of denaturant will change its polypeptide conformation to a more completely unfolded one. As can be seen from Table 7.I, the value of k_3 is greater in the absence of urea than in its presence, although the values of k_5 are the same. This indicates that although C_{LSH}^{SSG} has an opened conformation and the interchange reaction between its SH group and GSSG in the absence of urea occurs as easily as the reaction in the presence of 8 M urea, the distance between the SH group in C_{LSH}^{SSG} is appropriate to form the disulfide bond and the collision between them occurs more frequently in the absence of urea than in its presence where the process of disulfide formation is a statistically controlled event. As shown in Figure 7.7, the k_3 value decreased above pH 9. This may be due to a conformational change of C_{LSH}^{SSG} at high pH's by which the distance between the SH and SSG groups becomes inappropriate to form the disulfide bond.

As described above, in the reaction of C_{LSH}^{SH} with GSSG the yield of C_{LS}^{S} was substantial but the rate was extremely slow. The main reason for this slowness is that the cysteinyl residues of the C_{LSH}^{SH} molecule are buried in the interior of the protein molecule. I do not know whether the intrachain disulfide is formed through thiol-disulfide interchange reaction in vivo. However, whatever the mechanism of the disulfide formation in vivo, the cysteinyl residues buried in the interior of the C_{LSH}^{SH} molecule are not easily oxidized to disulfide; the disulfide should be formed rapidly before the complete folding of the C_L domain occurs. In fact, the recent work of Bergman and Kuehl (1979) have shown that the intrachain disulfide bonds of MPC 11 light chain are formed very rapidly before the completion of the primary structure.

As described in the present Chapter, the reduced C_L fragment has a native-like conformation and the folding of the polypeptide chain prevents the disulfide formation. This indicates that disulfide bond formation does not always serve as a useful probe of protein folding. Failure to form disulfide bonds owing to burial of SH groups in the hydrophobic interior of the protein molecule would be also observable during refolding process from other reduced proteins. Furthermore, Hamaguchi and his colleagues (Kishida et al., 1976; Tanaka et al., 1978; Kato et al., 1978) showed that formation of the interchain disulfide bonds between two light chains and between light and heavy chains is governed not only by the proximity of the two thiol groups that participate in the disulfide formation but also by the differences in the ionization constant and reactivity between the two thiol groups.

These findings indicate that to correlate disulfide formation with protein folding it is important to clarify the conformations of intermediates formed during regeneration in addition to the pathway of disulfide formation.

Creighton (1978) established the pathway of disulfide bond formation in bovine pancreatic trypsin inhibitor and correlated with the pathway of the folding of the polypeptide chain. He observed that one of the two-disulfide bonded intermediates cannot form directly the third native disulfide bond even though it had two native disulfide bonds, and suggested that it has basically an unfolded conformation and it must undergo conformational transitions involving disulfide interchange to different two-disulfide bonded intermediate which can form the third disulfide bond rapidly. According to my present findings, however, this might be due to the cysteinyl residues of this intermediate being buried in the interior of the molecule and being uncapable of forming the third disulfide bond even though they are located closely to each other. Recently, Creighton (1981) has denied my indication. Creighton also studied the conformations of intermediates of pancreatic trypsin inhibitor (Creighton et al., 1978) and ribonuclease A (Creighton, 1979) trapped by alkylation to confirm the correlation between the pathway of disulfide formation and the conformational transitions. However, since alkylation of buried SH groups may alter the protein conformation as found for the C_L fragment (Chapter 3), it will be necessary to confirm whether the alkylated intermediate has the same conformation as the SH-free intermediate.

As can be seen from Table 7.I, the rate constants, k_{-2} and k_{-5}, for the interchange reaction of protein SH group with GSSG are different depending on whether urea is present or not. The rate constant k_{-5} was obtained directly and accurately from the disappearance of C_{LSSG}^{SSG} (see Figure 7.5). The reason for this is not clear.

Finally, the rate constants of conformational transition obtained in this Chapter are compared with those determined in Chapter 5. On the basis of the three-species mechanism, I estimated the rates of unfolding and refolding of C_L fragment in the absence of denaturant in Chapter 5. Whereas the unfolding rate ($k_1 = 6 \times 10^{-4}$ s^{-1}) obtained in this Chapter using the two-state mechanism is in fair agreement with that ($k_{32} = 1 \times 10^{-3}$ s^{-1}) obtained by the three-species mechanism, the refolding rate ($k_{-1} = 3 \times 10^{-2}$ s^{-1}) estimated here is considerably smaller than that ($k_{23} = 0.18$ s^{-1}) estiamted by the three-species mechanism. In the analysis of the kinetic data of the disulfide formation in terms of the two-state approximation, the rate of slow isomerization process of U_1 to U_2 in the three-species mechanism is involved in the rate of refolding. This resulted in the underestimate of the refolding rate in the two-state approximation. On the other hand, the same process of the unfolding of the native molecule can be seen both in the kinetics of the disulfide formation described here and in the unfolding and refolding kinetics described in Chapter 5, and thus the both kinetic data give the same rate constant of unfolding.

Summary

In order to establish the mechanism of protein folding, the unfolding and refolding of the C_L fragment of the immunoglobulin light chain were studied with an emphasis on the role of the intrachain disulfide bond

1. Role of intrachain disulfide bond in conformation and stability of C_L fragment

The conformation and stabilities of the C_L fragment isolated from a type λ light chain and the C_L fragment in which the intrachain disulfide bond had been reduced were studied by measuring CD, fluorescence, and ultraviolet absorption. The results indicated that no great conformational change occurs on reduction of the disulfide, unless the SH groups are alkylated. Intact C_L was more resistant than reduced C_L to GuHCl. The denaturation curves were analyzed using an equation based on the binding of GuHCl and the free energy changes of denaturation in the absence of the denaturant were estimated as about 6 $kcal \cdot mol^{-1}$ for intact C_L and about 1.8 $kcal \cdot mol^{-1}$ for reduced C_L. The difference in stability between intact C_L and reduced C_L was explained to a great extent in terms of the entropy change associated with reduction of the intrachain disulfide bond of the fragment in the denatured state.

II. Folding mechanism of intact C_L fragment

The kinetics of reversible unfolding and refolding by GuHCl of C_L fragment were studied. The kinetic measurements were made at pH 7.5 and 25°C using tryptophyl fluorescence and far-ultraviolet circular dichroism.

The kinetics of unfolding of the C_L fragment showed two phases in the conformational transition zone and a single phase above the transition zone. A double-jump experiment confirmed the presence of two forms of the unfolded molecule. These results were thoroughly explained on the basis of the three-species mechanism, $U_1 \rightleftarrows U_2 \rightleftarrows N$, where U_1 and U_2 are the slow-folding and fast-folding species, respectively, of unfolded protein and N is native protein. The equilibrium constant for the process of U_2 to U_1 was estimated to be about 10 and was independent of the conditions of denaturation. These findings were consistent with the view that the $U_1 \rightleftarrows U_2$ reaction is proline isomerization. The rates of interconversion between N and U_2 changed greatly with the concentration of GuHCl. On the other hand, the refolding kinetics below the transition zone showed behavior unexpected from the three-species mechanism. Whereas the apparent rate constant of the slow phase of refolding was independent of the refolding conditions, its amplitude decreased markedly with the decrease in the final concentration of GuHCl. On the basis of this and other results, formation of an intermediate during refolding was ascertained and the refolding kinetics were consistently explained in terms of a more general mechanism

involving a kinetic intermediate probably containing non-native proline isomers. The intermediate seemed to have a folded conformation similar to native protein. Comparison of the refolding kinetics of the C_L fragment with those of other domains of the immunoglobulin molecule suggested that Pro 143 is responsible for the appearance of the slow phase.

III. Folding mechanism of reduced C_L fragment

The reduced C_L fragment assumes a conformation very similar to the intact C_L fragment. The kinetics of reversible unfolding and refolding of the reduced C_L fragment by GuHCl at pH 7.5 and 25°C were studied and were compared with those of the intact C_L fragment. Tryptophyl fluorescence, far ultraviolet circular dichroism and reactivity of the SH groups toward DTNB were used to follow the kinetics.

The results obtained were thoroughly explained on the basis of the three-species mechanism, $U_1 \rightleftarrows U_2 \rightleftarrows N$, where U_1 and U_2 are slow-folding and fast-folding species, respectively, of unfolded protein and N is the native protein. The rate constants of interconversion between U_1 and U_2 and the rate constant for the process from N to U_2 were very similar to the respective values for the intact C_L fragment. Only the rate constant for the process from U_2 to N was greatly different between the intact and reduced C_L fragments; the

rate constant for the reduced C_L fragment was about 100 times smaller than that for the intact C_L fragment. These results indicated that the slow isomerization of the unfolded molecule are independent of the presence of the disulfide bond and that the kinetic role of the intrachain disulfide bond is to accelerate the folding process. This kinetic role in the folding of the C_L fragment was explainable in terms of only the decreased entropy in the unfolded state of the intact C_L fragment due to the presence of the disulfide bond.

IV. Refolding of immunoglobulin light chain

The kinetics of the refolding of type λ light chains in 0.1 M GuHCl at pH 7.5 and 25°C from 4 M GuHCl were studied by CD, ultraviolet absorption, and fluorescence spectrophotometry.

The kinetics were complex and consisted of at least three phases, an undetectable fast phase which completed within the dead time (30 sec) of the measurement, a fast phase with an apparent rate constant of 2×10^{-2} s^{-1}, and a slow phase with an apparent rate constant of 3×10^{-3} s^{-1}. The apparent rate constant of the slow phase was very similar to that of the C_L fragment in the same refolding condition. The activation energy of the slow phase was the same for a light chain and the C_L fragment. On the other hand, the refolding reactions of V_L fragments were too fast to be measured in the experiment using manual mixing. These results indicated that the refolding kinetics of the C_L domain are very similar to those of isolated C_L fragment

and that refolding of the V_L domain precedes refolding of the C_L domain, even though both domains have similar immunoglobulin-fold. However, the results of refolding experiments on light chains, and V_L and C_L fragments in the presence of ANS, as well as other lines of evidence, indicated that the refolding kinetics of the light chain molecule cannot be expressed as exact sum of the refolding reactions of isolated V_L and C_L fragment.

V. Formation of intrachain disulfide bond in C_L fragment

Regeneration by glutathione of the C_L fragment was studied in the absence and presence of 8 M urea. The species that appeared during the reaction of the reduced C_L fragment with oxidized glutathione were trapped by alkylation with iodoacetamide and identified by electrophoresis in 15% polyacrylamide gel at pH 9.5. The kinetics of the reactions starting from various species formed during the reaction of the reduced C_L fragment were also studied, and the overall reaction kinetics of the formation of the intrachain disulfide bond in the C_L fragment were established in the absence and presence of urea.

The reaction of the reduced C_L fragment with oxidized glutathione was much slower but the yield of the C_L fragment with the disulfide bond was much higher in the absence than in the presence of 8 M urea. The slowness of the reaction in the absence of urea is due to the

two cysteinyl residues of the reduced C_L fragment being buried in the interior of the molecule and because oxidized glutathione is capable of reacting with the thiols only in the opened form of the protein molecule. The high yield is due to the cysteinyl thiol and the mixed disulfide in the intermediate forming an intrachain disulfide bond through thio-disulfide interchange reaction being exposed to solvent and located at the appropriate proximity. These findings indicate first, that the appropriate proximity of a pair of cysteinyl residues is essential to form a disulfide bond and second, that they are not easily oxidized to disulfide if they are buried in the interior of the protein molecule.

Acknowledgements

The author would like to express great appreciation to Professor Kozo Hamaguchi of Faculty of Science, Osaka University for his continuing guidance, many valuable discussions, and continuous encouragement throughout this work.

The author is also grateful to Dr. Takachika Azuma and Dr. Kiyoshi Ikeda of Faculty of Science, Osaka University for their continuing guidance and valuable discussions. The author would like to express his gratitude to Prof. H. Matsubara and Dr. S. Hase of Faculty of Science, Osaka University for advice and help in sequence determination and amino aicd analysis. The author wishes to thank Dr. E. Inada of Osaka Police Hospital and Prof. S. Migita of Kanazawa University for providing Bence Jones proteins used in this work. The author wishes to thank Mr. A. Sumi for help in preparing the C_L fragment and for valuable discussions. The author wishes to thank Dr. S. Kuramitsu, Dr. Y. Yang, Dr. Y. Nakae, Mr. K. Teshima, Mr. T. Yamauchi, Mr. T. Okajima, and other colleagues in my laboratory for valuable discussions and kind help in this work.

References

Acharya, A.S. & Taniuchi, H. (1976) J. Biol. Chem. 251, 6934-6946

Amzel, L.M. & Poljak, R.L. (1979) Ann. Rev. Biochem. 48, 961-997

Anfinsen, C.B. (1973) Science 181, 223-230

Anfinsen, C.B. & Scheraga, H.A. (1975) Adv. Protein Chem. 29, 205-300

Arata, Y. & Shimizu, A. (1979) Biochemistry 18, 2513-2520

Azuma, T., Hamaguchi, K., & Migita, S. (1972) J. Biochem. 73, 1457-1467

Azuma, T., Hamaguchi, K., & Migita, S. (1974) J. Biochem. 76, 685-693

Azuma, T., Kobayashi, O., Goto, Y., & Hamaguchi, K. (1978) J. Biochem. 83, 1485-1492

Baldwin, R.L. (1975) Ann. Rev. Biochem. 44, 453-475

Baldwin, R.L. (1978) Trends Biochem Sci. 3, 66-68

Baldwin, R.L. (1980) in Protein Folding (Jaenicke, R., ed.) pp. 369-384, Elsevier/North Holland, Amsterdam

Baldwin, R.L. & Creighton, T.E. (1980) in Protein Folding (Jaenicke, R., ed.) pp. 217-260, Elsevier/North Holland, Amsterdam

Beale, D. & Feinstein, A. (1976) Quart. Rev. Biophys. 9, 135-180

Bergman, L.W. & Kuehl, W.M. (1979) J. Biol. Chem. 254, 8869-8876

Blombäck, B., Blombäck, M., Edman, P., & Hessel, B. (1966) Biochim. Biophys. Acta 115, 371-396

Bradshaw, R.A., Kanarek, L., & Hill, R.L. (1967) J. Biol. Chem. 242, 3789-3798

Brandts, H.F., Halvorson, H.R., & Brennan, M. (1975) Biochemistry 14, 4953-4963

Burgess, A.W. & Scheraga, H.A. (1975) J. Theor. Biol. 52, 403-420

Cassim, J.Y. & Yang, J.T. (1969) Biochemistry 8, 1947-1951

Chen, B.L. & Poljak, R.J. (1974) Biochemistry 13, 1295-1302

Cheng, H.N. & Bovey, F.A. (1977) Biopolymers, 16, 1465-1472

Chou, P.Y. & Fasman, G.D. (1974a) Biochemistry 13, 211-222

Chou, P.Y. & Fasman, G.D. (1974b) Biochemistry 13, 222-245

Chou, P.Y. & Fasman, G.D. (1978) Adv. Enzymol. 47, 45-148

Cool, K.H., Schmid, F.X., & Baldwin, R.L. (1979) Proc. Nat. Acad. Sci. U.S.A. 76, 6157-6161

Cowgill, R.W. (1967) Biochim. Biophys. Acta 140, 37-44

Creighton, T.E. (1977) J. Mol. Biol. 113, 295-312

Creighton, T.E. (1978) Prog. Biophys. molec. Biol. 33, 231-297

Creighton, T.E. (1979) J. Mol. Biol. 129, 411-431

Creighton, T.E. (1980a) in Protein Folding (Jaenicke, R. ed.) pp.427-441, Elsevier/ North Holland, Amsterdam

Creighton, T.E. (1980b) J. Mol. Biol. 137, 61-80

Creighton, T.E. (1981) J. Mol. Biol. 151, 211-213

Creighton, T.E., Kalef, E., and Arnon, R. (1978) J. Mol. Biol. 123, 129-147

Crisanti, M.M. & Matthews, C.R. (1981) Biochemistry 20, 2700-2706

Cunningham, B.A. (1976) Federation Proc. 35, 1171-1176

Davies, D.R., Padlan, E.A., & Segal, D.M. (1975) Ann. Rev. Biochem. 44, 639-667

Davis, B.J. (1964) Ann. New York Acad Sci. 121, 404-427

Deisenhofer, J. (1961) Biochemistry 20, 2361-2370

Edsall, J.T. & Wyman, J. (1958) Biophysical Chemistry, vol. 1, Academic Press, New York

Edelman, G.M. & Gall, W.E. (1969) Ann. Rev. Biochem. 38, 415-466

Fasman, G.D., ed. (1976) Handbook of Biochemistry and Molecular Biology, 3rd ed., Proteins-Volume III, pp. 403-420, CRC Press Inc., Ohio

Fersht, A. (1977) Enzyme Structure and Mechanism, W.H. Freeman and Company Limited, California

Flory, P.J. (1956) J. Am. Chem. Soc. 78, 5222-5235

Frost, A.A. & Pearson, R.G. (1961) Kinetics and Mechanism, 2nd ed., pp. 160-199, John Wiley and Sons, Inc., New York

Garel, J.-R. & Baldwin, R.L. (1973) Proc. Nat. Acad. Sci. U.S.A. 70, 3347-3351

Garel, J.-R. & Baldwin, R.L. (1975) J. Mol. Biol. 94, 611-620

Garel, J.-R., Nall, B.T., & Baldwin, R.L. (1976) Proc. Nat. Acad. Sci. U.S.A. 73, 1853-1857

Gething, M.J.H. & Davidson, B.E. (1972) Eur. J. Biochem. 30, 352-353

Ghose, A.C. (1972) Biochim. Biophys. Acta 278, 337-343

Ghose, A.C. (1973) Biochem. Biophys. Res. Commun. 52, 240-245

Grathwohl, C. & Wüthrich, K. (1976) Biopolymers 15, 2043-2057

Hagerman, P.J. (1977) Biopolymers 16, 731-747

Hagerman, P.J. & Baldwin, R.L. (1976) Biochemistry 15, 1462-1473

Hamaguchi, K. (1976) Tanpakushitsu Kinō no Bunshiron, University of Tokyo Press, Tokyo (in Japanese)

Hamaguchi, K. (1978) Protein, Nucleic Acid and Enzyme 23, 1199-1204 (in Japanese)

Hamaguchi, K. & Kurono, A. (1963) J. Biochem. 54, 111-122

Henrici, P. (1962) Discrete Variable Methods in Ordinary Differential Equations, John Wiley and Sons, Inc., New York

Huber, R. & Steigemann, W. (1974) FEBS Letters 48, 235-237

Ikai, A., Fish, W.W., & Tanford, C. (1973) J. Mol. Biol. 73, 165-184

Isenman, D.E., Painter, R.H., & Dorrington, K.J. (1975) Proc. Nat. Acad. Sci. U.S.A. 72, 548-552

Isenman, D.E., Lancet, D., & Pecht, I. (1979) Biochemistry 18, 3327-3336

Johnson, R.E., Adams, P., & Rupley, J.A. (1978) Biochemistry 17, 1479-1484

Jullien, M & Baldwin, R.L. (1981) J. Mol. Biol. 145, 265-280

Kabat, E.A. (1978) Adv. Protein Chem. 32, 1-75

Karlsson, F.A., Peterson, P.A., & Berggård, I. (1972a) J. Biol. Chem. 247, 1065-1073

Karlsson, F.A., Björk, I., & Berggård, I. (1972b) Immunochemistry 9, 1129-1138

Karplus, M. & Weaver, D.L. (1976) Nature 260, 404-406

Kato, M., Azuma, T., Isobe, T. & Hamaguchi, K. (1978) J. Biochem. 84, 1475-1483

Kato, S., Okamura, M., Shimamoto, N., & Utiyama, H. (1981) Biochemistry 20, 1080-1085

Kishida, F., Azuma, T., & Hamaguchi, K. (1976) J. Biochem. 79, 91-105

Lapanje, S. & Rupley, J.A. (1979) Biochemistry 12, 2370-2372

Leher, S.S. (1971) Biochemistry 10, 3254-3263

Levitt, M. (1981) J. Mol. Biol. 145, 251-263

Lim, V.I. (1978) FEBS Letters 89, 10-14

Longworth, J.W., McLaughlin, C.L., & Solomon, A. (1976) Biochemistry 15, 2953-2958

Matsubara, H. & Sasaki, R.M. (1969) Biochem. Biophys. Res. Commun. 35, 175-181

Marquart, M., Deisenhofer, J., Huber, R., & Palm, W. (1980) J. Mol. Biol. 141, 369-391

Nall, B.T., Garel, J.-R., & Baldwin, R.L. (1978) J. Mol. Biol. 118, 317-330

Nemethy, G. & Scheraga, H.A. (1979) Proc. Nat. Acad. Sci. U.S.A. 76, 6050-6054

Pace, C.N. (1975) Crit. Rev. Biochem. 3, 1-43

Pace, C.N. & Vanderburg, K.E. (1979) Biochemistry 18, 288-292

Pain, R.H. (1981) Nature 290, 187-188

Plunkett, G. & Ryan, C.A. (1980) J. Biol. Chem. 255, 2752-2755

Pohl, F.M. (1976) FEBS Letters 65, 293-296

Poland, D.C. & Scheraga, H.A. (1965) Biopolymers 3, 379-399

Poljak, R.J., Amzel, L.M., Avey, H.P., Chen, B.L., Phizackerley, R.P., & Saul, F. (1973) Proc. Nat. Acad. Sci. U.S.A. 70, 3305-3310; data were obtained from A.M.S.O.M.(6.1.2.1.1.)

Pollet, R., Rossi, G., & Edelhoch, H. (1972) J. Biol. Chem. 247, 5921-5927

Ptitsyn, O.B. & Rashin, A.A. (1975) Biophys. Chem. 3, 1-20

Rowe, E.S. & Tanford, C. (1973) Biochemistry 12, 4822-4827

Ridge, J.A., Baldwin, R.L., & Labhardts, A.M. (1981) Biochemistry 20, 1622-1630

Schiffer, M., Girling, R.L., Ely, K.R., & Edmundson, A.B. (1973) Biochemistry 12, 4620-4631

Schmid, F.X. (1981) Eur. J. Biochem. 144, 105-109

Schmid, F.X. & Baldwin, R.L. (1979) J. Mol. Biol. 133, 285-287

Schmid, F.X. & Blaschek, H. (1981) Eur. J. Biochem. 144, 111-117

Schulz, G.E. & Schirmer, R.H. (1979) Principles of Protein Structure, Springer-Verlag, New York

Segawa, S., Husimi, Y., & Wada, A. (1973) Biopolymers 12, 2521-2537

Shimizu, A., Honzawa, M., Yamamura, Y., & Arata, Y. (1980) Biochemistry 19, 2784-2790

Spackman, D.H., Stein, W.H., & Moore, S., (1958) Anal. Chem. 30, 1190-1206

Stellwagen, E. (1979) J. Mol. Biol. 135, 217-229

Stern, O. & Volmer, M. (1919) Z. Physiol. 20, 183-188

Straub, F.B. (1967) Proc. 7th Int. Congress Biochem (Tokyo) 41-50

Stryer, L. (1965) J. Mol. Biol. 13, 482-495

Sumi, A. & Hamaguchi, K. in preparation

Takagi, T. & Isemura, T. (1966) Biochim. Biophys. Acta 130, 233-240

Takagi, T. & Ito, N. (1972) Biochim. Biophys. Acta 257, 1-10

Takagi, T., Okano, R., & Miyazawa, T. (1973) Biochim. Biophys. Acta 310, 11-19

Takagi, T. & Izutsu, T. (1974) J. Biochem. 75, 441-446

Takahashi, S., Kontani, T., Yoneda, M., & Ooi, T. (1977) J. Biochem. 82, 1127-1133

Tanaka, Y., Azuma, T., & Hamaguchi, K. (1978) J. Biochem. 83, 1249-1263

Tanford, C. (1968) Adv. Protein Chem. 23, 121-282

Tanford, C. (1970) Adv. Protein Chem. 24, 1-95

Tanford, C., Aune, K.C., & Ikai, A (1973) J. Mol. Biol. 73, 185-197

Teale, F.W.J. (1960) Biochem. J. 76, 381-388

Tonomura, B., Nakatani, H., Onishi, M., Yamaguchi-Ito, J., & Hiromi, K. (1978) Anal. Biochem. 84, 370-383

Torchinsky, Y.M. (1981) Sulfur in Proteins, pp. 199-217, Pergamon Press, Oxford

Tsong, T.Y., Baldwin, R.L., & Elson, E.L. (1972) Proc. Nat. Acad. Sci. U.S.A. 69, 1809-1812

Utiyama, Y. (1980) Protein, Nucleic Acid and Enzyme 25, 1041-1052 (in Japanese)

Urry, D.W. & Pettegrew, J.W. (1967) J. Am. Chem. Soc. 89, 5276-5283

Vincent, J.-P., Chicheportiche, R., Lazdunski, M. (1971) Eur. J. Biochem. 23, 401-411

Weber, G. & Young, L.B. (1964) J. Biol. Chem. 239, 1415-1423

Weber, K. & Osborn, M. (1969) J.Biol. Chem. 244, 4406-4412

Wetlaufer, D.B. & Ristow, S. (1973) Ann. Rev. Biochem. 42, 135-158

White, F.H., Jr. (1976) Biochemistry 15, 2906-2912

Whitesides, G.M., Lilburn, J.E., & Szajewski, R.P. (1977) J. Org. Chem. 42, 332-338

Yutani, K. (1978) Protein, Nucleic Acid and Enzyme 23, 1190-1198 (in Japanese)

Yoshida, C., Yoshikawa, M., & Takagi, T. (1976) J. Biochem. 80, 449-454

Publications

1. Refolding of the Immunoglobulin Light Chain

   Goto, Y., Azuma, T., & Hamaguchi, K. (1979) J. Biochem. 85, 1427-1438

2. The Role of the Intrachain Disulfide Bond in the Conformation and Stability of the Constant Fragment of the Immunoglobulin Light Chain

   Goto, Y. & Hamaguchi, K. (1979) J. Biochem. 86, 1433-1441

3. Formation of the Intrachain Disulfide Bond in the Constant Fragment of the Immunoglobulin Light Chain

   Goto, Y. & Hamaguchi, K. (1981) J. Mol. Biol. 146, 321-340

4. Unfolding and Refolding of the Constant Fragment of the Immunoglobulin Light Chain

   Goto, Y. & Hamaguchi, K. (1982) J. Mol. Biol., in press

5. Unfolding and Refolding of the Reduced Constant Fragment of the Immunoglobulin Light Chain: Kinetic Role of the Intrachain Disulfide Bond

   Goto, Y. & Hamaguchi, K. (1982) J. Mol. Biol., in press

6. Monomer-Dimer Equilibria of a Bence Jones Protein and its Variable Fragment

   Azuma, T., Kobayashi, O., Goto, Y., and Hamaguchi, K. (1978) J. Biochem. 83, 1485-1492